INVESTIGATING THE ROLE OF *LACTOBACILLUS REUTERI* AND THE MICROBIOTA IN BONE HEALTH

By

Darin Quach

A DISSERTATION

Submitted to
Michigan State University
in partial fulfillment of the requirements
for the degree of

Microbiology and Molecular Genetics - Doctor of Philosophy

2016

ABSTRACT

INVESTIGATING THE ROLE OF *LACTOBACILLUS REUTERI* AND THE MICROBIOTA IN BONE HEALTH

By

Darin Quach

Osteoporosis is a disease characterized by low bone mass, which can subsequently lead to an increased risk of sustaining a bone fracture. With the advancements made in research and medicine in the past century, the average lifespan has increased substantially. However, this has also lead to an increase in the elderly population that is susceptible to age-related diseases such as osteoporosis. It is currently estimated that over 300 million people worldwide are impacted by osteoporosis. Taking into consideration the side effects stemming from medications used to treat this illness, there has been an increase in research efforts to develop novel therapeutics for osteoporosis. One area of research that has garnered recent interest involves investigating the therapeutic potential of the gut microbiota in bone health. As a result, an overarching goal in this area of research revolves around identifying microbes that impact bone health and understanding the mechanisms mediating these responses.

In this thesis, I present the beneficial use of the probiotic bacterium *Lactobacillus reuteri* (*L. reuteri*) in an *in vivo* murine model of osteoporosis mediated by estrogen deficiency. Using female Balb/c mice that are rendered estrogen deficient following ovariectomy, we demonstrated that supplementation with *L. reuteri* was capable of preventing bone loss. In addition to this, we identified that the process of osteoclastogenesis was down-regulated following *L. reuteri* treatment in these mice suggesting that this could be the mechanism by which *L. reuteri* confers its benefit on bone health.

Osteoclasts are the main cell type responsible for bone resorption. Using an *in vitro* model of osteoclastogenesis, we demonstrated that cell-free conditioned medium (CCM) from *L. reuteri* inhibited the maturation of osteoclasts from macrophages. We further characterized this

by demonstrating that *L. reuteri* CCM halted osteoclastogenesis at an intermediate stage characterized by fused polykaryons. Using an antagonist to the G protein coupled receptor GPR120, we decreased the ability of *L. reuteri* CCM to suppress osteoclastogenesis from 70% to 38% suggesting that *L. reuteri* is partially signaling through GPR120 to suppress osteoclastogenesis. Taking into account that GPR120 was a receptor for long chain fatty acids, we investigated the impact of lactobacillic acid (LA), a long chain fatty acid produced by *L. reuteri*, and observed that the suppression of osteoclastogenesis by *L. reuteri* involved the production of LA. Moreover, purified LA could suppress osteoclast formation in a dose dependent manner. To elucidate the effect of *L. reuteri* treatment on host cell physiology, we performed RNA sequencing at multiple time points during osteoclastogenesis. An analysis of the transcriptome data identified several pathways that were modulated following *L. reuteri* treatment. Further investigations indicated that NF-κB and p38 activation were impacted by *L. reuteri* in RAW264.7 cells. These sets of experiments have led to the identification of a possible effector molecule produced by *L. reuteri* and mechanism by which it acts to benefit bone health.

In the last part of this thesis, I present an *in vivo* murine model using germ free (GF) mice to study the impact of the gut microbiota on bone health. By colonizing GF mice with microbiotas with different compositions, the goal was to identify specific microbes that could be impacting bone health in either a positive or negative manner. Interestingly enough, we discovered that the microbial communities that were introduced into the different groups of mice in our studies did not impact bone health in comparison to the GF control group. This was in stark contrast to existing literature that reported a deleterious effect in bone health following the introduction of a gut microbiota. This reinforced the fact that our knowledge remains limited in terms of understanding how the gut microbiota impacts bone health. Nevertheless, the discoveries stemming from these studies contribute to the growing body of work in this discipline and will guide future research that aims to uncover novel therapeutic options to combat osteoporosis.

This work is dedicated to my parents and sisters, who have been my biggest supporters every step of the way during this long but incredibly rewarding journey.

ACKNOWLEDGEMENTS

There is a long list of individuals that have contributed to my successes thus far, but the person that I would like to acknowledge first is Dr. Robert Britton. Words cannot adequately express how fortunate I feel to be a part of your blossoming laboratory. Thank you for your continual efforts to help me develop into a better scientist and individual. In my perspective, I couldn't have asked for a more patient, understanding, and supportive mentor. I was concurrently pursuing a medical degree and Dr. Britton's effort to bridge medicine and research gave me great insight and will no doubt be something that I will always lean on as I further my career as a physician scientist.

To the other members of my guidance committee, Dr. Laura McCabe, Dr. Nara Parameswaran, Dr. Chris Abramovitch, and Dr. Chris Waters, thank you for all your efforts. They were always available whenever I needed direction for my project and their suggestions were truly invaluable. I had the pleasure of working closely with Dr. McCabe and Dr. Parameswaran, who essentially served as my co-mentors, because of the collaboration that have resulted in the findings presented in this thesis.

I truly believe that in addition to the great mentorship I received, another thing that aided in my success were all the individuals in the lab that I've had the pleasure to meet and work alongside of. I learned so much from each and every one of you. I really couldn't have asked for a better environment to work in.

Finally, I would like to thank my family for their unwavering support through the course of my education. To my parents who immigrated here in order to ensure the opportunities of a better life for my sisters and me, thank you. I wish both of you were around to see this and share in my joy. To my sisters, Emily and Helen, both of you also made your share of sacrifices to allow me to pursue my hopes and dreams and I'll always be grateful for that. Lastly, I would

like to thank Andrea, who was always around to support me, make me laugh, and pick me up after the recent passing of my parents.

TABLE OF CONTENTS

LIST OF TABLES ..... **xi**

LIST OF FIGURES ..... **xii**

KEY TO ABBREVIATIONS ..... **xiv**

CHAPTER 1. OVERVIEW OF OSTEOPOROSIS AND THERAPEUTIC MICROBIOLOGY **1**
1.1 Osteoporosis 2
1.1.1 Types of osteoporosis 2
1.1.2 Bone physiology 3
1.1.3 Dysregulation of osteoclastogenesis in postmenopausal osteoporosis 4
1.1.4 Current treatments for postmenopausal osteoporosis 6
1.2 Therapeutic Microbiology 8
1.2.1 Probiotics and bone health 8
1.2.2 Microbiota and bone health 9
1.3 Thesis overview 10
BIBLIOGRAPHY 13

CHAPTER 2. PROBIOTIC *L. REUTERI* TREATMENT PREVENTS BONE LOSS IN A MENOPAUSAL OVARIECTOMIZED MOUSE MODEL **18**
2.1 Abstract 19
2.2 Introduction 19
2.3 Materials and Methods 21
2.3.1 Experimental design 21
2.3.2 μCT bone imaging 21
2.3.3 Femur histomorphometry and dynamic measures 22
2.3.4 Bone RNA analysis 23
2.3.5 Serum measurements 24
2.3.6 Bacterial strains and culture 24
2.3.7 FACS analysis 24
2.3.8 Osteoclast generation and characterization 25
2.3.9 DNA preparation of tissue samples 25
2.3.10 PCR amplification for beta diversity analysis 26
2.3.11 454 sequencing and analysis 26
2.3.12 Statistical analysis 27
2.4 Results 27
2.5 Discussion 40
BIBLIOGRAPHY 45

CHAPTER 3. CHARACTERIZATION OF THE SUPPRESSION OF OSTEOCLASTOGENESIS BY *LACTOBACILLUS REUTERI* **49**
3.1 Introduction 50
3.2 Materials and Methods 52
3.2.1 Bacterial strains used in this study and growth conditions 52
3.2.2 Culture conditions and osteoclastogenesis differentiation assay 53
3.2.3 Chemicals and reagents used 53
3.2.4 Pharmacological inhibition studies 54
3.2.5 Cell viability or metabolic activity assay 54
3.2.6 RNA Extraction from RAW264.7 cells and sequencing 55
3.2.7 Analysis of RNA sequencing data 55

3.2.8 Quantitative reverse transcriptase (RT) polymerase chain reaction (qPCR).....55
3.2.9 Primer sequences for qPCR.....56
3.2.10 Western blot analysis.....56
3.2.11 Bone resorption assay.....57
3.2.12 Statistical analysis.....57
3.3 Results.....57
3.3.1 L. reuteri suppressed osteoclastogenesis in a dose-dependent manner.....57
3.3.2 Progression of osteoclastogenesis over time.....59
3.3.3 Impact of L. reuteri on bone resorption in RANKL-stimulated RAW264.7 cells.....63
3.3.4 An early signaling event in osteoclastogenesis was targeted by L. reuteri.....65
3.3.5 Blocking of GPR 120 attenuated the suppression of osteoclastogenesis by L. reuteri.....67
3.3.6 Lactobacillic acid suppressed in vitro osteoclastogenesis.....69
3.3.7 Transcriptomic profiling of RAW264.7 cells during L. reuteri treatment supports the suppression of osteoclastogenesis.....74
3.3.8 Activation of NF-κB and p38 in RAW264.7 cells was inhibited by L. reuteri.....84
3.4 Discussion.....91
BIBLIOGRAPHY.....94

CHAPTER 4. ROLE OF THE GUT MICROBIOTA IN BONE HEALTH.....101
4.1 Introduction.....102
4.2 Materials and Methods.....105
4.2.1 Germ Free Mouse Husbandry.....105
4.2.2 Preparation of Cecal and Fecal Samples and inoculation of the GF animals.....106
4.2.3 Gavage and Sample Collection.....106
4.2.4 Micro Computed Tomography (μCT) Analysis of Bone.....107
4.2.5 Static and Dynamic Histomorphometry.....108
4.2.6 Quantitative Real Time PCR (qRT-PCR).....108
4.2.7 Flow Cytometry.....109
4.2.8 Osteoclast Outgrowth Assay.....110
4.2.9 DNA extraction from mouse fecal samples, 16S rRNA gene amplication, and sequencing.....110
4.2.10 Microbial Community Analysis.....111
4.2.11 Statistical analyses.....112
4.3 Results.....112
4.3.1 Conventionalization with a human microbiota does not decrease bone mass in GF mice.....112
4.3.2 Presence of a normal mouse gut microbiota does not impact bone mass in female Swiss Webster or C57bl/6 mice.....115
4.3.3 Presence of a normal mouse gut microbiota does not impact bone mass in male Swiss Webster mice.....118
4.3.4 Histomorphometric analysis of the distal femur.....119
4.3.5 Flow cytometry and osteoclast outgrowth between GF and CONV-D mice.....121
4.3.6 Analysis of inflammatory markers from the gut and serum.....125
4.3.7 Fecal microbial community analysis.....127
4.4 Discussion.....180
BIBLIOGRAPHY.....183

CHAPTER 5. DISCUSSION AND CONCLUSION.....188
5.1 Future directions.....190
5.1.1 Integration of other probiotic studies and potential mechanisms to consider.....192

5.2 Conclusions 194
BIBLIOGRAPHY 195

APPENDIX 198
BIBLIOGRAPHY 204

LIST OF TABLES

Table 2.1. Femur bone parameters....29

Table 2.2. Vertebrae bone parameters....30

Table 2.3. Beta diversity analysis....37

Table 3.1 Genes with significantly changed expression between vehicle and *L. reuteri* treatment (Fold change > 3)....76

Table 3.2. Pathways differentially regulated between vehicle and *L. reuteri* treatment....76

Table 3.3. KEGG pathways differentially regulated at day 1 in RAW264.7 cells....76

Table 3.4. KEGG pathways differentially regulated at day 3 in RAW264.7 cells....77

Table 3.5. KEGG pathways differentially regulated at day 5 in RAW264.7 cells....80

Table 4.1. Description of human microbiotas....114

Table 4.2. Trabecular and Cortical Bone Parameters for Swiss Webster Mice....118

Table 4.3. Histomorphometry of Trabecular Bone in Distal Femur....120

Table 4.4. Abundances of OTUs for each mouse group....130

Table 4.5. OTU taxonomy table....154

LIST OF FIGURES

Figure 1.1. Overview of osteoclastogenesis. 5

Figure 1.2. Overview of bone loss in postmenopausal osteoporosis. 6

Figure 2.1. Ovariectomy (Ovx) mice treated with L. reuteri for 4 weeks display femur and vertebral trabecular bone volumes that are similar to ovary intact control mice. 28

Figure 2.2. L. reuteri treatment prevents Ovx-induced increases in RANKL and bone marrow osteoclastogenesis after 2 weeks of probiotic treatment. 31

Figure 2.3. Osteoclast and osteoblast markers don't show significant changes in response to Ovx +/- L. reuteri treatment at 4 weeks. 33

Figure 2.4. FACS analysis of bone marrow cells. 35

Figure 2.5. Two-dimensional projection of the principal coordinate analysis (PCoA) of bacterial 16S sequences from mouse jejunum samples along the first two principal axes. 37

Figure 2.6. Effect of L. reuteri secreted factors on osteoclast differentiation in RAW 264.7 cells. 39

Figure 3.1. Dose-dependent inhibition of osteoclast formation by *L. reuteri.* 58

Figure 3.2. Progression of osteoclastogenesis over time. 60

Figure 3.3. Bone resorption studies. 64

Figure 3.4. Impact of *L. reuteri* CCS on osteoclast differentiation at different time points. 66

Figure 3.5. Suppression of osteoclastogenesis by *L. reuteri* was mediated through GPR120 signaling. 68

Figure 3.6. Lactobacillic acid (LA) involved with the suppression of osteoclastogenesis. 70

Figure 3.7. Histamine production by *L. reuteri* not involved with inhibition of osteoclastogenesis. 72

Figure 3.8. Experimental layout for gene expression analysis. 73

Figure 3.9. MTT assay measuring reduction potential of RAW264.7 cells following stimulation by the <3kDa CCS fraction from *L. reuteri* for (a) 24 and (b) 72 hours. 83

Figure 3.10. Comparison of osteoclastogenesis genes by qPCR and RNA sequencing. 84

Figure 3.11. Effect of *L. reuteri* on RANKL-induced NF-κB/p65 phosphorylation. 86

Figure 3.12. Impact of *L. reuteri* on MAPK signaling. 88

Figure 3.13. Working model of osteoclastogenesis suppression by *L. reuteri* and LA. 90

Figure 4.1. Experimental layout for human microbiota and conventionalization mouse studies. 113

Figure 4.2. Trabecular bone volume fraction (BVF) of GF Swiss Webster mice after colonization with different human microbiotas. 114

Figure 4.3. Conventionalization of female GF Swiss Webster and C57bl/6 mice does not impact bone density. 116

Figure 4.4. Conventionalization of male GF Swiss Webster mice does not lead to bone loss. 119

Figure 4.5. Conventionalization does not impact MAR or TRAP staining of metaphyseal region of femur. 120

Figure 4.6. Conventionalization of GF Swiss Webster mice resulted in no changes in bone marrow cell populations. 122

Figure 4.7. Osteoclast outgrowth from bone marrow cells of GF Swiss Webster and conventionalized (CONV-D) mice. 124

Figure 4.8. Partitioning of osteoclast outgrowth from bone marrow cells of GF Swiss Webster and conventionalized (CONV-D) mice. 125

Figure 4.9. Expression analysis of the colon and serum analysis of TNF-α. 126

Figure 4.10. Alpha and beta diversity measures for conventionalized mice indicate higher diversity in SW mice and distinct clustering. 129

Figure 4.11. Conventionalization of Swiss Webster mice reduces cecal weight and length while *Turicibacter* monocolonization does not. 178

Figure 4.12. Turicibacter colonization did not impact BVF. 179

Figure A.1. Identification of mutants with decreased suppression of osteoclastogenesis. 202

Figure A.2. Gene annotation of putative mutants and locus map. 203

KEY TO ABBREVIATIONS

BFR	bone formation rate
BMC	bone mineral content
BMD	bone mineral density
BVF	bone volume fraction
CCM	cell-free conditioned medium
CCS	cell culture supernatant
CFA	cyclopropane fatty acid
CFA	cyclopropane fatty acid
CONV-D	conventionalized
CT	computed tomography
DMSO	dimethyl sulfoxide
DXA	dual energy x-ray absorptiometry
GF	germ free
GI	gastrointestinal
GPR	G protein coupled receptor
LA	lactobacillic acid
M-CSF	macrophage colony stimulating factor
MAPK	mitogen activated protein kinase
MAR	mineral apposition rate
MEM-alpha	minimal essential medium
NF-κB	Nuclear factor kappa B
OTU	operational taxonomic unit
OVX	ovariectomy

PBS	phosphate buffered saline
PCoA	principal coordinate analysis
PCR	polymerase chain reaction
qPCR	quantitative polymerase chain reaction
RANKL	receptor activator of NF-kB ligand
SEM	standard error of mean
SERMs	selective estrogen-receptor modulators
SERT	serotonin reuptake transporter
SPF	specific pathogen free
SW	Swiss Webster
Tb.N	trabecular number
Tb.So.	trabecular spacing
Tb.Th	trabecular thickness
TMD	tissue mineral density
TNF-α	tumor necrosis factor alpha
TRAP	tartrate resistant alkaline phosphatase
WHI	Women’s Health Initiative
WT	wild-type

CHAPTER 1. OVERVIEW OF OSTEOPOROSIS AND THERAPEUTIC MICROBIOLOGY

1.1 *Osteoporosis*

Osteoporosis is a disease characterized by decreased bone mass that often leads to an increased risk of sustaining a bone fracture [1]. Osteoporosis is the most common type of bone disease and, according to the National Osteoporosis Foundation, there are 54 million Americans who are currently osteoporotic or osteopenic with low bone mass. Current estimates of bone fractures in the US are between 1.5 and 2 million per year [2]. While osteoporosis affects both men and women, 4/5^{ths} of all cases are found in women. Ultimately, this equates to an economic burden of $19 billion dollars each year in health expenditures (direct cost), lost workdays, and decreased productivity (indirect costs) in the US [3,4]. By 2025, experts predict that these figures will rise by 25%. Aside from the cost required to treat this disease, morbidity and mortality increases substantially with age following most fractures [5]. For example, 2 in 3 men die or sustain another fracture within a year following a hip fracture [6,7]. Similarly, 1 in 5 women die within a year following a hip fracture [8].

1.1.1 *Types of osteoporosis*

Osteoporosis can be categorized as being either primary or secondary, based on the etiology of the disease. The primary form is the most common type and typically results from age-related bone loss. Primary osteoporosis can be further subdivided into types 1 and 2. Type 1 is due to sex steroid deficiency and women are more likely to be impacted than men [4]. Type 2 is often referred to as senile osteoporosis and affects both men and women over 70 years of age as age-related physiological changes in the body are observed. Secondary osteoporosis results either from other diseases, medication use, or is the result of unknown etiology. Examples include metastatic cancer, gastrointestinal disorders, drug side effects, chronic renal failure, poor nutrition, and genetic disorders such as osteogenesis imperfecta [9,10]. This form of osteoporosis can occur in both sexes and can occur at any age.

Regardless of the type of osteoporosis, its development relies on two major factors: 1) peak bone mass reached and 2) the rate of bone loss during the different intervals of life. A combination of both genetic and environmental factors ultimately determines an individual's susceptibility for developing osteoporosis. The impact of these influences on an individual's bone health begins *in utero*. Therefore, maintaining bone health requires constant attention throughout life since it undergoes constant turnover and is affected by so many variables.

1.1.2 *Bone physiology*

Bone development begins in the embryonic stage of life but bone is constantly remodeled throughout life. Bone is formed in a process called ossification and several cell types take part in bone metabolism. Several of the main cell types are derived from a mesenchymal cell lineage that includes chondrocytes, osteocytes, and osteoblasts. Chondrocytes are present at the bone growth plate and deposit a cartilaginous matrix composed of collagen and proteoglycans for bone growth. Osteocytes act as sensors that respond to loading stresses to regulate bone turnover. Osteoblasts function in bone formation by carrying out the synthesis and mineralization of the bone matrix. Another important cell type is the osteoclast, which is derived from a hematopoietic stem cell lineage. These giant multinucleated cells are responsible for bone resorption, or the removal of bone [11,12].

The processes of bone growth, modeling, and remodeling direct the development of bone. Modeling is the process where bones are shaped and is characterized by a phase where osteoblast-driven bone formation outweighs osteoclast-driven bone resorption. During childhood where the majority of modeling takes place, longitudinal and radial growth lengthens and increases bone girth, respectively. Aside from the geometric shape, the composition of minerals and proteins also determine bone strength. It is primarily composed of the minerals calcium,

phosphate, and magnesium (hydroxyapatite) in addition to collagen. Spanning from childhood to adolescence, there is a drastic increase in bone mass and bones are shaped as the adult skeleton develops. It is estimated that 40% of bone mass is obtained during adolescence and 90% by the age of 18 [13]. Bridging into adulthood, the rate of bone formation starts to decline and becomes coupled with bone resorption. By the mid to late 30s, an individual's peak bone mass is reached. At this point, bone mass starts to decline at different rates depending on the individual. Bone remodeling occurs to maintain mineral homeostasis, repair bone microdamage, and facilitate fracture healing.

1.1.3 *Dysregulation of osteoclastogenesis in postmenopausal osteoporosis*

Bone is a dynamic organ that undergoes continuous turnover to enable a number of functions including the maintenance of normal serum calcium levels, removal of minerals from areas of disuse, and addition of mineral to areas of the skeleton for healing and load-bearing functions. The main processes involved in bone remodeling are bone formation and bone resorption [14]. Following early growth and development where peak bone mass is attained, these processes are normally balanced. However, bone loss leading to osteoporosis can develop if there is a shift that favors bone resorption. Osteoclastogenesis is a multi-step process that begins with hematopoietic stem cells (Figure 1.1)[11,15]. Monocytes from this stem cell lineage are stimulated by cytokines and growth factors (e.g. M-CSF, RANKL) for differentiation. As differentiation progresses, cell-cell fusion occurs and results in the formation of a giant cell known as a polykaryon [15,16]. The polykaryon increases in cell size and termination differentiation results in a giant multinucleated cell capable of resorbing bone [17,18]. This pathway is targeted in several bone diseases and its enhancement leads to an imbalance in bone remodeling. An example of this stems from the impact of estrogen deficiency on osteoclastogenesis (Figure 1.2).

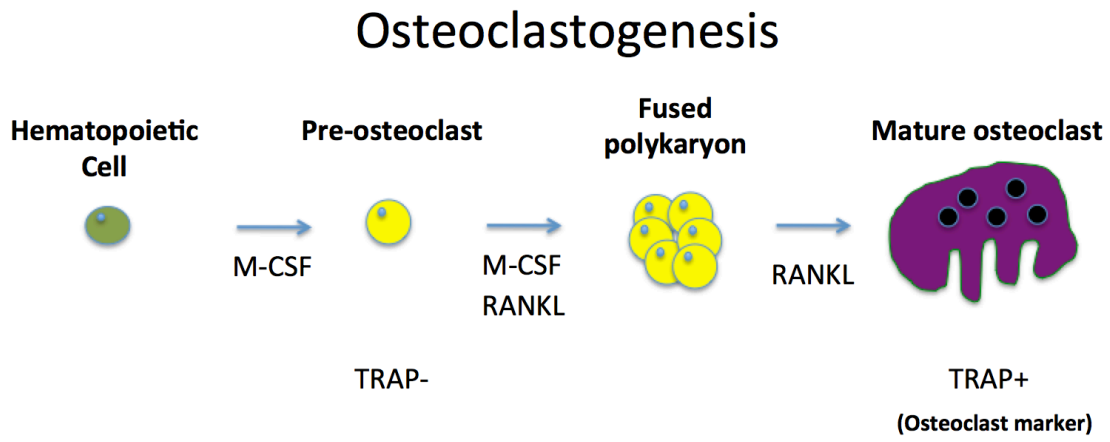

Figure 1.1. Overview of osteoclastogenesis.

Hematopoietic stem cells go through several stages of differentiation to form osteoclasts that are TRAP positive. Differentiating factors (e.g. M-CSF, RANKL) promote osteoclastogenesis.

Estrogen deficiency, which is observed during menopause, creates an imbalance between bone formation and resorption by increasing NF-κB activation and the production of pro-inflammatory cytokines such as TNF-α [19–23]. During estrogen deficiency, NF-κB activation inhibits osteoblast activity while promoting osteoclast activity resulting in bone loss [20,21]. The importance of NF-κB signaling in osteoporosis is further supported by findings showing that NF-κB inhibitors increase bone formation and decrease bone resorption in estrogen deficient mice [24,25]. Blocking TNF-α has also been shown to prevent bone loss in estrogen deficient mice [26]. Collectively, these studies strongly suggest that postmenopausal bone loss is, in part, due to pro-inflammatory cytokine production and increased immune activation.

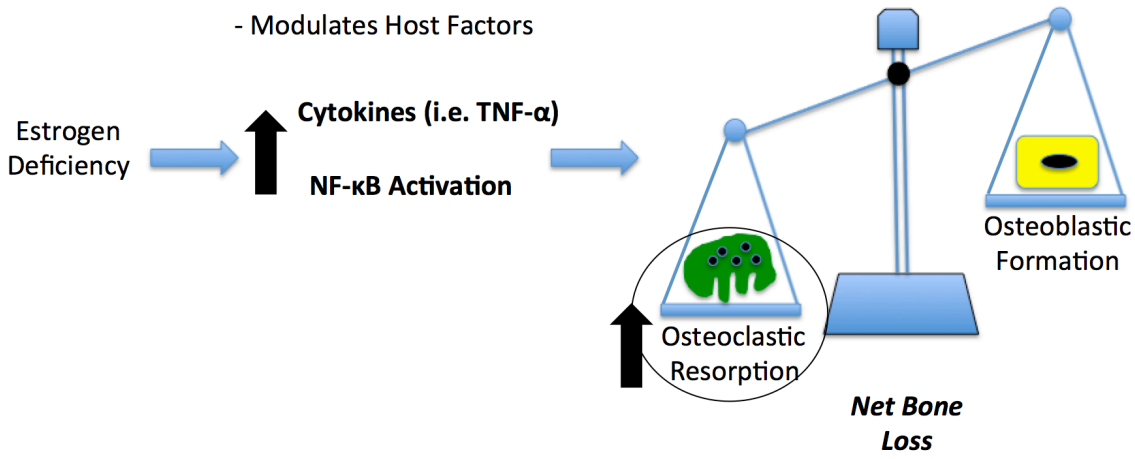

Figure 1.2. Overview of bone loss in postmenopausal osteoporosis.

Estrogen deficiency has been shown to impact the host immune response to promote bone resorption by creating an imbalance between bone resorption and bone formation.

1.1.4 *Current treatments for postmenopausal osteoporosis*

Therapeutic management of osteoporosis depends on the age of the individual and/or severity of bone loss. By the age of 50, men and women are advised to take daily vitamin D and calcium supplements. Nonpharmacologic recommendations include increased physical activity, assessment of the environment to mitigate fall risks, and decreased consumption of alcohol and/or smoking. At this stage, the overall goal is preventing the development of osteoporosis and to take precautions to limit the possibility of sustaining a future fracture.

According to guidelines established by the World Health Organization, osteoporosis is clinically defined by a having a T score of -2.5 or less at the hip, lumbar spine, or femoral neck. This equates to being 2.5 or more standard deviations below the peak bone mass that one achieves during childhood as measured by dual energy x-ray absorptiometry (DXA) scanning [9,27]. A

clinical diagnosis of osteoporosis warrants a more aggressive pharmacologic approach utilizing an antiresorptive or anabolic agent. These include bisphosphonates and estrogen or selective estrogen-receptor modulators (SERMs) [9]. The first line of treatment are bisphosphonates and they act as antiresorptives by inducing osteoclast apoptosis, leading to the inhibition of bone resorption [28]. Several randomized trials investigating the use of bisphosphonates have been shown to reduce the risk of bone fractures [29,30]. The second line of treatment is the use of estrogen or SERMs. In the Women's Health Initiative (WHI) trials, estrogen therapy significantly reduced the risk of fractures at multiple body sites including the hip, wrist, arm, and vertebrae [31,32].

While the use of bisphosphonates and estrogen have been shown to be extremely effective in preventing fracture risk, there are associated risks with each line of treatment. Common side effects of bisphosphonates include the development of esophagitis and overall malaise [29]. More serious, but rare, side effects include sustaining atypical femur fractures or osteonecrosis of the jaw [33,34]. Hormone replacement therapy with estrogen seems to be an obvious choice as a therapeutic since its absence is the main cause of postmenopausal osteoporosis. However, risks associated with estrogen use include an increased risk of breast cancer, thrombotic, and cardiovascular disease have led to recommendations against it as a first line treatment option [32]. These drawbacks, coupled with the projected increase in individuals affected by the disease, call for the development of novel therapeutics for osteoporosis.

1.2 *Therapeutic Microbiology*

1.2.1 *Probiotics and bone health*

The potential use of probiotics, defined by the World Health Organization as "live microorganisms which when administered in adequate amounts confer a health benefit on the host", for combating bone disease has recently gained substantial interest. Several studies have demonstrated the beneficial impact of probiotic organisms on bone health using several different animal models. For example, using an ovariectomy (OVX) model in both rats and mice designed to mimic postmenopausal conditions, it was shown that the administration of different *Lactobacilli* strains could prevent the loss of bone density following estrogen deficiency [35–37]. Moreover, studies conducted in normal models of aging also demonstrated the efficacy of *Lactobacillus* and *Lactococcus* to improve upon bone mineral density (BMD) and bone mineral content (BMC), which are measures commonly used to assess bone strength [38,35,37]. These observations, while exciting, still lack in fully describing a mechanism through which the probiotic organism exerts its health benefit.

Due to the fact that different parameters are impacted following probiotic treatment in a number of bone studies, the implication is that there is a high level of strain specificity and different probiotics act through different mechanisms to exert beneficial health effects. Moreover, the physiological and immune status of the host can also contribute to determining the efficacy of probiotic treatment. For example, it has been demonstrated that *Lactobacillus reuteri 6475* (*L. reuteri*) is able to prevent the onset of osteoporosis in estrogen deficient mice. However, in sex hormone sufficient animals, this strain only conferred a benefit to bone in male mice [39]. In order for female mice to respond to probiotic treatment, inflammation or estrogen deficiency had to be present [35,40]. In similar OVX studies, it was demonstrated that a mixture of other *Lactobacilli* was

capable of protecting mice against cortical bone loss as opposed to the protection against trabecular bone loss demonstrated by *L. reuteri* [36].

While human probiotic studies targeted at bone health are limited, one study has demonstrated reduced parathyroid hormone levels and increased serum calcium levels following the consumption of *Lactobacillus* fermented milk by women [41]. Conversely, it was observed in another study that consumption of fermented milk was ineffective in modulating calcium absorption in postmenopausal women [42]. Similar to what is observed in animal models, these conflicting results highlight the need for further investigation in order to gain a better understanding of the influence of probiotics on bone health.

1.2.2 *Microbiota and bone health*

The GI tract is the organ with the largest surface area in the human body. The digestive tract, which starts at the mouth and extends through the intestines ending at the anus, has an immense surface area at approximately 30 to 40 square meters [43]. It is responsible for a number of functions including the processing of food, absorption of nutrients, and excretion of waste products. In addition to these vital functions, it also serves as both a physical barrier that provides us protection as well as a means to interact with the external environment.

These functions are essential, as the human GI tract comes into contact with trillions of bacteria (gut microbiota) per day. These bacteria can be subdivided into hundreds of species with a vast array of metabolisms in tow [44]. It is generally accepted that humans have co-evolved with bacteria, and this relationship is mutualistic. This has been studied in the context of various diseases ranging from diabetes, obesity, and atherosclerosis to asthma [45–47]. More recently, the importance of the gut microbiota in bone health has been an area of focus following the discovery that the GI microbiota has the potential to regulate bone mass in mice.

One of the hallmark studies in the field concluded that the presence of a microbiota drastically decreased bone mass. Germ-free (GF) mice colonized with a conventional mouse microbiota were shown to lose bone density when compared to their GF counterparts [48]. Conversely, in a nutrition study, it was demonstrated that the presence of a gut microbiota was important for adequate weight gain and bone growth [49]. Other studies have shown that disrupting the microbiota with antibiotic treatment in mice could impact BMD and BMC. However, this effect was sex specific, as BMC in male mice was impacted in a negative fashion while female mice showed an increase in BMC and BMD [50]. Lastly, the pharmacological induction of estrogen deficiency was shown to decrease bone mass only in the presence of the gut microbiota [51]. In that study, it was also shown that there was no significant difference in bone mass between GF and conventionally raised animals. Taken together, the conflicting results stemming from these studies point to the fact that the regulation of bone mass by the microbiota depends on a number of factors including the composition of the microbiota, the intricacies of the animal model, and other variables that have yet to be discovered.

1.3 *Thesis overview*

Despite all the studies that have been conducted thus far investigating the impact of probiotics and the microbiota on bone health, our knowledge in this subject matter remains limited. Although, some studies have suggested that probiotics impacted mineral absorption or decreased osteoclastogenesis to improve bone health, a thorough understanding of how this is carried out still remains unknown. Results from the bone studies investigating the role of the microbiota suggest that bone health is dependent on the composition of the microbiota and host physiology is consistent with probiotics only being efficacious in a context dependent manner.

As a result, the work that will be presented in this thesis will attempt to contribute towards understanding the role of bacteria in regulating bone health.

This thesis focuses on characterizing the use of the probiotic *L. reuteri* in an estrogen deficiency mouse model of osteoporosis (Chapter 2). The treatment of OVX mice with *L. reuteri* prevented the onset of osteoporosis. Further characterization identified that the osteoclastogenesis pathway was impacted following *L. reuteri* treatment. As a result, the interaction between *L. reuteri* and osteoclasts became the focus of these studies aimed at understanding how *L. reuteri* exerts its beneficial bone effect.

The development and use of an *in vitro* osteoclastogenesis model to study the impact of *L. reuteri* identified a number of KEGG pathways that were differentially regulated by probiotic treatment (Chapter 3). Western blot studies indicated that NF-κB activation, which is a crucial signaling event for osteoclastogenesis, was suppressed by *L. reuteri*. Interestingly, it was previously shown that *L. reuteri* could modulate NF-κB activation [52]. This provides a specific mechanism to target in future bone studies with *L. reuteri*.

Phenotypic analysis of the osteoclastogenesis process led to the observation that osteoclasts were being arrested at a specific stage of development (Chapter 3). Similar results have been demonstrated through studies involving the use of fatty acids to suppress osteoclastogenesis [53–56]. As a result, this prompted the investigation of Lactobacillic acid (LA), which is an immunomodulatory compound produced by *L. reuteri*. Studies with LA or a mutant strain of *L. reuteri* unable to produce LA indicated that it is involved with the suppression of osteoclast formation. Additional studies with a pharmacological inhibitor of a receptor for long chain fatty acids, GPR120, demonstrated that this pathway was targeted by *L. reuteri* to impact osteoclastogenesis.

The role of the microbiota on bone health was also investigated (Chapter 4). The impact of the microbiota on bone health appears to be dependent on the community composition. To pursue the idea that specific community members could be identified that impact bone health, I began by colonizing GF mice with different defined communities, the goal was to be able to identify specific community members that impacted bone health. However, the presence of the microbiota regardless of its composition, did not impact bone health. The characterization of the bacterial community will serve as an important reference for future studies investigation bone health and the microbiota.

BIBLIOGRAPHY

BIBLIOGRAPHY

1. Lane, N. E. Epidemiology, etiology, and diagnosis of osteoporosis. *Am. J. Obstet. Gynecol.* **194,** (2006).

2. Burge, R. *et al.* Incidence and Economic Burden of Osteoporosis-Related Fractures in the United States, 2005–2025. *J. Bone Miner. Res.* **22,** 465–475 (2007).

3. C., P. *et al.* Direct and indirect costs of non-vertebral fracture patients with osteoporosis in the US. *Pharmacoeconomics* **28,** 395–409 (2010).

4. Cauley, J. A. Public health impact of osteoporosis. *J. Gerontol. A. Biol. Sci. Med. Sci.* **68,** 1243–51 (2013).

5. Bliuc, D. *et al.* Mortality risk associated with low-trauma osteoporotic fracture and subsequent fracture in men and women. *JAMA* **301,** 513–21 (2009).

6. Willson, T., Nelson, S. D., Newbold, J., Nelson, R. E. & LaFleur, J. The clinical epidemiology of male osteoporosis: A review of the recent literature. *Clin. Epidemiol.* **7,** 65–76 (2015).

7. Von Friesendorff, M., McGuigan, F. E., Besjakov, J. & Åkesson, K. Hip fracture in men-survival and subsequent fractures: A cohort study with 22-year follow-up. *J. Am. Geriatr. Soc.* **59,** 806–813 (2011).

8. Brauer, C. A., Coca-perraillon, M., Cutler, D. M. & Rosen, A. B. Incidence and Mortality of Hip Fractures in the United States. **302,** 1573–1579 (2009).

9. Cosman, F. *et al.* Clinician's Guide to Prevention and Treatment of Osteoporosis. *Osteoporos. Int.* **25,** 2359–2381 (2014).

10. Stein, E. & Shane, E. Secondary osteoporosis. *Endocrinol. Metab. Clin. North Am.* **32,** 115–134 (2003).

11. Boyle, W. J., Simonet, W. S. & Lacey, D. L. Osteoclast differentiation and activation. *Nature* **423,** 337–42 (2003).

12. Zhang, R. *et al.* Bone Resorption by Osteoclasts. *Science (80-.).* **289,** 1504–1508 (2000).

13. Bailey, D. a, McKay, H. a, Mirwald, R. L., Crocker, P. R. & Faulkner, R. a. A six-year longitudinal study of the relationship of physical activity to bone mineral accrual in growing children: the university of Saskatchewan bone mineral accrual study. *J. bone Miner. Res.* **14,** 1672–1679 (1999).

14. Eriksen, E. F. Cellular mechanisms of bone remodeling. *Rev. Endocr. Metab. Disord.* **11,** 219–227 (2010).

15. Teitelbaum, S. L., Tondravi, M. M. & Ross, F. P. Osteoclasts, macrophages, and the molecular mechanisms of bone resorption. *J. Leukoc. Biol.* **61,** 381–388 (1997).

16. Kukita, T. *et al.* RANKL-induced DC-STAMP is essential for osteoclastogenesis. *J. Exp. Med.* **200,** 941–6 (2004).

17. Aharon, R. & Bar-Shavit, Z. Involvement of aquaporin 9 in osteoclast differentiation. *J. Biol. Chem.* **281,** 19305–19309 (2006).

18. Yagi, M. *et al.* DC-STAMP is essential for cell-cell fusion in osteoclasts and foreign body giant cells. *J. Exp. Med.* **202,** 345–51 (2005).

19. Clarke, B. L. & Khosla, S. Physiology of bone loss. *Radiol Clin N Am* **48,** 483–95 (2010).

20. Strait, K., Li, Y., Dillehay, D. L. & Weitzmann, M. N. Suppression of NF-kappaB activation blocks osteoclastic bone resorption during estrogen deficiency. *Int. J. Mol. Med.* **21,** 521–5 (2008).

21. Krum, S. a, Chang, J., Miranda-Carboni, G. & Wang, C.-Y. Novel functions for NFκB: inhibition of bone formation. *Nat. Rev. Rheumatol.* **6,** 607–11 (2010).

22. Srivastava, S. *et al.* Estrogen decreases TNF gene expression by blocking JNK activity and the resulting production of c-Jun and JunD. *J. Clin. Invest.* **104,** 503–13 (1999).

23. Weitzmann, M. N. & Pacifici, R. Estrogen deficiency and bone loss: An inflammatory tale. *J. Clin. Invest.* **116,** 1186–1194 (2006).

24. Alles, N. *et al.* Suppression of NF-kappaB increases bone formation and ameliorates osteopenia in ovariectomized mice. *Endocrinology* **151,** 4626–4634 (2010).

25. Chang, J. *et al.* Inhibition of osteoblastic bone formation by nuclear factor-κB. *Nat. Med.* **15,** 682–689 (2009).

26. Kimble, R. B., Bain, S. & Pacifici, R. The functional block of TNF but not of IL-6 prevents bone loss in ovariectomized mice. *J. Bone Miner. Res.* **12,** 935–941 (1997).

27. Karjalainen, J. P., Riekkinen, O., Töyräs, J., Jurvelin, J. S. & Kröger, H. New method for point-of-care osteoporosis screening and diagnostics. *Osteoporos. Int.* **27,** 971–977 (2016).

28. Weinstein, R. S., Roberson, P. K. & Manolagas, S. C. Giant osteoclast formation and long-term oral bisphosphonate therapy. *N. Engl. J. Med.* **360,** 53–62 (2009).

29. Khosla, S. *et al.* Benefits and risks of bisphosphonate therapy for osteoporosis. *J. Clin. Endocrinol. Metab.* **97,** 2272–2282 (2012).

30. Crandall, C. J. *et al.* Comparative effectiveness of pharmacologic treatments to prevent fractures: An updated systematic review. *Ann. Intern. Med.* **161,** 711–723 (2014).

31. Jackson, R. D. *et al.* Effects of conjugated equine estrogen on risk of fractures and BMD in postmenopausal women with hysterectomy: results from the women's health initiative

randomized trial. *J. Bone Miner. Res.* **21,** 817–828 (2006).

32. Cauley, J. a *et al.* Effects of Estrogen Plus Progestin on Risk of Fracture and Bone Mineral Density. **290,** 1729–1738 (2014).

33. Khan, A. A. *et al.* Diagnosis and management of osteonecrosis of the jaw: A systematic review and international consensus. *J. Bone Miner. Res.* **30,** 3–23 (2015).

34. Shane, E. *et al.* Atypical subtrochanteric and diaphyseal femoral fractures: Second report of a task force of the American society for bone and mineral research. *J. Bone Miner. Res.* **29,** 1–23 (2014).

35. Britton, R. A. *et al.* Probiotic L. reuteri Treatment Prevents Bone Loss in a Menopausal Ovariectomized Mouse Model. *Journal of Cellular Physiology* **229,** 1822–1830 (2014).

36. Ohlsson, C. *et al.* Probiotics Protect Mice from Ovariectomy-Induced Cortical Bone Loss. *PLoS One* **9,** e92368 (2014).

37. Chiang, S. S. & Pan, T. M. Antiosteoporotic effects of lactobacillus-fermented soy skim milk on bone mineral density and the microstructure of femoral bone in ovariectomized mice. *J. Agric. Food Chem.* **59,** 7734–7742 (2011).

38. Kimoto-Nira, H. *et al.* Anti-ageing effect of a lactococcal strain: analysis using senescence-accelerated mice. *Br. J. Nutr.* **98,** 1178–1186 (2007).

39. Mccabe, L. R., Irwin, R., Schaefer, L. & Britton, R. A. Probiotic use decreases intestinal inflammation and increases bone density in healthy male but not female mice. *J. Cell. Physiol.* **228,** 1793–1798 (2013).

40. Collins, F. L. *et al.* Lactobacillus reuteri 6475 Increases Bone Density in Intact Females Only under an Inflammatory Setting. *PLoS One* **11,** e0153180 (2016).

41. Narva, M., Nevala, R., Poussa, T. & Korpela, R. The effect of Lactobacillus helveticus fermented milk on acute changes in calcium metabolism in postmenopausal women. *Eur. J. Nutr.* **43,** 61–68 (2004).

42. Cheung, A. L. T. F. *et al.* Fermentation of calcium-fortified soya milk does not appear to enhance acute calcium absorption in osteopenic post-menopausal women. *Br J Nutr* **105,** 282–286 (2011).

43. Helander, H. F. & Fändriks, L. Surface area of the digestive tract - revisited. *Scand. J. Gastroenterol.* **49,** 681–9 (2014).

44. Walter, J. & Ley, R. The Human Gut Microbiome: Ecology and Recent Evolutionary Changes. *Annu. Rev. Microbiol.* **65,** 411–429 (2011).

45. Cani, P. D. *et al.* Changes in gut microbiota control inflammation in obese mice through a mechanism involving GLP-2-driven improvement of gut permeability. *Gut* **58,** 1091–1103 (2009).

46. Koeth, R. a *et al.* Intestinal microbiota metabolism of l-carnitine, a nutrient in red meat, promotes atherosclerosis. *Nat. Med.* **19,** 576–85 (2013).

47. Korpela, K. *et al.* Intestinal microbiome is related to lifetime antibiotic use in Finnish pre-school children. *Nat. Commun.* **7,** (2016).

48. Sjögren, K. *et al.* The gut microbiota regulates bone mass in mice. *J. Bone Miner. Res.* **27,** 1357–1367 (2012).

49. Schwarzer, M. *et al.* Lactobacillus plantarum strain maintains growth of infant mice during chronic undernutrition. **351,** (2016).

50. Cox, L. M. *et al.* Altering the intestinal microbiota during a critical developmental window has lasting metabolic consequences. *Cell* **158,** 705–721 (2014).

51. Li, J.-Y. *et al.* Sex steroid deficiency-associated bone loss is microbiota dependent and prevented by probiotics. *J. Clin. Invest.* **126,** 2049–63 (2016).

52. Iyer, C. *et al.* Probiotic Lactobacillus reuteri promotes TNF-induced apoptosis in human myeloid leukemia-derived cells by modulation of NF-??B and MAPK signalling. *Cell. Microbiol.* **10,** 1442–1452 (2008).

53. Cornish, J. *et al.* Modulation of osteoclastogenesis by fatty acids. *Endocrinology* **149,** 5688–5695 (2008).

54. Drosatos-Tampakaki, Z. *et al.* Palmitic acid and DGAT1 deficiency enhance osteoclastogenesis, while oleic acid-induced triglyceride formation prevents it. *J. Bone Miner. Res.* **29,** 1183–1195 (2014).

55. Kim, H.-J., Yoon, H.-J., Kim, S.-Y. & Yoon, Y.-R. A medium-chain fatty acid, capric acid, inhibits RANKL-induced osteoclast differentiation via the suppression of NF-κB signaling and blocks cytoskeletal organization and survival in mature osteoclasts. *Mol. Cells* **37,** 598–604 (2014).

56. Kwon, J.-O., Jin, W. J., Kim, B., Kim, H.-H. & Lee, Z. H. Myristoleic acid inhibits osteoclast formation and bone resorption by suppressing the RANKL activation of Src and Pyk2. *Eur. J. Pharmacol.* **768,** 189–98 (2015).

CHAPTER 2. PROBIOTIC *L. REUTERI* TREATMENT PREVENTS BONE LOSS IN A MENOPAUSAL OVARIECTOMIZED MOUSE MODEL

These results have been published in the article: Britton RA, Irwin R, Quach D, Schaefer L, Zhang J, Lee T, Parameswaran N, and McCabe LR. Journal of Cellular Physiology.

Development of the *in vivo* experiments was a collaborative effort between Robert A. Britton, Regina Irwin, Nara Parameswaran, and Laura R. McCabe. All authors with the exception of Robert A. Britton, Nara Parameswaran, and Laura R. McCabe participated in animal tissue collection and sample processing at the conclusion of the *in vivo* experiments. Regina Irwin and Jing Zhang conducted the measurements for the bone parameters. Taehyung Lee performed the flow cytometric analysis. Laura Schaefer conducted the microbial community analysis. I developed the *in vitro* assay that studied the interaction between *L. reuteri* and osteoclasts.

2.1 *Abstract*

Estrogen deficiency is a major risk factor for osteoporosis that is associated with bone inflammation and resorption. Half of women over the age of 50 will experience an osteoporosis related fracture in their lifetime, thus novel therapies are needed to combat post-menopausal bone loss. Recent studies suggest an important role for gut-bone signaling pathways and the microbiota in regulating bone health. Given that the bacterium *Lactobacillus reuteri* ATCC PTA 6475 (*L. reuteri*) secretes beneficial immunomodulatory factors, we examined if this candidate probiotic could reduce bone loss associated with estrogen deficiency in an ovariectomized (Ovx) mouse menopausal model. Strikingly, L. reuteri treatment significantly protected Ovx mice from bone loss. Osteoclast bone resorption markers and activators (Trap5 and RANKL) as well as osteoclastogenesis are significantly decreased in L. reuteri-treated mice. Consistent with this, L. reuteri suppressed Ovx-induced increases in bone marrow CD4þ T-lymphocytes (which promote osteoclastogenesis) and directly suppressed osteoclastogenesis in vitro. We also identified that L. reuteri treatment modifies microbial communities in the Ovx mouse gut. Together, our studies demonstrate that L. reuteri treatment suppresses bone resorption and loss associated with estrogen deficiency. Thus, L. reuteri treatment may be a straightforward and cost-effective approach to reduce post-menopausal bone loss.

2.2 *Introduction*

Finding effective novel treatments for bone loss is a priority, since it is estimated that by 2020 more than 61 million women and men will have osteoporosis (National-Osteoporosis-Foundation, 2009). Menopause is a major risk factor for osteoporosis. In fact, one in two women over the age of 50 will experience an osteoporosis-related fracture in their lifetime. Estrogen

deficiency in post-menopausal women promotes bone loss, increases bone resorption, and enhances fracture risk [1–3]. Similarly, ovariectomy (Ovx) depletes estrogen in mice leading to bone loss at multiple skeletal sites and increased bone turnover [4,5]. Bone loss ensues due to a greater increase in bone resorption compared to bone formation [5,6]. Studies demonstrate that bone inflammation is increased with estrogen deficiency and is linked to osteoclastogenesis and hence bone resorption [1,5,6]. Despite all of the current treatments available for promoting bone health, the number of osteoporotic patients is on the rise in the United States and worldwide. A lack of awareness that one is at risk early in life, an increasing elderly population, and patient noncompliance due to unwanted medication side effects are likely contributors to this outcome. In addition, conventional bone loss treatments are not always effective. Therefore, new approaches to increase bone density are needed.

The role of the intestinal microbiota in regulating human health and disease is receiving increasing attention [7,8]. While the intestine is known to be key for calcium and vitamin D metabolism, the effect of bacterial community changes on bone health, especially in estrogen deficiency, has not been thoroughly examined. Reports have indicated that prebiotics (non-digestible poly- saccharides that modulate gut microbial composition) can increase bone density [9–11] especially in combination with probiotics [12]. Probiotics (microorganisms that provide health benefit to the host when ingested in adequate amounts) have also been shown to increase cortical bone thickness in chicken [13] as well as reduce bone loss in aging mice [14] and improve bone density in male mice [15]. More recently, studies indicate that germ-free mice have greater bone density compared to mice harboring a conventional microbiota, further supporting a link between the intestine and bone [16]. The mechanistic basis by which the gut and the intestinal microbiota regulate bone density, however, is not known.

Lactobacillus reuteri is an established probiotic species that has proven beneficial in clinical trials [17,18]. *L. reuteri* is one of a handful of lactobacilli indigenous to the human and mouse GI tract [19] and has never been associated with causing disease. *L. reuteri* ATCC PTA

6475 produces antimicrobial compounds such as reuterin as well as molecules that have potent anti-TNF activity in vitro [20,21]. Previously we identified that *L. reuteri* 6475 improves bone density in male mice [15]. Therefore, we hypothesized that *L. reuteri* 6475 could modulate the intestinal microbiota and/or regulate systemic and bone inflammation, resulting in sup- pressed bone loss in Ovx mice. Consistent with our premise, L. reuteri treatment prevents Ovx-induced bone loss thereby implicating probiotic ingestion as a straightforward and cost- effective approach to prevent menopause-induced bone loss.

2.3 *Materials and Methods*

2.3.1 *Experimental design*

Balb/c mice 12 weeks of age non-Ovx and Ovx were obtained from Harlan Laboratories (Indianapolis, IN). Mice were allowed to acclimate to animal room for 1 week prior to start of experiment. After 1 week, mice were treated by gavaging with 300ml ($1*10^9$ cfu/ml) with *L. reuteri* ATCC PTA 6475 or MRS broth, (vehicle control) three times per week for 4 weeks and *L. reuteri* was also added to the drinking water at a concentration of $1.5*10^8$ cfu/ml unless otherwise noted in the figure legend. Mice were given Teklad 2019 chow (Madison, WI) and water ad libitum and were maintained on a 12 h light/dark cycle. Food and water intake were monitored and did not differ between groups (data not shown). All animal procedures were approved by the Michigan State University Institutional Animal Care and Use Committee.

2.3.2 *µCT bone imaging*

Fixed femurs were scanned using a GE Explore Locus microcomputed tomography (µCT) system at a voxel resolution of 20mm obtained from 720 views. Beam angle of increment was 0.5, and beam strength was set at 80 peak kV and 450 uA. Each run consisted of control (non-

Ovx) and Ovx and Ovx + L. reuteri- treated mouse bones, and a calibration phantom to standardize grayscale values and maintain consistency. On the basis of autothreshold and isosurface analyses of multiple bone samples, a fixed threshold (760) was used to separate bone from bone marrow. Bone measurements were blinded; thus, knowledge of what mouse condition the analyzed bone was from was unknown until the final data was pooled. Trabecular bone analyses were performed in a region of trabecular bone defined at 1% of the total length length (~0.17mm) proximal to the growth plate of and extending 2mm toward the diaphysis excluding the outer cortical bone. Trabecular bone mineral content, bone volume fraction, thickness, spacing, and number values were computed by a GE Healthcare MicroView software application for visualization and analysis of volumetric image data. Cortical measurements were performed in a 2*2*2mm cube centered midway down the length of the bone using a threshold of 1000 to separate bone from marrow.

2.3.3 *Femur histomorphometry and dynamic measures*

Femurs were fixed in 10% formalin and transferred to 70% ethanol after 24 h. Fixed samples were processed on an automated Thermo Electron Excelsior tissue processor for dehydration, clearing, and infiltration using a routine overnight processing schedule. Samples were then embedded in Surgipath-embedding paraffin on a Sakura Tissue Tek II-embedding center. Paraffin bocks were sectioned at 5mm on a Reichert Jung 2030 rotary microtome. Slides were stained for TRAP activity and counterstained with hematoxylin according to manufacturer protocol (387A-1KT, Sigma, St. Louis, MO). Osteoblast and osteoclast surface area was measured and expressed as a percentage of total bone surface in the femur trabecular region ranging from the growth plate to 2mm distal. For dynamic histomorphometric measures of bone formation, mice were injected intraperitoneally with 200ml of 10 mg/ml calcein (Sigma, St. Louis, MO) dissolved in sterile saline at 7 and 2 days prior to harvest. L3-L4 vertebrae were fixed in formalin at time of harvest then transferred to 70% ethanol 48 h later. Vertebrae were then

embedded, sectioned, and examined under UV light. Five images were taken and the distance between the calcein lines (bone formation rate, BFR) and their length along the bone surface was measured and used to calculate mineral apposition rate (MAR).

2.3.4 *Bone RNA analysis*

Immediately following euthanasia tibias were cleaned of muscle and connective tissue, snap frozen in liquid nitrogen and stored at -80 °C. Frozen tibias were crushed under liquid nitrogen conditions with a Bessman Tissue Pulverizer (Spectrum Laboratories, Rancho Dominguez, CA). RNA was isolated using TriReagent (Molecular Research Center, Cincinnati, OH), and integrity assessed by formaldehyde–agarose gel electrophoresis. cDNA was synthesized by reverse transcription using Superscript II Reverse Transcriptase Kit and oligo dT(12–18) primers (Invitrogen, Carlsbad, CA) and amplified by real-time PCR with iQ SYBR Green Supermix (BioRad, Hercules, CA), and gene specific primers were synthesized by Integrated DNA Technologies (Coralville, IA). Hypoxanthine guanine phosphoribosyl transferase (HPRT) mRNA levels do not fluctuate with Ovx were used as an internal control. Amplicon specificity was confirmed by melting curve, size, and sequence analysis. Primers for real-time PCR were designed or previously described: osteocalcin, Trap5b and HPRT [22]. Receptor activator of nuclear factor kappa-B ligand (RANKL) was amplified using 5'-TTTGCAGGACTCGAC TCT GGA G-3' and 5'-TCC CTC CTT TCA TCA GGT TAT GAG-3' [23,24]. Osterix was amplified using 5'-CCC TTC TCA AGC ACC AAT GG-3' and 5'-AGG GTG GGT AGT CAT TTG CAT AG-3' [25]. Real time PCR was carried out for 40 cycles using the iCycler (Bio-Rad) and data were evaluated using the iCycler software. Each cycle consisted of 95 °C for 15 sec, 60°C for 30 sec (except for osteocalcin which had an annealing temperature of 65 °C), and 72 °C for 30 sec. cDNA-free samples, a negative control, did not produce amplicons. Melting curve and gel analyses (sizing, isolation, and sequencing) were used to verify single products of the appropriate base pair size.

2.3.5 *Serum measurements*

Blood was collected at the time of harvest, allowed to clot at room temperature for 5 min, then centrifuged at 4000 rpm for 10 min. Serum was removed, frozen in liquid nitrogen, and stored at -80 °C. Serum went through no more than two freeze/thaw cycles. Serum TRAP5b and Osteocalcin were measured using a Mouse TRAP and OC assay kits (SB-TR103, Immunodiagnostic Systems Inc., Fountain Hills, AZ and BT-470, Biomedical Technologies Inc., Stoughton, MA respectively) according to the manufacturer's protocol.

2.3.6 *Bacterial strains and culture*

L. reuteri ATCC PTA 6475 was cultured under anaerobic conditions in deMan, Rogosa, Sharpe media (MRS, Difco) for 16– 18 h at 37 °C. On the following day, the overnight culture was sub-cultured into fresh MRS and grown until log phase (OD600=0.4). Cells are harvested by centrifugation at 4000 rpm for 10 min. Minimum Essential Medium (MEMα, Invitrogen) conditioned medium was generated by resuspending the bacterial pellet in pre- warmed MEMα and incubating with gentle shaking at 37°C for 3 h. Cells were harvested and the supernatant is separated from the bacterial cell pellet, pH neutralized, and filter-sterilized using PVDF membrane filters (0.22μm pore size, Millipore). An equivalent of OD600=1.0 was lyophilized for long-term storage at -80 °C.

2.3.7 *FACS analysis*

After the appropriate time points of *L. reuteri*/Ovx treatment, bone marrow cells were collected and cells were stained for various immune cell populations as described [26,27]. Stained cells were analyzed in Flow cytometry and gated for various populations using FlowJo software, as described before [28].

2.3.8 *Osteoclast generation and characterization*

For primary osteoclastogenesis assays, bone marrow cells were flushed from mouse femurs and plated at 900,000 cells per 24 well. Flushed cells were fed with αMEM(Invitrogen) containing 10% FBS (Atlanta Biologicals, Inc.) and were treated with 2 ng/ml RANKL (R&D Systems) and 30 ng/ml M-CSF (R&D Systems) to induce osteoclastogenesis. The bone marrow cells were allowed to grow undisturbed for 4 days at which point they were fed with the complete media above. Twenty-four hours later cells were stained for tartrate-resistant acid phosphatase (TRAP) (Sigma-Aldrich Co. LCC). Cells were examined by microscopy and photographed (five fields per well) and multinucleated cells that stained TRAP positive were counted and averaged per condition. RAW 264.7 cells, a murine macrophage cell line, were obtained from ATCC and maintained in phenol red-free MEMα and charcoal-stripped fetal bovine serum (Invitrogen) at 37°C with 5% CO2. In 12-well tissue culture plates (Costar), 100,000 cells/well were seeded. On the following day, cells were washed with PBS and then stimulated with RANKL (100 ng/ml) and M-CSF (10 ng/ml). At this time, lyophilized *L. reuteri* MEMα conditioned medium was re-solubilized in culture medium and added to the cells. The medium and *L. reuteri* MEMα conditioned medium were replaced on days 3 and 5. At day 6, cells were fixed and stained for tartrate-resistant acid phosphatase (TRAP) according to manufacturer's protocol (Sigma cat no. 387A). Multinucleated giant cells that stained for TRAP were considered osteoclasts.

2.3.9 *DNA preparation of tissue samples*

Intestinal tissue samples were transferred to Mo Bio Ultra Clean Fecal DNA Bead Tubes (MoBio) containing 360ml Buffer ATL (Qiagen) and homogenized for one minute in a a BioSpec Mini-Beadbeater. 40ml Proteinase K (Qiagen) was added and samples were incubated for 30 min at 55 °C, homogenized again for 1 min, and incubated at 55°C for an additional 30 min. DNA was extracted with the Qiagen DNeasy Blood and Tissue kit.

2.3.10 *PCR amplification for beta diversity analysis*

Bacterial 16S sequences spanning variable regions V4-V6 were amplified by PCR from intestinal DNA using barcoded V4-V6 primers designed by the Human Microbiome Project. 20ml reactions for each sample were prepared in triplicate and contained 0.75 units Accuprime High Fidelity Taq DNA polymerase (Invitrogen), 1X Accuprime PCR Buffer II (Invitrogen), 0.4mMprimers, and 400mgDNA.Reactions were performed in an Eppendorf Pro thermal cycler with 3 min at 94°C followed by 30 cycles of 94 °C for 30 sec, 60°C for 45 sec, 72°C for 2 min. Triplicate reactions were then pooled, purified using Agencourt AMPure XP magnetic beads (Beckman Coulter), and quantified using the QuantIt High Sensitivity DNA assay kit (Invitrogen).

2.3.11 *454 sequencing and analysis*

Sequencing was performed on a Roche 454 GS Junior Sequencer using Roche's GS Junior Titanium EmPCR Lib-L kit and Titanium Sequencing kit. Sequences were processed for analysis using the mothur software package version 1.21 [29] using the Schloss laboratory standard operating procedure available on the mothur Wiki website (http://www.mothur.org/wiki/). A total of 71,061 quality bacterial 16S sequences (median 3773 sequences per sample) were obtained from mouse jejunum samples and 82,903 sequences (median 3875 sequences per sample) were obtained from ileum samples. Of these sequences, 96.2% in jejunum/90% in ileum were classified as belonging to the Proteobacteria, Firmicutes, or Bacteroidetes phyla. Rare OTUs occurring 1 or 2 times across the data set were removed to minimize bias due to sequencing error. To minimize bias due to uneven sequencing depth across samples, randomly selected subsets of 600 sequences per sample in jejunum/1000 sequences per sample in ileum were generated in mothur to calculate operational taxonomic units (OTU) at 97% similarity. L. reuteri 6475 was not detected in the communities. Species richness measurements for Chao1 for each sample were calculated in mother on 12 independent subsamplings for each sample, averaged, and tested for statistically significant

differences between the experimental groups using analysis of variance (ANOVA) and Tukey's range test in the PAST software package (PAST: Paleontological Statistics Software Package for Education and Data Analysis. Palaeontologia Electronica 4(1): 9pp.). Beta diversity analysis was performed using mothur and PAST and visualized using PCoA plots generated in R (R Development Core Team, 2011). R: A language and environment for statistical computing. R Foundation for Statistical Computing, Vienna, Austria. ISBN 3-900051-07-0, URL http://www.R-project. org/). Taxonomic classification was performed using RDP Classifier [30]. SIMPER analyses in PAST and PCoA analyses in R were performed to identify OTUs that contributed to microbial community differences between the experimental groups.

2.3.12 *Statistical analysis*

All measurements are presented as the mean±SE or SD as noted. ANOVA was performed followed by post hoc analysis (Tukey) when results of ANOVA indicated significance ($\alpha < 0.05$).

2.4 *Results*

The effect of probiotic ingestion, specifically *L. reuteri* 6475, on ovariectomized (Ovx)-induced bone loss was examined in 12-week old Balb/c mice. One week after ovariectomy the mice were treated with *L. reuteri* 6475 or vehicle (broth) 3 times a week. After 4 weeks, microcomputed tomography was used to assess bone loss at two sites, femur and vertebrae. As expected, the trabecular bone of the Ovx mouse distal femur and L3 vertebrae displayed a bone volume loss (50% and 25%, respectively; Fig. 1B). *L. reuteri* treatment of Ovx mice, on the other hand, completely prevented femur and vertebral trabecular bone volume loss resulting in a BV/TV similar to control mice (Fig. 1B). Other trabecular parameters of the femoral and vertebral regions, which were negatively affected by Ovx (trabecular thickness, number, and spacing), were also protected by *L. reuteri* treatment (Tables 1 and 2). On the other hand,

femoral diaphysis cortical bone parameters did not display a large enough change to be significant in Ovx mice (Table 1). Treatment of sham-operated female mice had no effect on trabecular bone volume (Fig. 1C) consistent with our previous report [15].

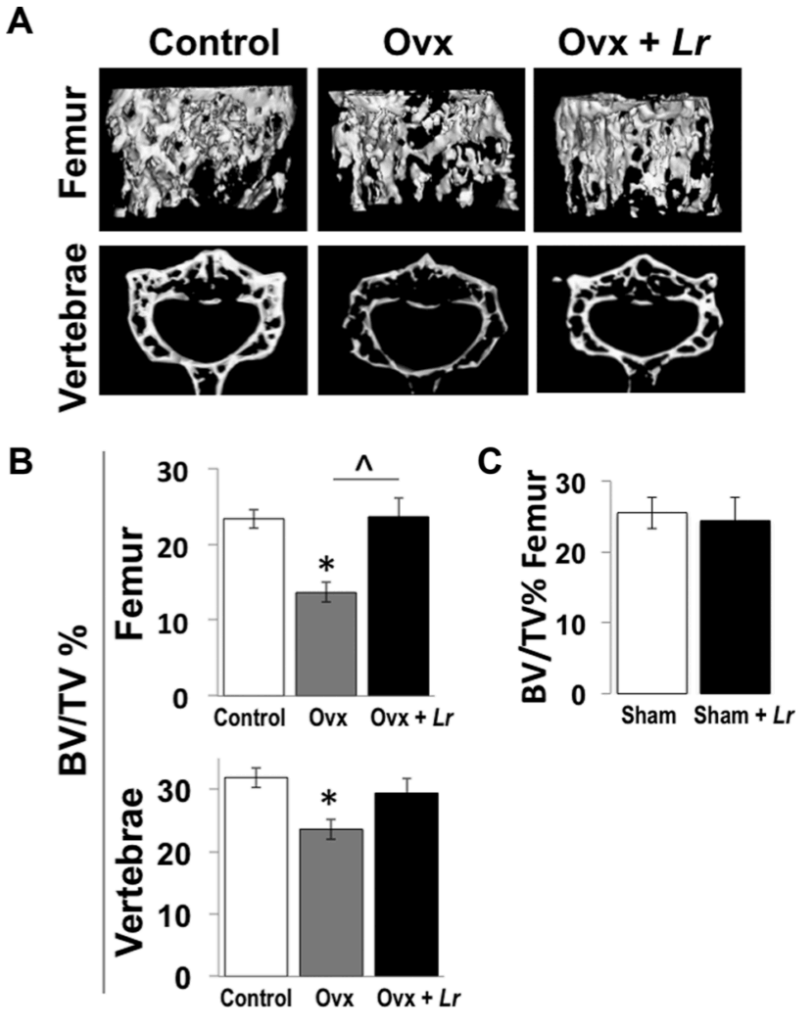

Figure 2.1. Ovariectomy (Ovx) mice treated with L. reuteri for 4 weeks display femur and vertebral trabecular bone volumes that are similar to ovary intact control mice.

Representative micro- computed tomography isosurface images (A) and percent bone volume fraction (BV/TV) quantitative pooled data (B, C) obtained from the trabecular bone region of the distal femur and L3 vertebrae of non-Ovx control (white bar), Ovx (gray bar), and Ovx + *L. reuteri* treated (black bar) mice (A, B) and from sham versus sham plus *L. reuteri* treatment (C).

Figure 2.1. (cont'd)

L. reuteri was given by gavage only as described in the methods. Values are averages ± standard error, n=8 per group, *P<0.05 compared to Non-Ovx, ^p<0.05 compared to Ovx as determined by one-way ANOVA followed by Tukey HSD.

Table 2.1. Femur bone parameters

	Non-Ovx	Ovx	Ovx+*Lr*
Trabecular			
BV/TV	23.3 ± 1.2	$13.6 \pm 1.3^{*}$	$23.6 \pm 2.5^{\wedge}$
BMD (mg/cc)	230 ± 6	$179 \pm 7^{*}$	$222 \pm 11^{\wedge}$
BMC (mg)	0.38 ± 0.02	$0.27 \pm 0.01^{*}$	$0.35 \pm 0.02^{\wedge}$
Tb. Th. (μm)	45.4 ± 1.2	$35.8 \pm 2.2^{*}$	41.3 ± 1.9
Tb. N. (1/mm)	5.14 ± 0.24	3.80 ± 0.29	$5.66 \pm 0.50^{\wedge}$
Tb. Sp. (μm)	152 ± 10	$234 \pm 20^{*}$	$145 \pm 17^{\wedge}$
Cortical			
Tt. Ar. (mm^2)	1.53 ± 0.03	1.46 ± 0.02	1.49 ± 0.04
Ct. Ar. (mm^2)	0.97 ± 0.03	0.88 ± 0.01	0.93 ± 0.03
Ma. Ar. (mm^2)	056 ± 0.01	0.58 ± 0.01	0.56 ± 0.01
Ct Ar/Tt. Ar.	0.63 ± 0.01	0.60 ± 0.01	0.62 ± 0.01
Thickness (mm)	0.27 ± 0.01	0.25 ± 0.01	0.27 ± 0.01
Inner P. (mm)	2.83 ± 0.02	2.86 ± 0.04	2.80 ± 0.02
Outer P. (mm)	4.54 ± 0.04	4.44 ± 0.04	4.47 ± 0.06

Femur distal trabecular bone and diaphyseal cortical bone parameters. Non-Ovx, intact mice; Ovx, ovariectomized; Ovx+*L.r.*, Ovx mice treated with *Lactobacillus reuteri*. BV/TV, bone volume fraction; BMD, bone mineral density; BMC, bone mineral content; Tb. Th., trabecular thickness; Tb. N., trabecular number; Tb. Sp., trabecular spacing; Tt. Ar., total area; Ct. Ar., cortical area; Ma. Ar., marrow area; Ct. Ar./Tt. Ar., cortical area fraction; Inner P., inner perimeter; Outer P., outer perimeter. Data are averages ± standard error, n = 8 per group.
$^{*}P < 0.05$ to Non-Ovx, $^{\wedge}P < 0.05$ to Ovx by one-way ANOVA followed by Tukey HSD.

To identify the effect of *L. reuteri* 6475 treatment on bone remodeling, we examined both osteoblast and osteoclast parameters in 3-week post-Ovx mice. We identified that 2- weeks of *L. reuteri* treatment was able to prevent Ovx-induced increases in bone mRNA levels of RANKL, an osteoclastogenesis activator cytokine (Fig. 2A). Probiotic treatment also reduced bone TRAP5 mRNA levels, an osteoclast marker (Fig. 2A). Serum TRAP5 levels were modestly decreased in the *L. reuteri*-treated Ovx mice (data not shown). To further assess if osteoclastogenesis is altered, femur marrow cells were obtained from mice in each group and cultured to stimulate osteoclast differentiation. While cells obtained from Ovx mice displayed increased osteoclastogenesis, cells obtained from Ovx mice treated with *L. reuteri* were similar to controls (Fig. 2B). Taken together, these results suggest that *L. reuteri* suppresses osteoclast activity in this mouse model. We did not observe differences in any osteoblast parameters among conditions after treatment (Fig. 2C).

Table 2.2. Vertebrae bone parameters

	Non-Ovx	Ovx	Ovx+*Lr*
Trabecular			
BMD (mg/cc)	218 ± 8	$182 \pm 8^{*}$	204 ± 10
BMC (mg)	0.36 ± 0.01	$0.29 \pm 0.01^{*}$	0.36 ± 0.01
Tb. N. (1/mm)	6.72 ± 0.19	6.24 ± 0.31	7.17 ± 0.35
Tb.Th. (μm)	47.4 ± 1.81	$37.5 \pm 1.00^{*}$	$40.8 \pm 1.48^{*}$
Tb. Sp. (μm)	102 ± 5	126 ± 9	100 ± 7

Vertebrae distal trabecular bone parameters. Non-Ovx, intact mice; Ovx, ovariectomized; Ovx+*L.r.*, Ovx mice treated with *Lactobacillus reuteri*. BV/TV, bone volume fraction; BMD, bone mineral density; BMC, bone mineral content; Tb. Th., trabecular thickness; Tb. N., trabecular number; Tb. Sp., trabecular spacing; Data are averages ± standard error, n = 8 per group.
$^{*}P < 0.05$ to Non-Ovx by one-way ANOVA followed by Tukey HSD.

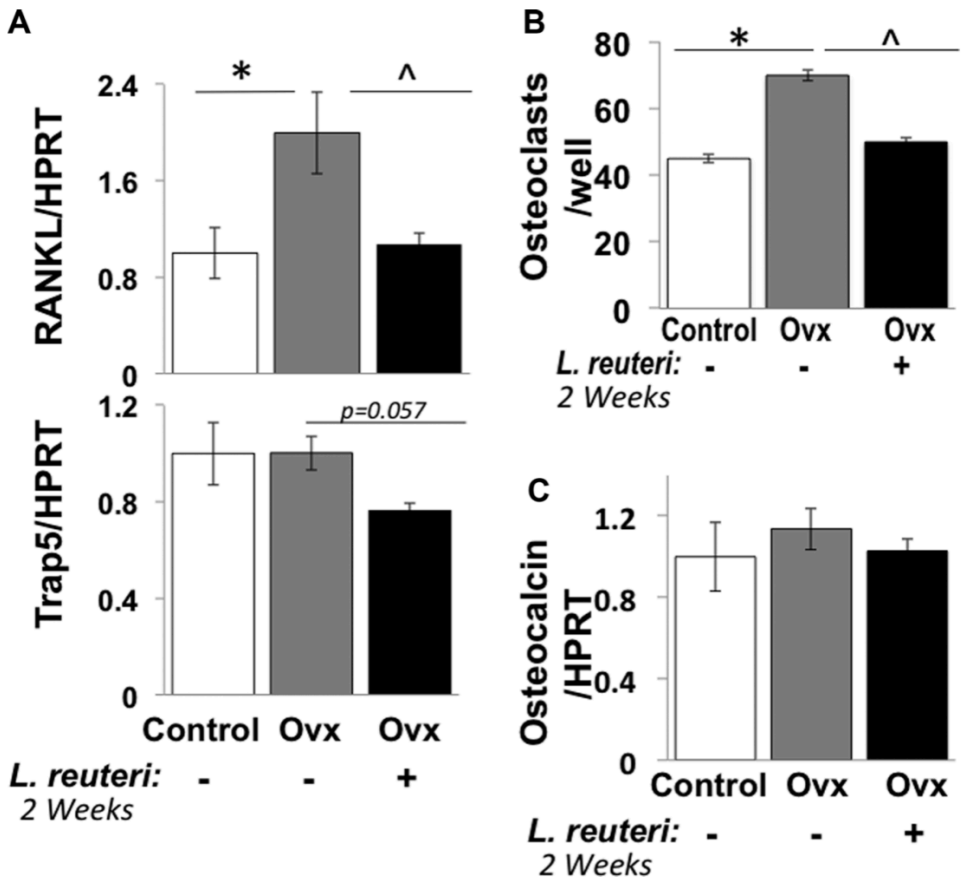

Figure 2.2. L. reuteri treatment prevents Ovx-induced increases in RANKL and bone marrow osteoclastogenesis after 2 weeks of probiotic treatment.

Conditions are non-Ovx, intact mice (white bar); Ovx, ovariectomized mice (gray bar); Ovx + Lr, Ovx mice gavaged with L. reuteri for 2 weeks (black bar). (A) Levels of TRAP5 and RANKL RNA in whole tibia bone. Levels were expressed relative to HPRT, a non-modulated house-keeping gene. (B) Harvested mouse bone marrow cells from the mice above were cultured in vitro with RANKL and M-CSF and the number of osteoclasts counted per well. (C) Osteocalcin mRNA levels were measured in whole tibia bone and expressed relative to HPRT. Data values are average ± standard error, n>8 per group, *P<0.05 to Non-Ovx, ^P<0.05 to Ovx by one-way ANOVA followed by Tukey HSD.

We further examined dynamic and static osteoblast parameters at the 4-week *L. reuteri* treatment time point (in mice more than 4 months old at this time). However, at this point we did not observe significant differences between control and Ovx mice or *L. reuteri*-treated Ovx mice. Specifically, the level of bone formation rate, osteoblast surface or tibial osteocalcin and osterix mRNA did not differ between any of the three conditions (Fig. 3). Similarly, osteoclast parameter markers did not differ among the groups at this time point (Fig. 3). This is likely due to changes in osteoclastogenesis having already occurred by 5 weeks after ovariectomy. However, note that tibial RANKL RNA levels displayed a trend to increase with Ovx and a decrease in Ovx mice treated with *L. reuteri*, which is consistent with the 2-week treatment time point.

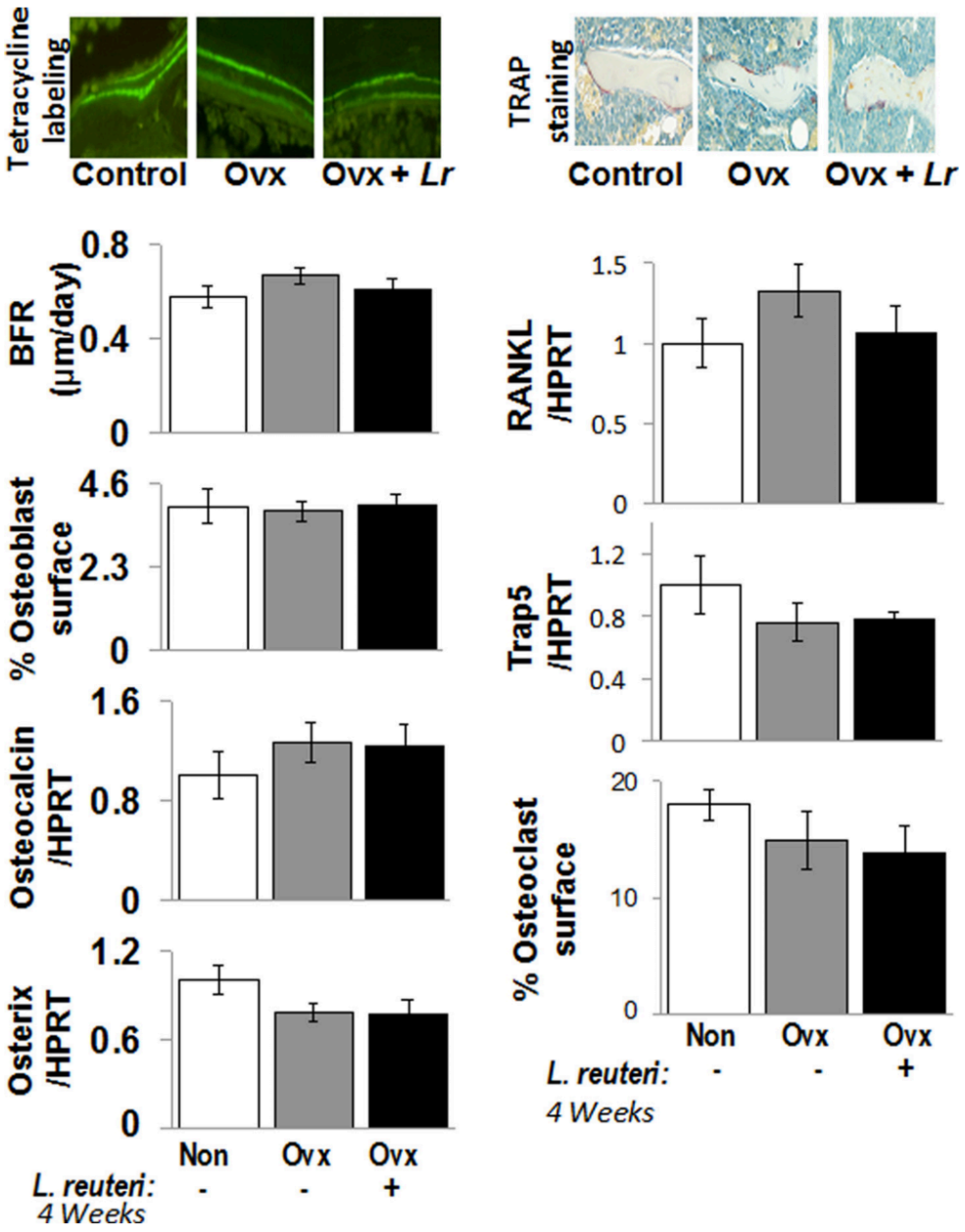

Figure 2.3. Osteoclast and osteoblast markers don't show significant changes in response to Ovx +/- L. reuteri treatment at 4 weeks.

Top left: Representative fluorescent microscope photographs depicting the two pulses of calcein incorporation. The space between the two bands represents the mineral apposition rate (MAR). Top right: Representative microscope photographs of TRAP stained femur metaphyseal sections. Osteoclasts stain purple. Left Bar Graphs: Bone formation rate (BFR), osteoblast

Figure 2.3. (cont'd)

surface/total trabecular surface, and tibial RNA levels of osteocalcin and osterix (relative to HPRT an unaltered housekeeping gene). Right Bar Graphs: Tibial RNA levels of RANKL and Trap5 relative to HPRT, as well as osteoclast surface/total trabecular surface. Conditions are non-Ovx (white); Ovx, ovariectomized mice (gray); and Ovx + Lr, Ovx mice gavaged with Lactobacillus reuteri for 4 weeks (black). Values are averages ± standard error, n=8 per group, *P<0.05 to Non-Ovx by one-way ANOVA followed by Tukey HSD.

Utilizing these animals harvested after treatment with *L. reuteri* for 2 weeks we examined the influence of *L. reuteri* on bone marrow CD4 T cells, which are known to affect osteoclast activity [5]. As shown in Figure 4, there was a significant increase in the percentage of CD4 T-cells in Ovx mice compared to controls. Treatment with *L. reuteri* caused significant decrease in CD4 T-lymphocytes (compared to Ovx mice). These changes suggest that *L. reuteri* 6475 could be reducing osteoclastogenesis through suppression of osteoclast inducing signals from T-cells.

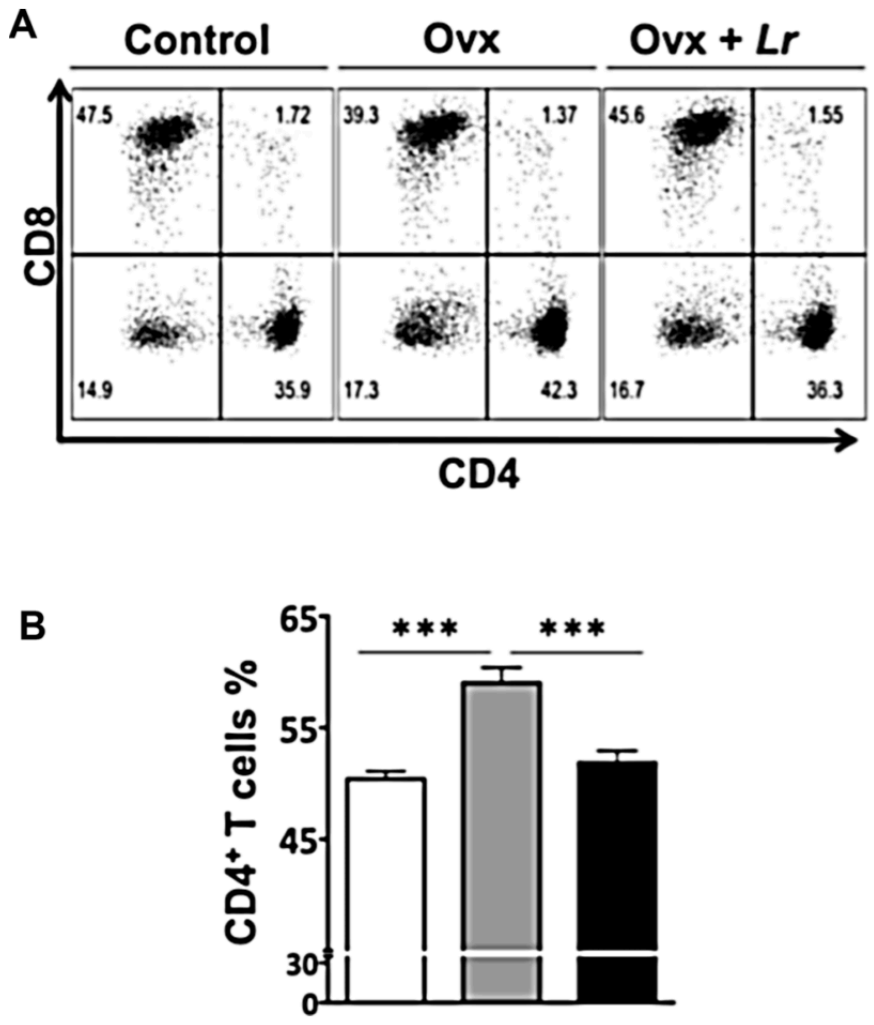

Figure 2.4. FACS analysis of bone marrow cells.

Control, OVX and OVX+LR mice were treated as described and femurs collected during euthanasia at 2 weeks after treatment. Femurs were flushed and bone marrow cells were collected, processed and stained for cell surface markers for identifying the various immune cells as described in the methods. CD4 T-lymphocytes were identified as CD3/CD4 T-cells; Dot plots are shown at the top and cumulative data presented in graph in the bottom. In the dot plots, the numbers in the quadrants indicate the percentage of cells. N=8 for each condition; ***P<0.001 as determined by ANOVA followed by Bonferroni.

Because *L. reuteri* could directly affect the intestinal microbiota, we assessed alterations in intestinal microbial diversity since the microbiota could contribute to changes in intestinal function, immune function, and possibly bone density [16]. Samples from *L. reuteri* 6475-treated mice had significantly higher measurements of richness than those from non-treated mice, including Chao 1 estimate values (ANOVA $P<0.0023$) and ACE richness values (ANOVA $P<0.0014$). Analysis of the jejunum samples using diversity metrics that utilize only species richness (Jaccard) or richness and evenness (Bray-Curtis) showed statistically significant separation between the three communities, non Oxx, Ovx, and Ovx + *L. reuteri* (Bray-Curtis $R=0.34$, $P<0.018$, Jaccard $R=0.42$, $P<0.0004$; Fig. 5). Pairwise comparisons demonstrated that although Ovx did not significantly alter microbial community structure compared to non-Ovx animals; treating animals with L. reuteri resulted in a significant change in jejunal communities compared with wild-type and Ovx animals (Table 3, Fig. 5). We also identified operational taxonomic units (OTUs) that were associated with differences between these communities and found that several OTUs classified as Clostridiales were significantly more abundant in *L. reuteri*- treated animals than in non-treated animals. Conversely, we found that several OTUs classified as Bacteriodales trended toward being decreased in *L. reuteri*-treated Ovx animals compared to untreated Ovx and non-Ovx controls. Similar changes in microbial diversity were observed in the ileum (data not shown). Thus, we have uncovered profound shifts in specific members in microbial communities that are associated with the suppression of bone loss by *L. reuteri* 6475.

Table 2.3. Beta diversity analysis

Distance metric	Comparison	R Value (*P value*)
Bray-Curtis	wtbroth-ovxbroth-ovxlacto	0.3393 (*0.0176*)*
	wtbroth-ovxbroth	0.05382 (*0.3106*)
	wtbroth-ovxlacto	0.5979 (*0.0246*)*
	ovxbroth-ovxlacto	0.3448 (*0.0629*)
Jaccard	wtbroth-ovxbroth-ovxlacto	0.5344 (*0.0005*)*
	wtbroth-ovxbroth	0.1736 (*0.2751*)
	wtbroth-ovxlacto	0.8094 (*0.0076*)*
	ovxbroth-ovxlacto	0.4938 (*0.0100*)*

Diversity in jejunal tissue was assessed and analyzed by ANOSIM. Subsampling cutoff = 374 sequences.
*Indicates statistical significance.

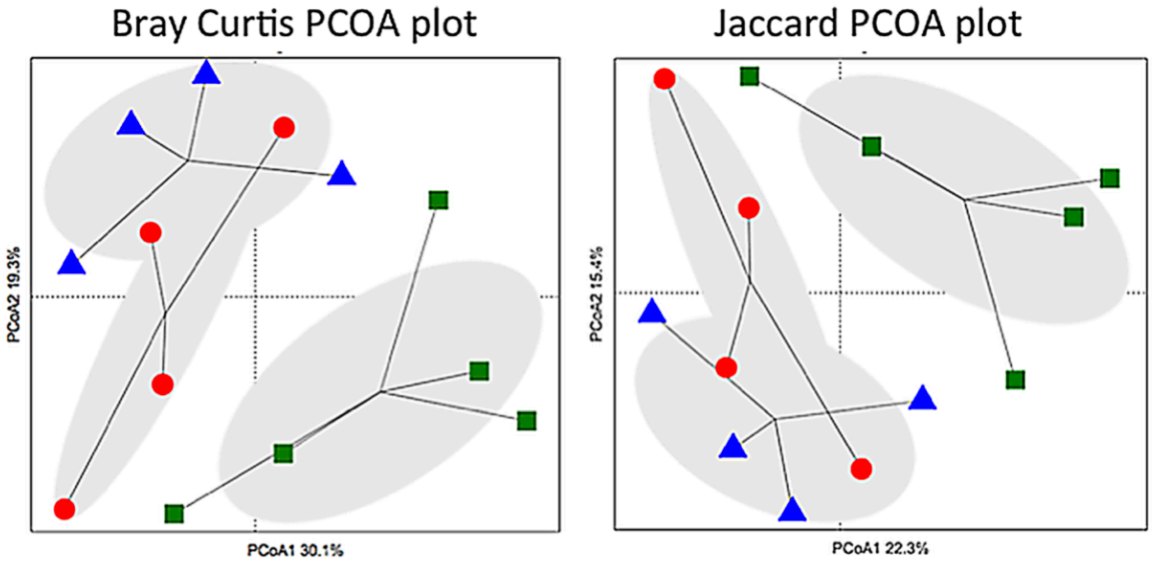

Figure 2.5. Two-dimensional projection of the principal coordinate analysis (PCoA) of bacterial 16S sequences from mouse jejunum samples along the first two principal axes.

Left. PCoA was calculated using the Bray–Curtis similarity measures (coordinate axis 1 percent variation explained = 30.1%, coordinate axis 2 =19.3%). Right. PCoA was calculated using the

Figure 2.5. (cont'd)

Jaccard similarity measure (coordinate axis 1 percent variation explained = 22.3%, coordinate axis 2 = 15.4%). Non-OVX mice (Δ), OVX mice (O), *L.reuteri*-treated OVX mice (■).

Finally, to address the possibility that *L. reuteri* 6475 could be directly affecting bone resorption by producing a factor that affects osteoclastogenesis, we induced osteoclast formation in a murine macrophage cell line in the presence or absence of *L. reuteri* 6475 conditioned medium. While control cultures and vehicle-treated cultures displayed active osteoclastogenesis marked by the presence of many large multinucleated, TRAP5 positive cells, the presence of *L. reuteri* supernatant in the culture prevented RANKL and M-CSF induced osteoclastogenesis by 70% (Fig. 6). This indicates that *L. reuteri* 6475 secretes a soluble factor capable of directly suppressing osteoclast formation *in vitro*.

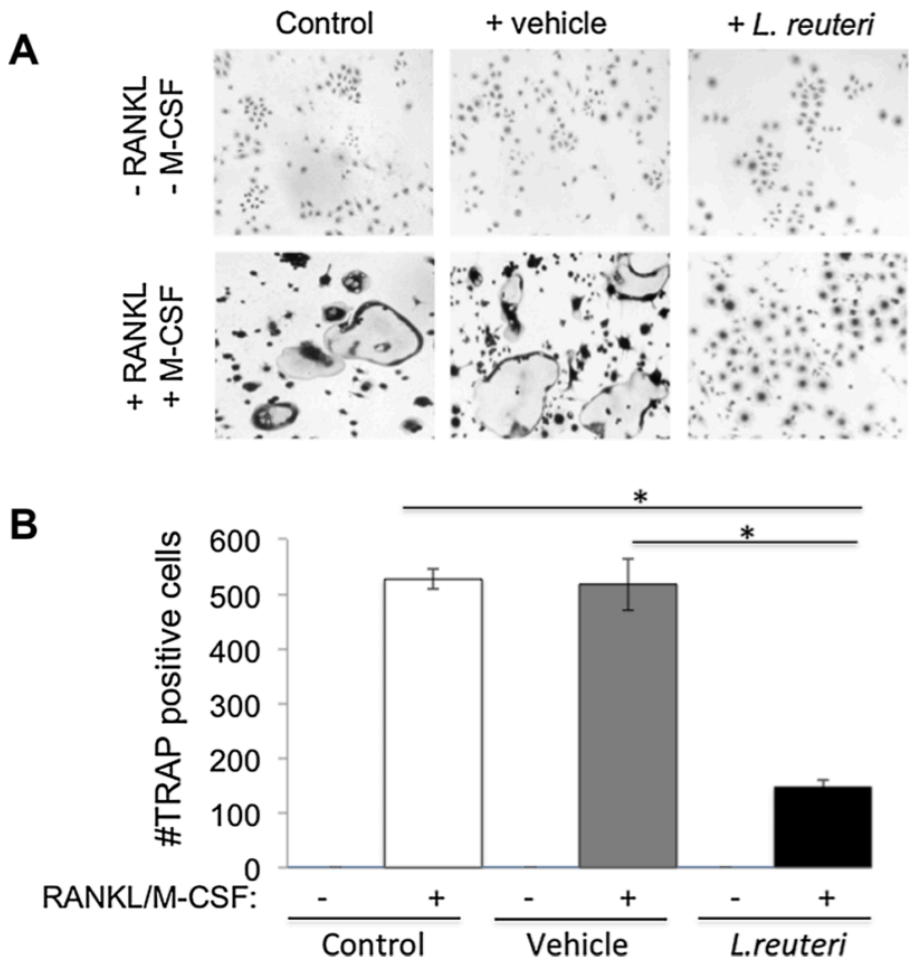

Figure 2.6. Effect of L. reuteri secreted factors on osteoclast differentiation in RAW 264.7 cells.

(A) Representative images of TRAPþ multinuclear giant cells at 7 days after RANKL and M-CSF treatment. (a) Cells only (Negative control) (b) RANKL and M-CSF (Positive control) (c) MEM-α (d) MEM-α plus RANKL and M-CSF (e) L. reuteri conditioned MEM-α (LR CM) (f) LR CM plus RANKL and M-CSF. (B) Quantification of TRAPþ multinuclear (>3 nuclei/cell) giant cells at 7 days after treatment with RANKL (100 ng/ml) and M-CSF (10 ng/ml) per visual field under light microscopy. Values are averages ± standard deviations. Conditions were done in triplicate and the entire experiment repeated 4 times. *P<0.05 by Students t-test.

2.5 *Discussion*

Probiotics are increasingly being used worldwide to treat health problems. Studies indicate that probiotics may be effective in the treatment of some gastrointestinal diseases such as colic, irritable bowel, and inflammatory bowel disease (Thomas and Greer, 2010; Whelan and Quigley, 2013). In addition, probiotics have also showed promise in ameliorating other ailments that are distal to the gut, including eczema, asthma, and allergies [31]. Our studies demonstrate that oral administration of the candidate probiotic *L. reuteri* 6475 can enhance bone health under estrogen deficiency conditions. Benefits were observed in both the appendicular and axial skeleton, indicating a broad ranging bone effect. Furthermore, *L. reuteri* 6475 treatment of Ovx mice restored all trabecular bone parameters.

Previous work has indicated that the intestinal microbiota may impact bone health. Rodents and birds treated with prebiotics, such as inulin, oligofructose, and galactooligosaccharides, can also display increased bone density [9–11,32]. For example, galactooligosaccharide intake resulted in a dose dependent increase in rat femur trabecular bone volume [11]. However, inulin treatment had no effect on bone parameters in pigs [33]. Interestingly, some studies demonstrate that prebiotic treatment can increase the presence of bifidobacteria in the stool [11], but the direct role of this bacterial genus and whether osteoblast or osteoclast activity was affected was not determined. A few studies have examined the role of probiotic treatment on bone and show increased bone density, but also do not show how treatment affects bone remodeling [13,14].

Does *L. reuteri* 6475 affect anabolic and/or catabolic bone remodeling pathways? Identifying changes in osteoclast and osteoblast activities in our study proved somewhat difficult. We did not observe large differences in bone remodeling parameters between non-Ovx and Ovx mice at 2 or 4 weeks of age. This may be due to the use of adult mice (which we felt was most

applicable to estrogen-deficient women) rather than preadolescent mice, which have a faster rate of bone growth/ remodeling and may more readily display changes (but are also growing). However, one common finding was that *L. reuteri* 6475 reduced Ovx mouse Trap5 and RANKL bone RNA levels at 2 and 4 weeks post-treatment. It may be that RNA levels provide the greatest detection sensitivity in our model. Further *in vitro* studies will help delineate whether *L. reuteri* affects RANKL production from T-cells or osteoblasts or both. Alternatively, *L. reuteri* might decrease the number of osteoclastogenic T-cells in the marrow. Consistent with this, marrow CD4 T cells, which have been shown to be important mediators of osteoclastogenesis in estrogen deficiency [34], were significantly decreased in the presence of *L. reuteri* 6475. At least two mechanisms have been proposed as to how T-cells might mediate OVX-induced bone loss. While one involves direct activation of T-cells and production of TNFα, the other involves activation of stromal cells by T-cells to produce osteoclastogenic cytokines leading to enhanced bone loss. Future studies will determine whether a specific TNFα- producing T-cell population is also decreased by *L. reuteri* in Ovx mice. Compared to the changes in CD4 T cells, CD8 T cells decreased in Ovx mice and increased in response to probiotic treatment. Future studies will examine whether other immune cell populations (relevant to osteoclastogenesis) in the bone marrow and other systemic sites are also modulated by probiotic treatment and how these changes affect bone health.

Consistent with these in vivo results, our in vitro osteoclastogenesis experiments demonstrate a potential direct role of *L. reuteri* 6475 in decreasing osteoclast activity because the medium of L. reuteri cultures is capable of suppressing osteoclast differentiation in a cell culture model of osteoclastogenesis. This cannot be attributed to any pH effect since the medium was neutralized prior to treating the cells. *L. reuteri* is known to secrete a variety of factors including the antimicrobial reuterin and molecules that reduce TNFα activity in vitro [20]. The latter could be a key factor in the response that we see in vitro since TNFα stimulates bone resorption [35]. Such

a factor could also cross the gut epithelium and affect local, systemic, and bone marrow immune responses and/or have direct effects on osteoclasts. In addition, we have reported that *L. reuteri* ATCC PTA 6475 produces histamine, which contributes to one of the immunomodulatory activities exhibited by *L. reuteri* ATCC PTA 6475. Specifically, *L. reuteri* production of histamine can suppress TNFα signaling through modulation of PKA and ERK signaling [21] providing a mechanistic link between this probiotic, TNFα signaling suppression and the prevention of Ovx-induced bone loss. Future mechanistic studies deleting the expression of these molecules such as reuterin or histamine production will test their role in *L. reuteri*'s bone benefits. Regardless of the mechanism, the fact that markers of osteoclastogenesis as well as cells important in osteoclastogenesis, are modulated by *L. reuteri* 6475 demonstrates important role for probiotics in this estrogen-deficiency model of bone loss.

Interestingly, we did not observe any *L. reuteri*-induced change in osteoblast activity/markers at the time points we studied. This is in contrast to studies in male mice (bred under pathogen free conditions), which display an anabolic response to L. reuteri 6475 that is characterized by increased bone formation rate and osteoblast markers [15]. It may be that we were not at the optimal time point to detect a bone formation response in the treated Ovx mice. A variety of factors could contribute to gender differences including different gut microbiomes, bone remodeling rates, immunoresponsiveness and/or composition of marrow immune cells that can affect bone formation and resorption [5].

One possible indirect mechanism by which *L. reuteri* 6475 could impact the suppression of bone loss in Ovx animals is by alteration of the immune response by changing intestinal microbial communities found in Ovx animals. Dysbiosis of gut communities can promote or exacerbate diseases including obesity, diabetes, and IBD [36–40] while alterations in the host immune system can also modify the structure and function of the intestinal microbiota to promote disease.

Interestingly, bone density can be enhanced by the absence of luminal bacteria [16]. This underlies that the gut microbiota (greater than 1000 species composition) comprises a community of microbes that promotes health, but that there is a cost to having these microbes in such close association with us. Given that the absence of gut bacteria is beneficial to bone, gut bacteria in a standard mouse likely has an overall negative effect on bone health that may be overcome by ingestion of *L. reuteri* 6475. Consistent with this we found significant changes in microbial communities upon *L. reuteri* 6475 treatment of Ovx animals in the small intestine when compared to Ovx and non-Ovx control communities. Interestingly, several OTUs that were classified as Clostridiales are the main groups of bacteria that are driving the separation of the *L. reuteri*-treated Ovx communities from the other two groups. Interestingly, several murine clostridia have been implicated in the regulation of the immune system by driving the upregulation of colonic Treg cells [41], and thus an increase in this bacterial class may be directly linked to anti-inflammatory effects in the bone. At this point, these are associations between microbial communities and bone health and we are actively pursuing if the microbiota plays a direct role in Ovx mediated bone loss.

Taken together, *L. reuteri* 6475 treatment can benefit bone health in estrogen deficient mice. We demonstrate a role for this probiotic in the suppression of osteoclast activity, which is known to increase with estrogen deficiency. The idea of a natural product for the treatment of menopause-induced osteoporosis is appealing since existing therapies have side effects. Future studies looking at the long term impact of probiotic treatment on gut and bone health, as well as probiotic treatment after well established osteopenia, will be important for providing clinically relevant insight into treating menopause induced bone loss. Importantly, our studies also warrant future mechanistic research in this exciting area utilizing gastrointestinal health to treat bone disease.

Acknowledgments The authors thank the Investigative Histology Laboratory in the Department of Physiology, Division of Human Pathology and the Biomedical Imaging Center at Michigan State University for their assistance with histology and imaging, respectively. These studies were supported by funding from the National Institute of Health, National Center for Complementary and Alternative Medicine (R21-RAT005472 and 1RO1AT007695), Biogaia, and by a Strategic Partnership Grant from Michigan State University. All authors state that they have no conflict of interest.

BIBLIOGRAPHY

BIBLIOGRAPHY

1. Manolagas, S. C. From estrogen-centric to aging and oxidative stress: A revised perspective of the pathogenesis of osteoporosis. *Endocr. Rev.* **31,** 266–300 (2010).

2. McNamara, L. M. Perspective on post-menopausal osteoporosis: establishing an interdisciplinary understanding of the sequence of events from the molecular level to whole bone fractures. *J R Soc Interface* **7,** 353–372 (2010).

3. Riggs, B. L. Role of the vitamin D-endocrine system in the pathophysiology of postmenopausal osteoporosis. *J. Cell. Biochem.* **88,** 209–215 (2003).

4. Bouxsein, M. L. *et al.* Ovariectomy-induced bone loss varies among inbred strains of mice. *J. Bone Miner. Res.* **20,** 1085–1092 (2005).

5. Li, J.-Y. *et al.* Ovariectomy disregulates osteoblast and osteoclast formation through the T-cell receptor CD40 ligand. *Proc. Natl. Acad. Sci. U. S. A.* **108,** 768–773 (2011).

6. Jilka, R. L. *et al.* Loss of estrogen upregulates osteoblastogenesis in the murine bone marrow evidence for autonomy from factors released during bone resorption. *J. Clin. Invest.* **101,** 1942–1950 (1998).

7. Bäckhed, F. *et al.* Defining a healthy human gut microbiome: current concepts, future directions, and clinical applications. *Cell Host Microbe* **12,** 611–622 (2012).

8. Lemon, K. P., Armitage, G. C., Relman, D. A. & Fischbach, M. A. Microbiota-Targeted Therapies : An Ecological Perspective. **4,** (2012).

9. Abrams, S. A. *et al.* A combination of prebiotic short- and long-chain inulin-type fructans enhances calcium absorption and bone mineralization in young adolescents. *Am. J. Clin. Nutr.* **82,** 471–476 (2005).

10. Coxam, V. Current Data with Inulin-Type Fructans and Calcium, Targeting Bone Health in Adults. *J. Nutr.* **137,** 2527S–2533 (2007).

11. Weaver, C. M. *et al.* Galactooligosaccharides Improve Mineral Absorption and Bone Properties in Growing Rats through Gut Fermentation - Journal of Agricultural and Food Chemistry (ACS Publications). 6501–6510 (2011). at <http://pubs.acs.org/doi/abs/10.1021/jf2009777>

12. Scholz-Ahrens, K. E. & Schrezenmeir, J. Inulin and oligofructose and mineral metabolism: the evidence from animal trials. *J. Nutr.* **137,** 2513S–2523S (2007).

13. Mutuş, R. *et al.* The effect of dietary probiotic supplementation on tibial bone characteristics and strength in broilers. *Poult. Sci.* **85,** 1621–1625 (2006).

14. Kimoto-Nira, H. *et al.* Anti-ageing effect of a lactococcal strain: analysis using senescence-accelerated mice. *Br. J. Nutr.* **98,** 1178–1186 (2007).

15. Mccabe, L. R., Irwin, R., Schaefer, L. & Britton, R. A. Probiotic use decreases intestinal inflammation and increases bone density in healthy male but not female mice. *J. Cell. Physiol.* **228,** 1793–1798 (2013).

16. Sjögren, K. *et al.* The gut microbiota regulates bone mass in mice. *J. Bone Miner. Res.* **27,** 1357–1367 (2012).

17. Tubelius, P., Stan, V. & Zachrisson, A. Increasing work-place healthiness with the probiotic Lactobacillus reuteri: a randomised, double-blind placebo-controlled study. *Environ. Health* **4,** 25 (2005).

18. Weizman, Z., Asli, G. & Alsheikh, A. Effect of a probiotic infant formula on infections in child care centers: comparison of two probiotic agents. *Pediatrics* **115,** 5–9 (2005).

19. Valeur, N., Engel, P., Carbajal, N., Connolly, E. & Ladefoged, K. Colonization and Immunomodulation by Lactobacillus reuteri ATCC 55730 in the Human Gastrointestinal Tract Colonization and Immunomodulation by Lactobacillus reuteri ATCC 55730 in the Human Gastrointestinal Tract. *Society* **70,** 1176–1181 (2004).

20. Thomas, C. M. & Versalovic, J. Probiotics-host communication: Modulation of signaling pathways in the intestine. *Gut Microbes* **1,** 148–163 (2010).

21. Thomas, C. M. *et al.* Histamine derived from probiotic lactobacillus reuteri suppresses tnf via modulation of pka and erk signaling. *PLoS One* **7,** (2012).

22. Harris, L., Senagore, P., Young, V. B. & McCabe, L. R. Inflammatory bowel disease causes reversible suppression of osteoblast and chondrocyte function in mice. *Am. J. Physiol. Gastrointest. Liver Physiol.* **296,** G1020–G1029 (2009).

23. Zhao, S., Zhang, Y. K. Y., Harris, S., Ahuja, S. S. & Bonewald, L. F. MLO-Y4 osteocyte-like cells support osteoclast formation and activation. *J. Bone Miner. Res.* **17,** 2068–2079 (2002).

24. Motyl, K. & Mccabe, L. R. Streptozotocin , Type I Diabetes Severity and Bone. **11,** 296–315

25. Jadlowiec, J. *et al.* Phosphophoryn regulates the gene expression and differentiation of NIH3T3, MC3T3-E1, and human mesenchymal stem cells via the integrin/MAPK signaling pathway. *J. Biol. Chem.* **279,** 53323–53330 (2004).

26. Fukata, M. *et al.* The myeloid differentiation factor 88 (MyD88) is required for CD4+ T cell effector function in a murine model of inflammatory bowel disease. *J. Immunol.* **180,** 1886–1894 (2008).

27. Patial, S. *et al.* G-protein coupled receptor kinase 5 mediates lipopolysaccharide-induced NF??B activation in primary macrophages and modulates inflammation in vivo in mice. *J. Cell. Physiol.* **226,** 1323–1333 (2011).

28. Lee, T. *et al.* β-Arrestin-1 deficiency protects mice from experimental colitis. *Am. J. Pathol.* **182,** 1114–23 (2013).

29. Schloss, P. D. *et al.* Introducing mothur: Open-source, platform-independent, community-supported software for describing and comparing microbial communities. *Appl. Environ. Microbiol.* **75,** 7537–7541 (2009).

30. Wang, Q., Garrity, G. M., Tiedje, J. M. & Cole, J. R. Na??ve Bayesian classifier for rapid assignment of rRNA sequences into the new bacterial taxonomy. *Appl. Environ. Microbiol.* **73,** 5261–5267 (2007).

31. Yoo, J., Tcheurekdjian, H., Lynch, S. V, Cabana, M. & Boushey, H. a. Microbial manipulation of immune function for asthma prevention: inferences from clinical trials. *Proc. Am. Thorac. Soc.* **4,** 277–282 (2007).

32. Scholz-Ahrens, K. E. *et al.* Prebiotics, probiotics, and synbiotics affect mineral absorption, bone mineral content, and bone structure. *J. Nutr.* **137,** 838S–46S (2007).

33. Jolliff, J. S. & Mahan, D. C. Effect of dietary inulin and phytase on mineral digestibility and tissue retention in weanling and growing swine. *J. Anim. Sci.* **90,** 3012–3022 (2012).

34. Pacifici, R. Role of T cells in ovariectomy induced bone loss-revisited. *J. Bone Miner. Res.* **27,** 231–239 (2012).

35. Teitelbaum, S. L. Osteoclasts: what do they do and how do they do it? *Am J Pathol* **170,** 427–435 (2007).

36. Kühbacher, T. *et al.* Bacterial and fungal microbiota in relation to probiotic therapy (VSL#3) in pouchitis. *Gut* **55,** 833–841 (2006).

37. Oakley, B. B., Fiedler, T. L., Marrazzo, J. M. & Fredricks, D. N. Diversity of human vaginal bacterial communities and associations with clinically defined bacterial vaginosis. *Appl. Environ. Microbiol.* **74,** 4898–4909 (2008).

38. Sartor, R. B. Microbial Influences in Inflammatory Bowel Diseases. *Gastroenterology* **134,** 577–594 (2008).

39. Vaarala, O., Atkinson, M. A. & Neu, J. The 'perfect storm' for type 1 diabetes: The complex interplay between intestinal microbiota, gut permeability, and mucosal immunity. *Diabetes* **57,** 2555–2562 (2008).

40. Wen, L. *et al.* Innate immunity and intestinal microbiota in the development of Type 1 diabetes. *Nature* **455,** 1109–1113 (2008).

41. Atarashi, K. *et al.* Induction of Colonic Regulatory T Cells. *Science (80-.).* **331,** 337–342 (2011).

CHAPTER 3. CHARACTERIZATION OF THE SUPPRESSION OF OSTEOCLASTOGENESIS BY *LACTOBACILLUS REUTERI*

3.1 *Introduction*

Bone is a dynamic organ that undergoes constant remodeling during all stages of life. Physiologic bone remodeling requires the concerted action by two cell types, osteoclasts and osteoblasts, which are responsible for bone resorption and bone formation, respectively. Osteoclasts are derived from a hematopoietic stem cell lineage. During differentiation, mononuclear progenitors from a monocyte lineage fuse together and maturate over time to form giant, multinucleated cells [1]. These giant cells dock onto a targeted bone site and facilitates its breakdown through the secretion of acid and different enzymes. At the same remodeling site, osteoblasts that originate from a mesenchymal stem cell lineage, participate in the deposition of collagen and minerals (Ca^{2+}, PO_4^{3-}) that make up the bone matrix. Often times, the perturbation of this cellular process contributes greatly in the underlying pathogenesis of bone loss for various chronic inflammatory diseases [2–4]. For the example of osteoporosis mediated by estrogen deficiency, increased inflammation (i.e. TNF-α, IL-1, IL-6) and the activation of immune cells promote the differentiation and formation of osteoclasts [5–10]. This increase in osteoclastogenesis creates an imbalance favoring bone resorption in comparison to bone formation and leads to subsequent bone loss. As a result, the modulation of this pathway has been the focus of many studies aimed at the understanding and development of novel therapeutics to treat osteoporosis.

Studies on the potential use of probiotics, defined as live microorganisms that confer health benefits when consumed according to the Food and Agriculture Organization (FAO) and World Health Organization (WHO), for the treatment of bone diseases, have increased recently [11]. The efficacy of different probiotics on improving bone health could be demonstrated in various animal models [12–20]. However, the mechanisms by which probiotics impact bone health have yet to be elucidated.

In our previous studies, we show that OVX mice treated with the immunomodulatory probiotic *Lactobacillus reuteri* 6475 (*L. reuteri*) had decreased osteoclast formation from bone marrow outgrowth studies [18]. Moreover, using the *in vitro* RAW264.7 cell line, we demonstrate that the differentiation of this monocyte/macrophage cell line into osteoclasts was halted upon the addition of a <3kDa cell culture supernatant (CCS) fraction from *L. reuteri*. Other studies involving probiotics and bone health have highlighted the efficacy of different bioactive compounds in preventing bone loss and this prevention has often times been attributed to a suppression of osteoclastogenesis [13,21,22]. Taken together, these studies strongly indicate that the identification of molecule(s), produced by bacteria that target osteoclastogenesis may lead to understanding how bacteria regulate bone health and optimize probiotic strain selection for treating bone disease.

Cyclopropane fatty acid (CFA) is a fatty acid containing a cyclopropane ring. One CFA in particular, Lactobacillic acid (LA), is produced by *L. reuteri* and has been shown to be important for the suppression of TNF- α production from a human monocyte cell line [23]. The immunomodulatory activity of this strain contributed towards strain selection in the original studies in the OVX osteoporosis model since TNF-α plays such an important role in promoting osteoclastogenesis and bone loss [3,24–26]. LA is a 19-carbon chain long CFA derived from the conversion of vaccenic acid by cyclopropane fatty acid synthase [23]. Dihydrosterculic acid, another CFA, is also present in *L. reuteri* and is derived from oleic acid. Interestingly enough, oleic acid has been shown to suppress osteoclastogenesis [27,28]. Other fatty acids have also been shown to inhibit osteoclastogenesis through the inhibition of NF-κB activation, which is a crucial signaling event in osteoclast differentiation [21,29,30]. LA has yet to be studied in this context and warrants further investigation.

In this study, we expanded on the initial findings where *L. reuteri* suppressed osteoclastogenesis and further characterized this interaction by describing the host response following *L. reuteri* stimulation. Through a time course experiment, we established that an early

stage in osteoclastogenesis was being targeted by *L.* reuteri. This guided an RNA sequencing experiment where global transcriptional changes due to *L. reuteri* treatment were revealed. When these differentially expressed genes were mapped onto the pathways in the *Mus musculus* KEGG database, various pathways were down-regulated by *L. reuteri* with notable ones that included Osteoclast differentiation, TNF-α signaling, and NF-κB signaling. Consistent with this, we showed that *L. reuteri* treatment decreased the levels of phosphorylated p65 suggesting that NF-κB activation is also inhibited. Since LA is involved with the ability of *L. reuteri* to suppress TNF-α, we were prompted to investigate its role in suppressing osteoclastogenesis. Using exogenous LA and an *L. reuteri* mutant deficient in LA production, we have established that LA is capable of inhibiting *in vitro* osteoclastogenesis.

3.2 *Materials and Methods*

3.2.1 *Bacterial strains used in this study and growth conditions*

L. reuteri ATCC 6475 was provided to the Britton laboratory by Biogaia inc. (Sweden) and was cultured anaerobically in deMan, Rogosa, Sharpe media (MRS, Difco) for 18 h at 37°C. To generate *L. reuteri* cell culture supernatant (CCS), the overnight culture was subcultured into fresh MRS and grown until log phase (OD_{600} = 0.4) and cells were pelleted by centrifugation at 4000 rpm for 10 min. The pellet was washed twice with sterile PBS to remove any residual MRS. The *L. reuteri* CCS was generated by resuspending the bacterial cell pellet in Minimum Essential Medium (MEM-α, Invitrogen) with an OD_{600} = 3.0 and incubated for 3 h at 37°C with gentle orbital shaking (60 rpm). The bacterial cell pellet was harvested and the supernatant collected. Then, it was filter-sterilized with using a PVDF membrane filter (0.22 μm pore size, Millipore) and fractionated (Amicon filter, Millipore) to include only the <3 kDa fraction. The *L.*

reuteri CCS was lyophilized and stored at -80°C. Sterile MEM-α also underwent processing in parallel to serve as the vehicle control for each experiment.

3.2.2 *Culture conditions and osteoclastogenesis differentiation assay*

The immortalized murine macrophage cell line, RAW264.7, was obtained from ATCC and maintained in phenol red-free medium (MEM-α, Invitrogen) supplemented with charcoal stripped fetal bovine serum (Invitrogen) at 37°C with 5% CO_2. In 24-well tissue culture grade plates (Costar), $2*10^4$ cells were seeded. Following one day of incubation, cells were stimulated for differentiation with the addition of receptor activator of NF-kappa B ligand (RANKL, 100ng/ml, R&D systems). Lyophilized *L. reuteri* CCS was resuspended in culture medium and used to treat the cells. Each well contained 10% of the OD_{600} = 3.0 CCS generated as previously described. For dose response experiments, a CCS of 100% is equivalent to containing 50% of the OD_{600} = 3.0 in each well. Fresh medium is replenished after every 2 days for a week. On day 7, cells were fixed and stained for tartrate-resistant acid phosphatase (TRAP) using a commercially available staining kit (Sigma Cat. No. 387A). Giant cells with ≥ 3 nuclei that stained positive were considered osteoclasts.

3.2.3 *Chemicals and reagents used*

The GPR40 and GPR120 antagonists, DC260126 (Cat. No. 5357) and AH7614 (Cat. No. 5256), respectively, were purchased from Tocris Biosciences. Lactobacillic acid (LA, also known as phytomonic or cyclopropane fatty acid) was purchased from Cayman chemical. The antibodies, p38 (Cat. No. 8610), phosphorylated p38 (Cat. No. 4511), ERK (Cat. No. 3552), phosphorylated ERK (Cat. No. 4377), JNK (Cat. No. 9258), phosphorylated JNK (Cat. No 9251), p65 (Cat. No. 8242), phosphorylated p65 (Cat. No. 3033), and beta actin (Cat. No. 4970) used for this study were purchased from Cell Signaling Technology.

3.2.4 *Pharmacological inhibition studies*

For the antagonist studies, the osteoclastogenesis assay was performed as previously described with an additional preincubation step with the inhibitor. Prior to the addition of *L. reuteri* or LA, 1 μM of GPR40 or GPR120 was added for 1 h. The fresh medium that was replenished every 2 days contained 1 μM of GPR40 or GPR120. Following 7 days of culture, the cells were fixed, stained for TRAP, and the enumeration of osteoclasts was performed as previously described.

3.2.5 *Cell viability or metabolic activity assay*

MTT (3-(4,5-dimethylthiazol-2-yl)-2,5-diphenyltetrazolium bromide) was used to assess cell viability as a function of metabolic activity. This is signified by the NAD(P)H-dependent oxidoreductase enzymatic activity of a cell. In the presence of these enzymes, MTT becomes reduced to formazan, which is an insoluble product possessing chromogenic properties. Briefly, 1*10^4 RAW264.7 cells are seeded on a 96-well culture plate (Cat. No. 07-200-760, Fisher Scientific) and incubated at 37C with 5% CO2. Following 24 hours, the media is exchanged and the cells are stimulated with the vehicle control or cell culture supernatant from *Lactobacillus reuteri.* The cells are co-incubated with the different treatment conditions for 4 and 24 hours. Upon completion of each treatment, 0.02 ml of MTT solution (5 mg/ml) dissolved in MEMα + 10% FBS was added to each well and the plate is incubated at 37°C with 5% CO_2 for 4 hours. The plate is washed twice with PBS and then DMSO is added to each well to dissolve the formazan formed. The plate is shaken for 5 minutes and absorbance readings at 570 nm are taken to measure the amount of metabolic activity for each condition. The data is expressed as a ratio between the specific treatment groups to that of the control group containing untreated cells.

3.2.6 *RNA Extraction from RAW264.7 cells and sequencing*

RNA extraction was performed using TRIzol Reagent (Cat. No. 15596018, Thermo Fisher Scientific) according to the manufacturer's instructions. Library preparation and sequencing of *Mus musculus* transcriptome was performed by the Baylor Human Genome Sequencing Center. Sequencing was performed on an Illumina HiSeq 2000 platform. Sequencing data were mapped onto the *Mus musculus* 10 genome available from UCSC Genome Bioinformatics.

3.2.7 *Analysis of RNA sequencing data*

On average, there were 31,060,000 high quality bases sequenced per sample with a mean fragment length of 225 bases per read. There was an average of 51,905 transcripts detected per sample. The count table signifying the amount of reads that fell into each gene was generated with using Bioconductor in R. Differential expression analysis was performed by the DESeq package in R [31]. Pathway analysis was performed by GAGE in R [32].

3.2.8 *Quantitative reverse transcriptase (RT) polymerase chain reaction (qPCR)*

Following RNA extraction, cDNA synthesis was performed with Superscript III Reverse Transcriptase (Cat. No. 8080093, Thermo Fisher Scientific). A total of 1 µg of RNA was reverse transcribed. Briefly, an Eppendorf Mastercycler EP S was preheated to 65 °C. The mixture containing RNA, 100 ng of random hexamers, (Cat. No.C1181, Promega) and 1 µl of 10nM dNTPs (Cat. No. 18427088) was placed into the thermocycler for 5 mins. Following 1 min on ice, a mixture containing the reverse transcriptase and RNaseOUT was added to complete the cDNA synthesis. A cycle of 10 min at 25°C, 50 min at 50°C, and then 85°C for 5 min was used. The cDNA was used immediately or stored at -20°C. The qPCR reactions reactions contained 1 µl of cDNA, 1 µl of each forward and reverse primer (10 µM), 7 µl of nuclease free water, and 10 µl of Power SYBR Green PCR Master Mix (Cat. No. 4367659, Thermo Fisher Scientific). A 2-step PCR amplification protocol was used with acquisition at the annealing and melting curve

steps. The protocol included an initial denaturation at 95°C for 30 s, followed by 40 cycles of denaturing at 95°C for 10 s, annealing at 51°C for 20 s. A melting curve was performed at the end at 95°C for 15 s and ramping up from 60°C to 95°C at a rate of +0.2°C/sec. Data analysis was performed according to the method described by Pfaffl [33].

3.2.9 *Primer sequences for qPCR*

The following primer pairs were used for the RNA sequencing validation studies: (1) HPRT F 5' GCTATAAATTCTTTGCTGACCTGCT 3', HPRT R 5' AATTACTTTTATGTCCCCTGTTGACTG 3', (2) Nuclear factor of Activated T cells c1 (NFATc1) F 5' CATGCGAGCCATCATCGA 3', NFATc1 R 5' TGGGATGTGAACTCGGAAGAC 3', (3) Tartrate Resistant Alkaline Phosphatase (TRAP) F 5' GACAAGAGGTTCCAGGAGACC 3', TRAP R 5' GGGCTGGGGAAGTTCCAG 3', (4) Matrix metalloproteinase 9 (MMP9) F 5' CTGGACAGCCAGACACTAAAG 3', MMP9 R 5' CTCGCGGCAAGTCTTCAGAG 3', (5) Cathepsin K (CtsK) F 5' GAAGAAGACTCACCAGAAGCAG 3', CtsK R 5' TCCAGGTTATGGGCAGAGATT 3', (6) Dendritic cell-specific transmembrane protein (DC-STAMP) F 5' GGCTGACGGGAAACCGAGCC 3', DC-STAMP R 5' ACAGAAGCAGCAGTTGGCCCAG 3', (7) H+ ATPase F 5' ACGGTGATGTCACAGCAGACGT 3', H+ ATPase R 5' CCTCTGGATAGAGCCTGCCGCA 3'.

3.2.10 *Western blot analysis*

The osteoclastogenesis assay was performed as previously described and proteins were extracted using the commercially available Cell Extraction Buffer (Cat. No. FNN0011, Thermo Fisher Scientific). It was used according to the manufacturer's protocol. Timepoints were taken at 15, 30, 45, and 60 mins. Chemiluminescent imaging was performed with the ProteinSimple FluorChem E system. Analysis was performed by comparing densitometry measurements obtained using the ImageJ software package [34].

3.2.11 *Bone resorption assay*

Osteoassay (Cat. No. 3988) plates coasted with inorganic crystalline calcium phosphate were purchased from Corning Inc. The osteoclastogenesis assay was performed as previously described. Resorption pits were measured using the NIH imaging software, ImageJ [34].

3.2.12 *Statistical analysis*

The results presented are as means+/- SD or SEM. An unpaired Student's *t* test was used to assess differences between groups. The cutoff for significance was $p \leq 0.05$. One-way ANOVA analysis was applied when more than 2 groups were being compared.

3.3 *Results*

3.3.1 *L. reuteri suppressed osteoclastogenesis in a dose-dependent manner*

Expanding on a result previously shown [18], RAW264.7 cells were treated with osteoclastogenic media and stimulated with different doses of *L. reuteri* CCS. Inhibition of osteoclastogenesis was demonstrated in a dose-dependent manner (Figure 3.1).

A)

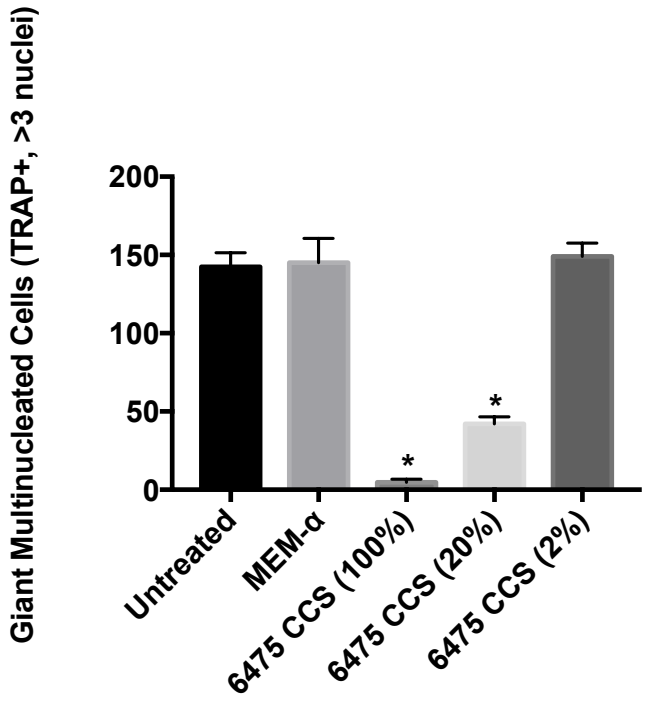

B)

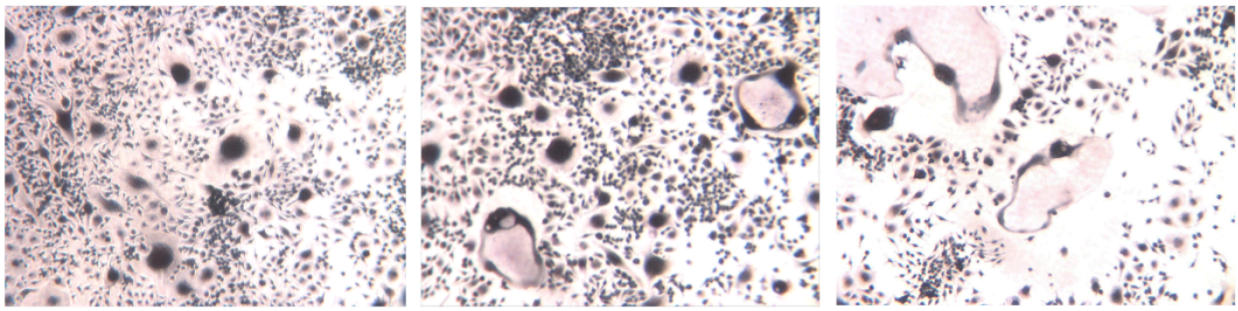

Figure 3.1. Dose-dependent inhibition of osteoclast formation by *L. reuteri.*

Osteoclast differentiation was induced with the addition of 100ng/mL RANKL. Giant multinucleated cells that stained positive for TRAP and with ≥ 3 nuclei were considered osteoclasts (A). Light microscopy images (B) were taken and demonstrate an increase in osteoclast formation with decreasing levels of *L. reuteri* CCS used. This was performed three

Figure 3.1. (cont'd)

times in total and the reported result is a representative experiment with associated standard deviation, *$p < 0.05$ compared to untreated and MEM-α (vehicle control) conditions as determined by one-way ANOVA.

3.3.2 *Progression of osteoclastogenesis over time*

Osteoclast differentiation is a multi-step process consisting of osteoclast precursor activation, fusion, and differentiation before fully mature osteoclasts are developed [1,35–38]. To gain a better understanding of the interaction between *L. reuteri* and RAW264.7 cells during osteoclastogenesis, the phenotypic progression was observed for the duration of the assay (Figure 3.2a). During one of the later steps in osteoclastogenesis, the fusion of mononuclear preosteoclasts results in the formation of giant multinucleated cells known as polykaryons [39–41]. This intermediate step is before cytoskeletal actin rearrangement and an increase in cytosolic space takes place to form fully mature osteoclasts [42,43]. Interestingly, it was observed that *L. reuteri* treatment resulted in an accumulation of fused polykaryons by days 5 and 7 (Figure 3.2b, c). These fused polykaryons resulting from *L. reuteri* treatment phenocopied the polykaryons observed during osteoclastogenesis and suggested that differentiation was halted at this stage [44–46]. While it appears that the osteoclastogenesis process could just be delayed rather than inhibited, additional experiments were performed where the duration of the experiment was extended to 17 days. Following treatment on day 5, there was a washout period where only fresh medium containing RANKL was replenished. At the end of day 17, similar results were obtained in that the cells treated *L. reuteri* still had suppressed osteoclastogenesis with an accumulation of polykaryons (Figure 3.2d). Taken together, these results indicated that *L. reuteri* halted osteoclastogenesis at a fused polykaryon stage and that the effects were long lasting at least out until 17 days.

A)

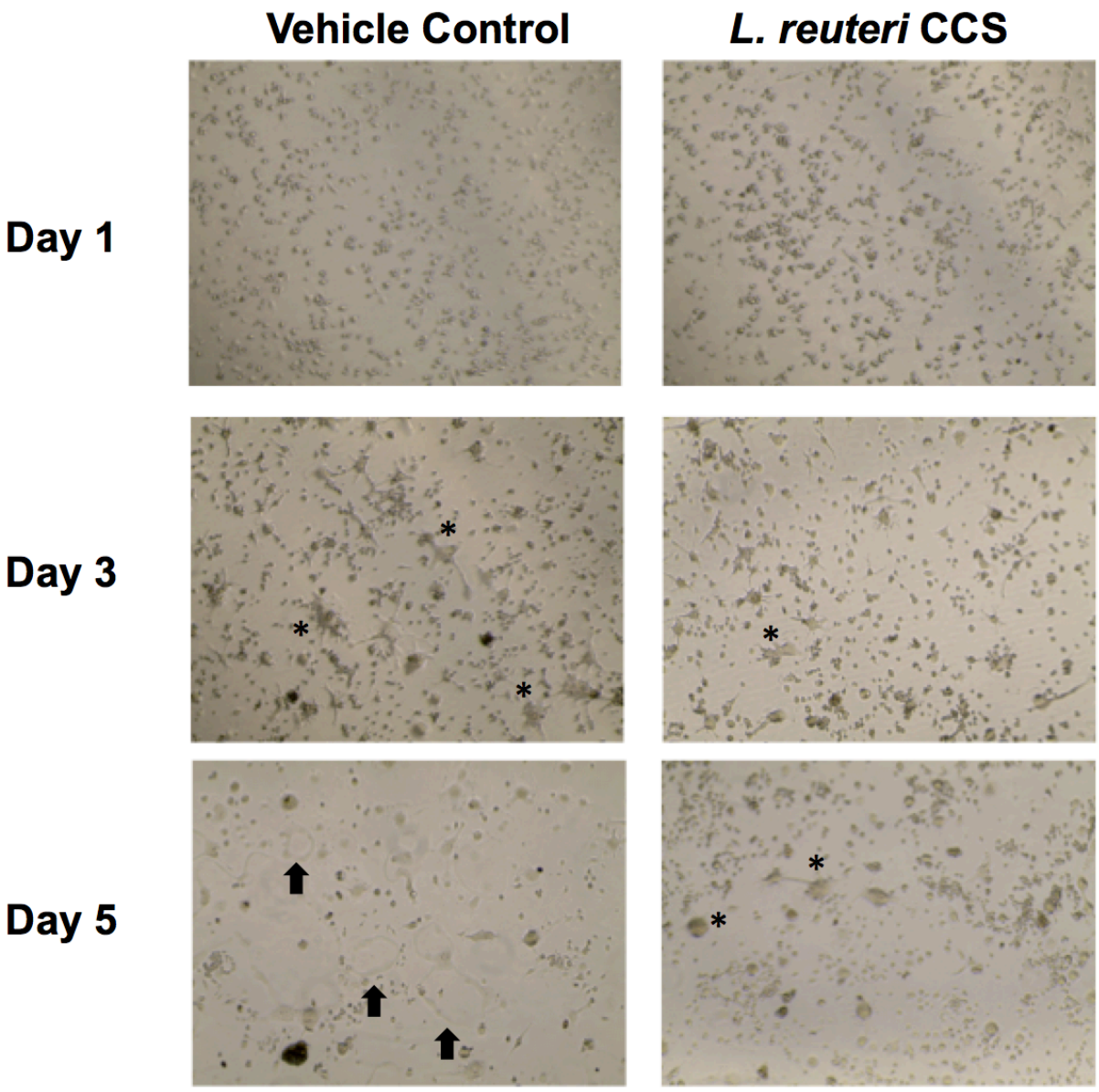

Figure 3.2. Progression of osteoclastogenesis over time.

RAW264.7 cells were stimulated for osteoclast differentiation with RANKL (100ng/ml) and treated with a vehicle (MEM-α) or *L. reuteri* CCS. (A) Differentiated osteoclasts (arrows) can be observed by day 5 in the vehicle treatment while *L. reuteri* suppressed mature osteoclast formation. (B, C) Fused polykaryons (asterisks) were present in both condition but *L. reuteri*

Figure 3.2. (cont'd)

treatment led to an accumulation of them by day 7. (D) After a 10 day washout period, osteoclast differentiation was still inhibited in cells treated by *L. reuteri* CCS at day 17. *$p < 0.05$ compared to untreated and MEM-α (vehicle control) conditions as determined by one-way ANOVA.

B)

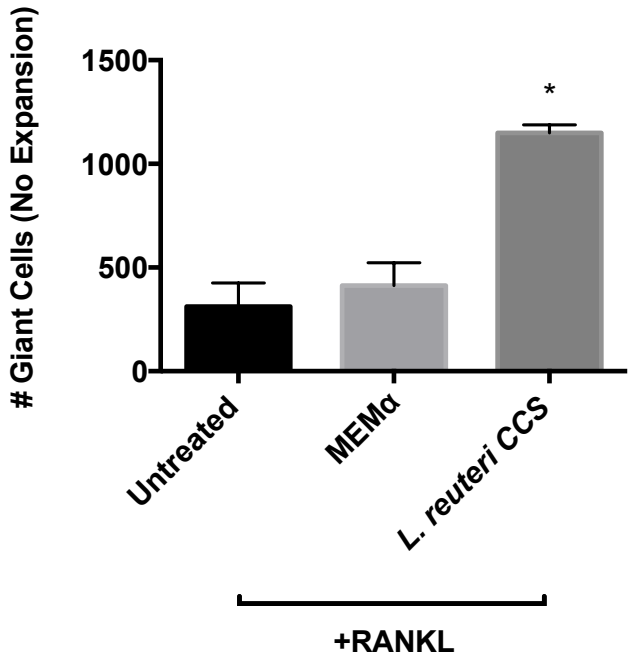

Figure 3.2. (cont'd)

C)

MEMα + RANKL

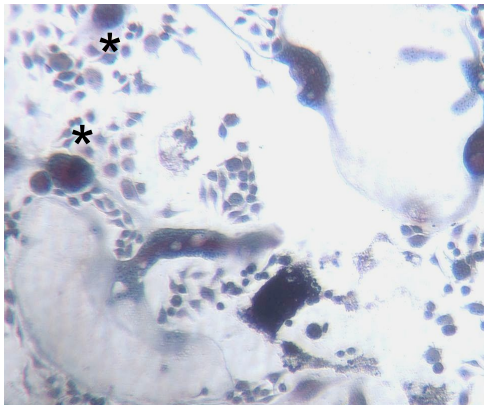

***L. reuteri* CCS + RANKL**

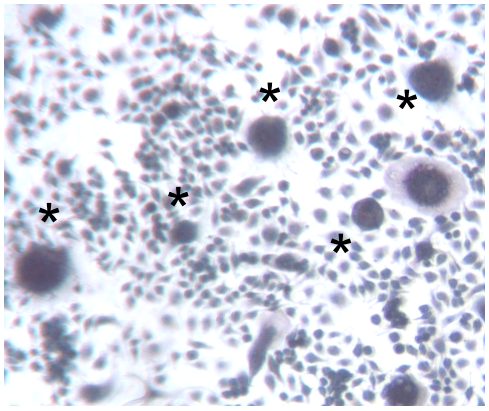

D)

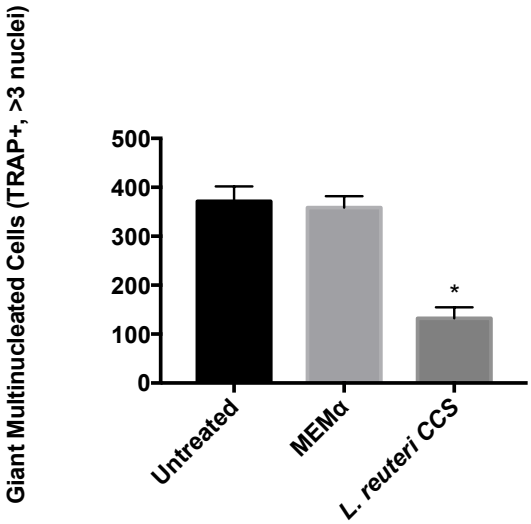

3.3.3 *Impact of L. reuteri on bone resorption in RANKL-stimulated RAW264.7 cells*

We have already demonstrated that CCS from *L. reuteri* inhibits RAW264.7 cell differentiation into osteoclasts, but the question of whether osteoclast function was impacted remained unanswered. To test this, we performed a bone resorption assay using plates coated with calcium phosphate that mimicked the bone environment. Consistent with the ability to suppress osteoclastogenesis, *L. reuteri* CCS significantly decreased the amount of mineral resorption compared to the controls (Figure 3.3).

A)

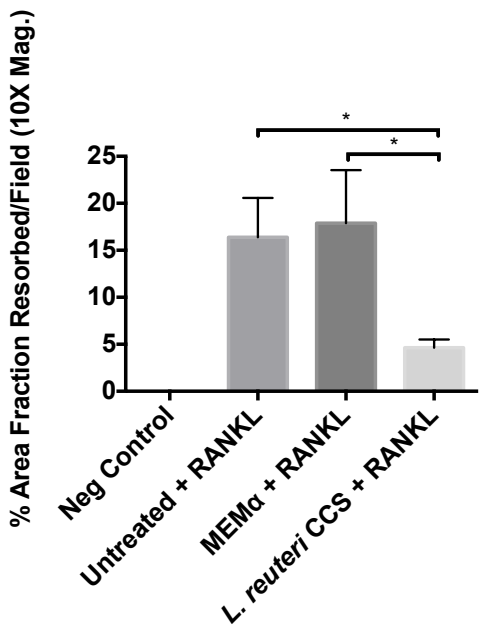

B)

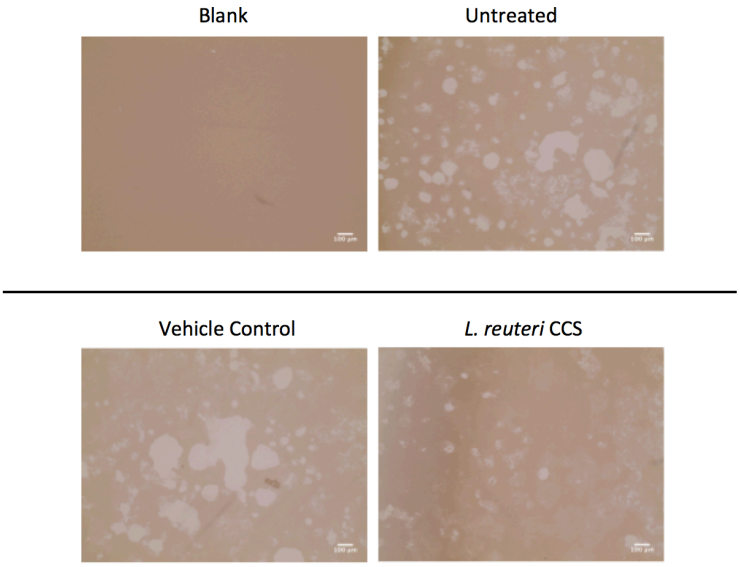

Figure 3.3. Bone resorption studies.

RAW264.7 cells were plated for on Osteoassay plates for 1 day and then stimulated concurrently with RANKL (100ng/ml) and either the vehicle control (MEM-α) or *L. reuteri* CCS. Fresh medium was replenished every 2 days. The analysis was performed using the Image J

Figure 3.3. (cont'd)

software package to measure densitometry. (A) *L. reuteri* CCS significantly decreased the amount of absorption from calcium and phosphate coated plates. (B) The microscopy images also support that less absorption had taken place in the presence of *L. reuteri* CCS. This was performed three times in total and the reported result is a representative experiment with associated standard deviation, $*p < 0.05$ compared to untreated and MEM-α (vehicle control) conditions as determined by one-way ANOVA.

3.3.4 *An early signaling event in osteoclastogenesis was targeted by L. reuteri*

To determine the stage of osteoclastogenesis being targeted by *L. reuteri*, we performed a time course experiment where RAW264.7 cells are stimulated by RANKL for differentiation and treated with *L. reuteri* CCS throughout the duration of the assay or just once on day 1, 3, or 5. The addition of *L. reuteri* CCS at day 1 sufficiently inhibited osteoclast differentiation while treatment at day 3 ($p = 0.07$) or 5 had no impact on osteoclastogenesis

Figure 3.4). These results, coupled with the phenotypic studies (Figure 3.2b, c), suggested that *L. reuteri* affected an early signaling event during osteoclastogenesis and halted the cells in a polykaryon stage.

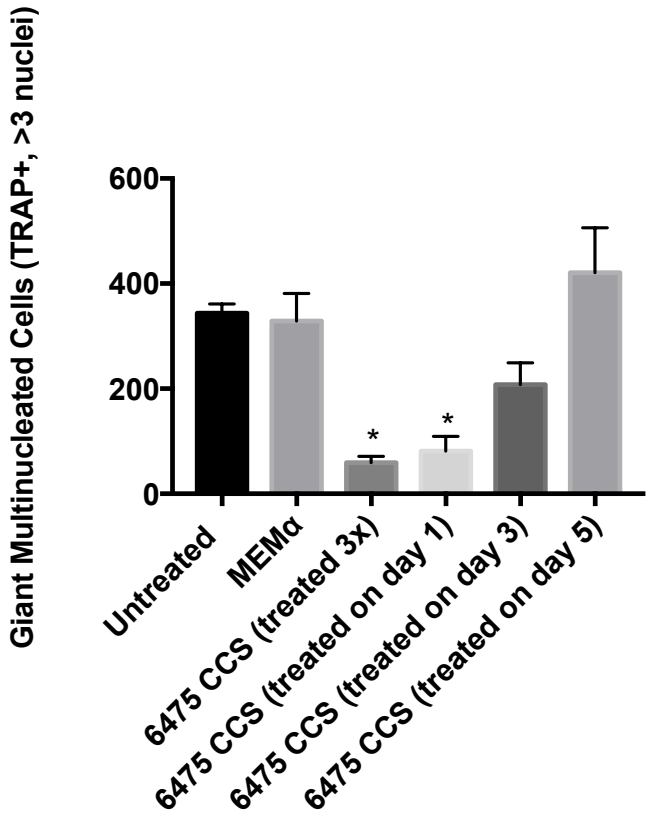

Figure 3.4**.** Impact of *L. reuteri* CCS on osteoclast differentiation at different time points.

RAW264.7 cells were plated and osteoclast differentiation was induced with the addition of 100ng/mL RANKL. *L. reuteri* CCS was added normally when the media was replenished (days 1, 3, and 5) or just once on day 1, 3, or 5. After 7 days, the number of giant multinucleated (≥ 3 nuclei) cells staining positive for TRAP were quantified. Treatment by *L. reuteri* CCS on day 1 was sufficient to suppress osteoclastogenesis. This was performed three times in total and the reported result is a representative experiment with associated standard deviation, *$p < 0.05$ compared to untreated and MEM-α (vehicle control) conditions as determined by one-way ANOVA.

3.3.5 *Blocking of GPR 120 attenuated the suppression of osteoclastogenesis by L. reuteri*

Interestingly, the inhibition of osteoclastogenesis and suspension at the polykaryon stage has been demonstrated in a number of studies [42,47,48]. In these studies, it was observed that medium and long chain fatty acids suppressed osteoclastogenesis. Free fatty acid receptor 4 (FFAR4), a G protein-coupled receptor, has been shown to be a receptor for long chain fatty acids [49,50]. It is also known as GPR120 and its role in anti-inflammation and sensitization of insulin has been demonstrated through stimulation from omega 3 fatty acids [50]. Interestingly, GPR120 was induced in RAW264.7 cells and bone marrow macrophages following RANKL treatment and its activation suppressed osteoclastogenesis [51]. Since this study demonstrated results suggesting that osteoclastogenesis was halted at a polykaryon stage, we hypothesized that *L. reuteri* CCS was inhibiting osteoclastogenesis through GPR120 activation. To test this, we performed an osteoclastogenesis study with the addition of a GPR120 antagonist (AH7614). Inhibition of GPR120 rendered *L. reuteri* less effective in suppressing osteoclastogenesis (Figure 3.5). GPR40 is also a receptor for long chain fatty acids and has been shown to have a positive impact on bone [52,53]. However, blocking GPR40 stimulated with an antagonist (DC260126) did not impact the ability of the CCS from *L. reuteri* to suppress osteoclastogenesis. These studies suggested that *L. reuteri* was inhibiting osteoclastogenesis through GPR120 but not GPR40.

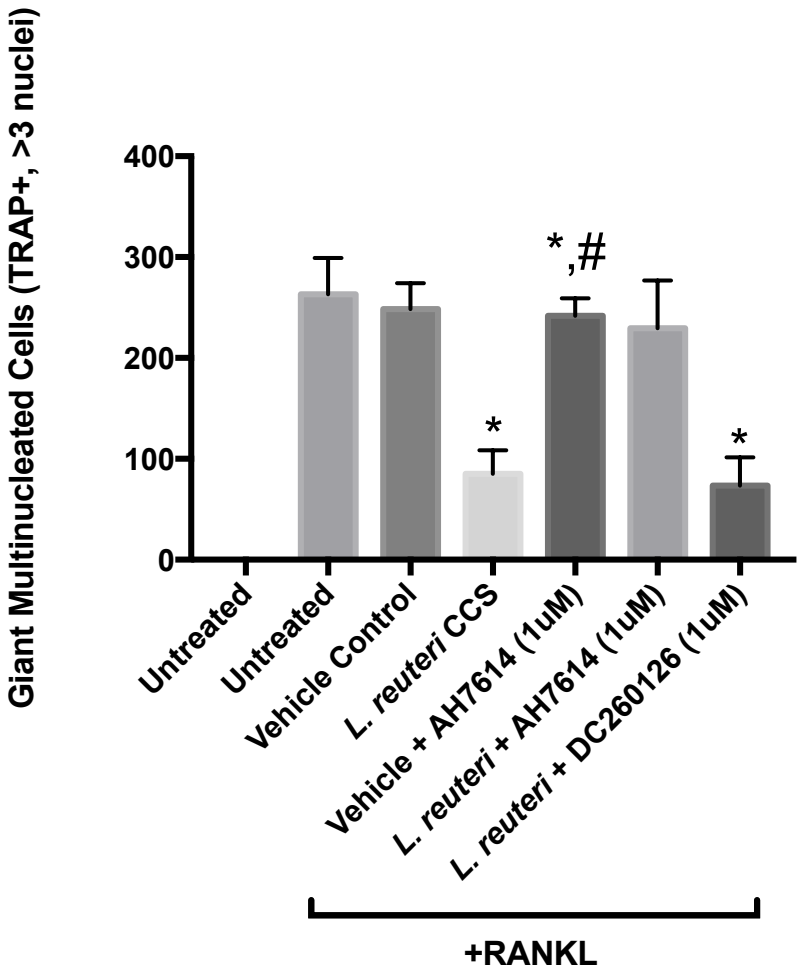

Figure 3.5**.** Suppression of osteoclastogenesis by *L. reuteri* was mediated through GPR120 signaling.

RAW264.7 cells were plated. After 24 h, the cells were pretreated with 1 μM of AH7614 for 1 h. Then, osteoclast differentiation was induced with the addition of 100ng/mL RANKL. Cell differentiation medium (containing RANKL and the inhibitor) was replenished every 2 days. The presence of the inhibitor attenuated the suppression of osteoclastogenesis by *L. reuteri*. This was performed three times in total and the reported result is a representative experiment with associated standard deviation, *$p < 0.05$ compared to untreated and MEM-α (vehicle control) conditions, #$p < 0.05$ compared to *L. reuteri* as determined by one-way ANOVA.

3.3.6 *Lactobacillic acid suppressed in vitro osteoclastogenesis*

It was previously shown that the ability of *L.* reuteri to suppress TNF-α production from a human monocyte line was related to the presence of LA, a long chain fatty acid with a cyclopropane ring [23]. Long chain fatty acids have been shown to suppress osteoclastogenesis [28,42]. These studies, coupled with our results suggesting that the activation of GPR120 was involved in the suppression of osteoclastogenesis by *L. reuteri*, made LA a compelling candidate to test in our model of osteoclast differentiation. Incubation of RAW264.7 cells, which were stimulated for osteoclast differentiation, with LA resulted in a dose-dependent inhibition of osteoclast formation (Figure 3.6). Additionally, an *L. reuteri* mutant unable to produce LA was less effective in suppressing osteoclastogenesis in comparison with WT *L. reuteri*. Lastly, the presence of an inhibitor to GPR120 decreased the ability to LA to suppress osteoclastogenesis.

A)

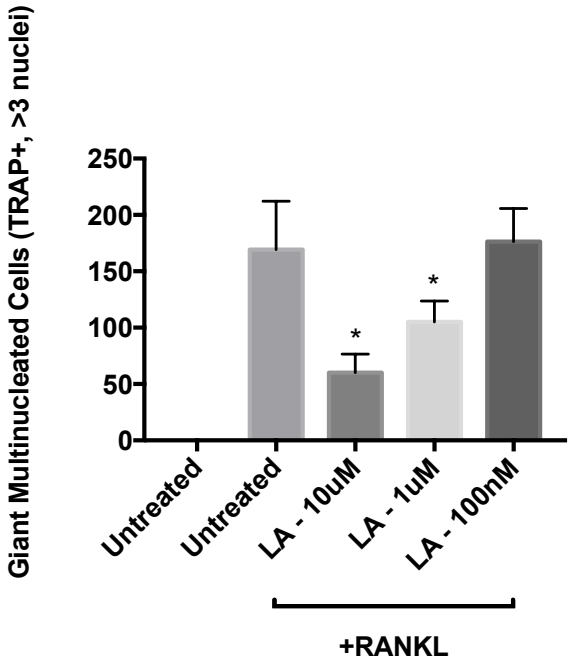

Figure 3.6**.** Lactobacillic acid (LA) involved with the suppression of osteoclastogenesis.

RAW264.7 cells were plated and osteoclast differentiation was induced with the addition of 100ng/mL RANKL. (A) Dose-dependent suppression of osteoclastogenesis was observed with LA at the concentrations of 10 μM, 1 μM, and 100 nM. (B) A mutant unable to produce LA in the *L. reuteri* genetic background was not as effective as the WT strain in suppressing osteoclastogenesis. (C) Pharmacological inhibition of GPR120 decreased the ability of LA to suppress osteoclast formation. This was performed three times in total and the reported result is a representative experiment with associated standard deviation, $*p < 0.05$ compared to untreated and MEM-α (vehicle control) conditions, $\#p < 0.05$ compared to *L. reuteri* as determined by one-way ANOVA.

Figure 3.6. (cont'd)

B)

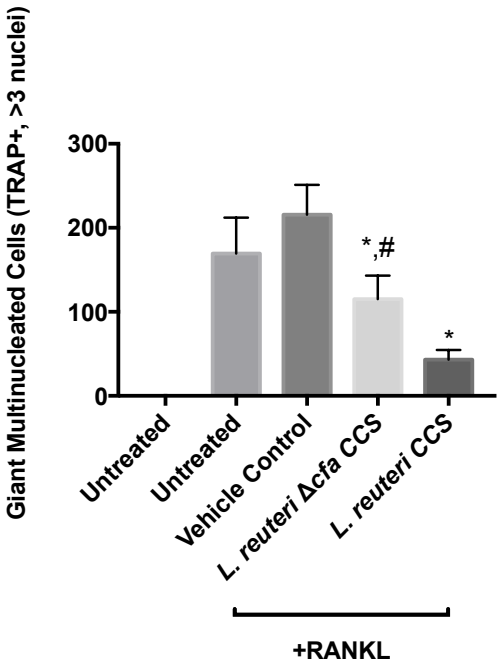

C)

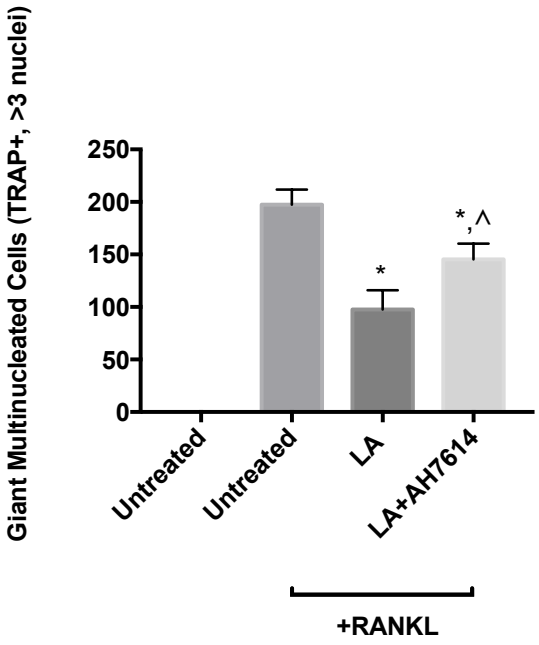

Histamine, another small molecule involved with inhibiting TNF-α production by *L. reuteri*, has also been shown to be important for regulating bone mass [54,55]. To test whether histamine contributed to *L. reuteri* suppressing osteoclastogenesis, CCS from a mutant deficient in histamine production was used to treat RAW264.7 cells stimulated for osteoclast differentiation. The lack of histamine production by *L. reuteri* did not impact its ability to suppress osteoclastogenesis (Figure 3.7).

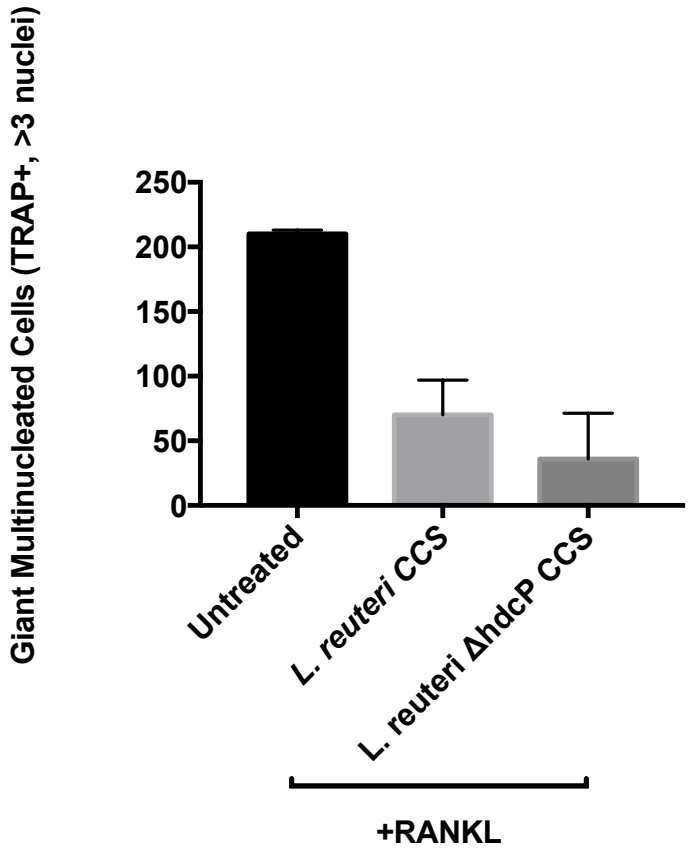

Figure 3.7**.** Histamine production by *L. reuteri* not involved with inhibition of osteoclastogenesis. RAW264.7 cells were plated and osteoclast differentiation was induced with the addition of 100ng/mL RANKL. A mutant unable to produce histamine in the *L. reuteri* genetic background was capable of suppressing osteoclastogenesis.

Through these sets of experiments, we demonstrated that LA directly inhibited osteoclast differentiation and this was mediated through GPR120. While the *L. reuteri* mutant lacking LA was less effective in suppressing osteoclastogenesis, partial inhibition was still observed.

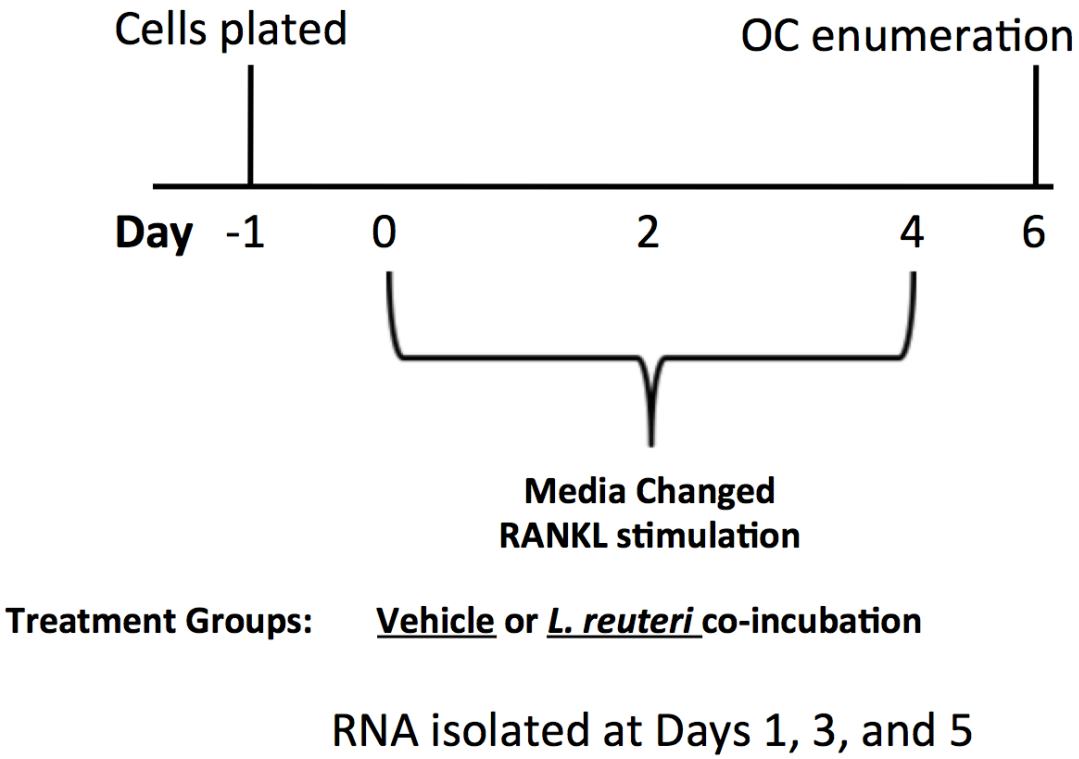

Figure 3.8**.** Experimental layout for gene expression analysis.

RAW264.7 cells were plated for 1 day and then stimulated concurrently with RANKL (100ng/ml) and either the vehicle control (MEM-α) or *L. reuteri* CCS. RNA was extracted at days 1, 3, and 5.

3.3.7 *Transcriptomic profiling of RAW264.7 cells during L. reuteri treatment supports the suppression of osteoclastogenesis*

To gain a better understanding of how *L. reuteri* impacts RAW264.7 cells, we performed an RNA sequencing experiment to measure the levels of gene expression from the entire transcriptome. Cells were stimulated for differentiation with RANKL and treated with the vehicle control or *L. reuteri* CCS. There were two biological replicates for each condition at each timepoint (Figure 3.8). Differential gene expression analysis was performed using the Bioconductor software package DESeq2 [56]. Using a fold change cutoff of 3, we observed 2,993 genes were differentially regulated by *L. reuteri* in comparison to the vehicle control (Table 3.1). However, there were substantially more genes differentially regulated at the days 3 and 5 timepoints. The gage software package was used to gain a better understanding of pathways that were differentially regulated by *L. reuteri* [32]. The cutoff for statistical significance was determined using a *q value* < 0.05 (*p value* that takes into account the false discovery rate based off of multiple comparisons). Similar to the gene expression data, more KEGG pathways were differentially regulated by *L. reuteri* at days 3 and 5 with 90 out of the total 98 occurring on those 2 timepoints (Table 3.2).

At day 1, very few changes were observed. There was an activation of 4 pathways and down-regulation of 4 pathways, but none that were involved with osteoclast differentiation (Table 3.3). Out of the up-regulated pathways, one was associated with innate immunity (Complement and coagulation cascades, mmu04610) and another associated with the detection of fatty acids (PPAR signaling pathway, mmu 03320). Notably, the down-regulated pathways suggested that cell cycle and/or proliferation were affected by *L. reuteri* treatment (Table 3.3). However, light microscopy and trypan blue exclusion staining did not reveal any discernible differences. Additionally, an MTT assay was utilized to detect metabolic activity and no differences were observed up to 3 days following *L. reuteri* treatment (Figure 3.9).

By day 3, there were 2 pathways that were up-regulated and 43 that were down-regulated (Table 3.4). Interestingly enough, the 2 pathways activated were neural pathways (Olfactory transduction, mmu04740; Neuroactive ligand-receptor interaction, mmu04080). Notable ones in the set of down-regulated pathways included Osteoclast differentiation (mmu04380), NF-kappa B signaling (mmu04064), MAPK signaling (mmu04010), and TNF signaling (mmu04668). Pathway analysis from the day 5 timepoint suggested that the majority of the processes being impacted involved cellular metabolism and immune signaling (Table 3.5). Consistent with day 3, Osteoclast differentiation, NF-kappa B signaling, MAPK signaling, and TNF signaling were down-regulated.

To validate the data set, we performed quantitative PCR analysis of genes that were well characterized in the osteoclast differentiation pathway. The genes measured were *NFatC1, TRAP*, *MMP9*, *CtsK*, *DC-STAMP*, and *ATP6v0d2* [57,58]. For all the genes tested, the RNA sequencing results closely paralleled the quantitative PCR results (Figure 3.10). Provided that this strain of *L. reuteri* has demonstrated immunomodulatory activity, the transcriptional analysis suggests that immune signaling may be targeted to impact osteoclastogenesis [23,55,59].

Table 3.1 Genes with significantly changed expression between vehicle and *L. reuteri* treatment (Fold change > 3)

	V1T1	**V3T3**	**V5T5**
Up-regulated	24	1334	1635
Down-regulated	21	3097	2611

Table 3.2**.** Pathways differentially regulated between vehicle and *L. reuteri* treatment

	V1T1	**V3T3**	**V5T5**
Up-regulated	4	2	4
Down-regulated	4	43	41

Table 3.3**.** KEGG pathways differentially regulated at day 1 in RAW264.7 cells

A) Up-regulated pathways due to *L. reuteri* treatment

Entry number	Pathway name	p.val	q.val
mmu04610	Complement and coagulation cascades	0.000214332	0.00985925
mmu04630	Jak-STAT signaling pathway	0.000425642	0.012771066
mmu04966	Collecting duct acid secretion	0.000428009	0.012771066
mmu03320	PPAR signaling pathway	0.004688236	0.066356575

Table 3.3. (cont'd)

B) Down-regulated pathways due to *L. reuteri treatment*

Entry number	Pathway name	p.val	q.val
mmu04110	Cell cycle	3.64E-11	6.70E-09
mmu03040	Spliceosome	1.43E-10	1.32E-08
mmu03030	DNA replication	1.24E-08	7.59E-07
mmu03013	RNA transport	1.73E-07	7.97E-06

Table 3.4. KEGG pathways differentially regulated at day 3 in RAW264.7 cells.

Pathways present at day 3 but absent at 5 are denoted by *.

A) Up-regulated pathways due to *L. reuteri* treatment

Entry number	Pathway name	p.val	q.val
mmu04110	Cell cycle	3.64E-11	6.70E-09
mmu03040	Spliceosome	1.43E-10	1.32E-08

B) Down-regulated pathways due to *L. reuteri* treatment

Entry number	Pathway name	p.val	q.val
mmu04110	Cell cycle	2.34E-25	4.31E-23
mmu04120	Ubiquitin mediated proteolysis	1.79E-22	1.65E-20
mmu04141	Protein processing in endoplasmic reticulum	3.81E-18	2.34E-16
mmu04114	Oocyte meiosis*	1.03E-16	4.73E-15
mmu03013	RNA transport	2.39E-14	8.21E-13
mmu04144	Endocytosis	2.68E-14	8.21E-13
mmu04145	Phagosome*	2.50E-12	6.56E-11

Table 3.4. (cont'd)

mmu00020	Citrate cycle (TCA cycle)	7.95E-12	1.46E-10
mmu04010	MAPK signaling pathway	9.01E-12	1.51E-10
mmu00230	Purine metabolism	1.42E-11	2.18E-10
mmu00240	Pyrimidine metabolism	1.67E-11	2.36E-10
mmu04142	Lysosome*	1.90E-11	2.50E-10
mmu04380	Osteoclast differentiation	2.87E-11	3.52E-10
mmu00510	N-Glycan biosynthesis*	3.61E-11	4.15E-10
mmu04620	Toll-like receptor signaling pathway*	6.43E-11	6.96E-10
mmu04910	Insulin signaling pathway	8.60E-11	8.79E-10
mmu04650	Natural killer cell mediated cytotoxicity*	1.17E-10	1.13E-09
mmu04210	Apoptosis	1.25E-10	1.15E-09
mmu04666	Fc gamma R-mediated phagocytosis	4.64E-10	4.06E-09
mmu04146	Peroxisome	6.31E-10	5.28E-09
mmu04115	p53 signaling pathway	1.19E-09	9.22E-09
mmu03018	RNA degradation	1.20E-09	9.22E-09
mmu04150	mTOR signaling pathway	1.57E-09	1.16E-08
mmu04662	B cell receptor signaling pathway	1.72E-09	1.21E-08
mmu04668	TNF signaling pathway	5.07E-09	3.41E-08
mmu04066	HIF-1 signaling pathway	5.19E-09	3.41E-08
mmu04062	Chemokine signaling pathway	1.72E-08	1.09E-07
mmu03030	DNA replication	2.32E-08	1.42E-07

Table 3.4. (cont'd)

mmu04070	Phosphatidylinositol signaling system	4.12E-08	2.37E-07
mmu04151	PI3K-Akt signaling pathway	4.83E-08	2.69E-07
mmu04660	T cell receptor signaling pathway	5.67E-08	2.90E-07
mmu00280	Valine, leucine and isoleucine degradation*	8.76E-08	4.36E-07
mmu04622	RIG-I-like receptor signaling pathway	1.14E-07	5.52E-07
mmu00562	Inositol phosphate metabolism	2.68E-07	1.26E-06
mmu04810	Regulation of actin cytoskeleton	4.38E-07	1.96E-06
mmu00010	Glycolysis / Gluconeogenesis*	7.27E-07	3.18E-06
mmu00071	Fatty acid degradation*	8.39E-07	3.59E-06
mmu04064	NF-kappa B signaling pathway	1.26E-06	5.16E-06
mmu00970	Aminoacyl-tRNA biosynthesis	2.93E-06	1.15E-05
mmu00563	Glycosylphosphatidylinositol(GPI)-anchor biosynthesis*	4.33E-06	1.66E-05
mmu04390	Hippo signaling pathway	4.79E-06	1.76E-05
mmu03320	PPAR signaling pathway*	5.42E-06	1.95E-05

Table 3.5**.** KEGG pathways differentially regulated at day 5 in RAW264.7 cells.

Pathways present at day 5 but absent at 3 are denoted by #.

A) Up-regulated pathways due to *L. reuteri* treatment

Entry number	Pathway name	p.val	q.val
mmu03010	Ribosome	8.97E-15	1.65E-12
mmu00190	Oxidative phosphorylation	3.36E-09	3.09E-07
mmu04740	Olfactory transduction	1.08E-05	0.000663709
mmu04260	Cardiac muscle contraction	0.000461131	0.021212004

B) Down-regulated pathways due to *L. reuteri* treatment

Entry number	Pathway name	p.val	q.val
mmu04110	Cell cycle	6.81E-31	1.25E-28
mmu04141	Protein processing in endoplasmic reticulum	1.79E-21	1.64E-19
mmu04120	Ubiquitin mediated proteolysis	1.50E-19	9.20E-18
mmu03013	RNA transport	1.30E-14	4.79E-13
mmu04144	Endocytosis	2.49E-14	7.65E-13
mmu04010	MAPK signaling pathway	5.29E-13	1.39E-11
mmu04115	p53 signaling pathway	1.28E-11	2.94E-10
mmu04914	Progesterone-mediated oocyte maturation#	3.29E-11	6.73E-10
mmu03030	DNA replication	4.70E-10	7.21E-09
mmu04722	Neurotrophin signaling pathway	1.07E-09	1.52E-08
mmu04150	mTOR signaling pathway	2.18E-09	2.73E-08

Table 3.5. (cont'd)

mmu00240	Pyrimidine metabolism	2.22E-09	2.73E-08
mmu04910	Insulin signaling pathway	2.48E-09	2.85E-08
mmu04151	PI3K-Akt signaling pathway	2.94E-09	3.18E-08
mmu04668	TNF signaling pathway	3.66E-09	3.74E-08
mmu04622	RIG-I-like receptor signaling pathway	4.91E-09	4.75E-08
mmu04210	Apoptosis	6.81E-09	5.97E-08
mmu03018	RNA degradation	2.72E-08	2.18E-07
mmu04650	Natural killer cell mediated cytotoxicity	3.78E-08	2.90E-07
mmu04064	NF-kappa B signaling pathway	4.48E-08	3.30E-07
mmu04660	T cell receptor signaling pathway	6.50E-08	4.60E-07
mmu00230	Purine metabolism	7.14E-08	4.87E-07
mmu03040	Spliceosome#	8.26E-08	5.43E-07
mmu04666	Fc gamma R-mediated phagocytosis	1.00E-07	6.37E-07
mmu04066	HIF-1 signaling pathway	1.30E-07	7.95E-07
mmu04070	Phosphatidylinositol signaling system	1.66E-07	9.87E-07
mmu00970	Aminoacyl-tRNA biosynthesis	4.54E-07	2.61E-06
mmu04662	B cell receptor signaling pathway	5.24E-07	2.92E-06
mmu04810	Regulation of actin cytoskeleton	6.29E-07	3.40E-06
mmu04510	Focal adhesion#	8.19E-07	4.31E-06
mmu04390	Hippo signaling pathway	1.81E-06	9.24E-06
mmu04664	Fc epsilon RI signaling pathway#	2.54E-06	1.26E-05
mmu00562	Inositol phosphate metabolism	4.56E-06	2.15E-05
mmu04062	Chemokine signaling pathway	4.85E-06	2.23E-05
mmu03008	Ribosome biogenesis in eukaryotes#	6.87E-06	3.08E-05

Table 3.5 (cont'd)

mmu03015	mRNA surveillance pathway#	9.27E-06	3.97E-05
mmu04621	NOD-like receptor signaling pathway	1.30E-05	5.31E-05
mmu04380	Osteoclast differentiation	1.68E-05	6.60E-05
mmu04146	Peroxisome	1.83E-05	7.01E-05
mmu00020	Citrate cycle (TCA cycle)	2.20E-05	8.28E-05
mmu04320	Dorso-ventral axis formation	2.43E-05	8.96E-05

A)

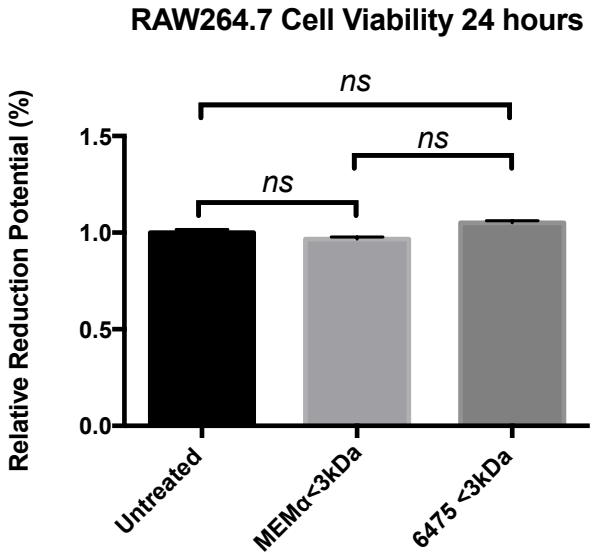

B)

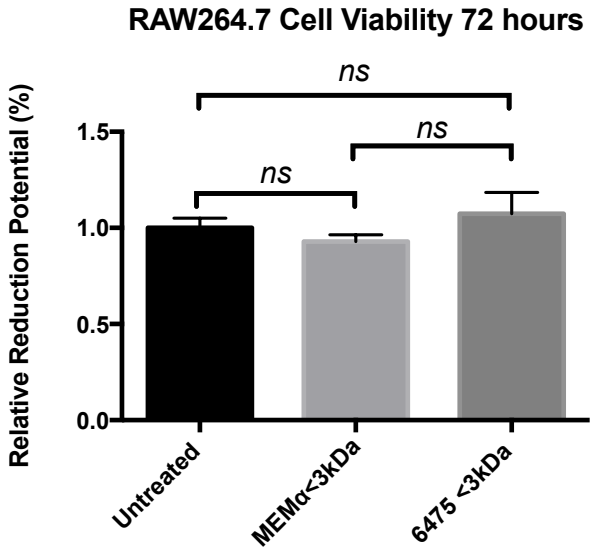

Figure 3.9. MTT assay measuring reduction potential of RAW264.7 cells following stimulation by the <3kDa CCS fraction from *L. reuteri* for (a) 24 and (b) 72 hours.

Results are reported as the average of all experiments (n=3) with associated standard error of mean.

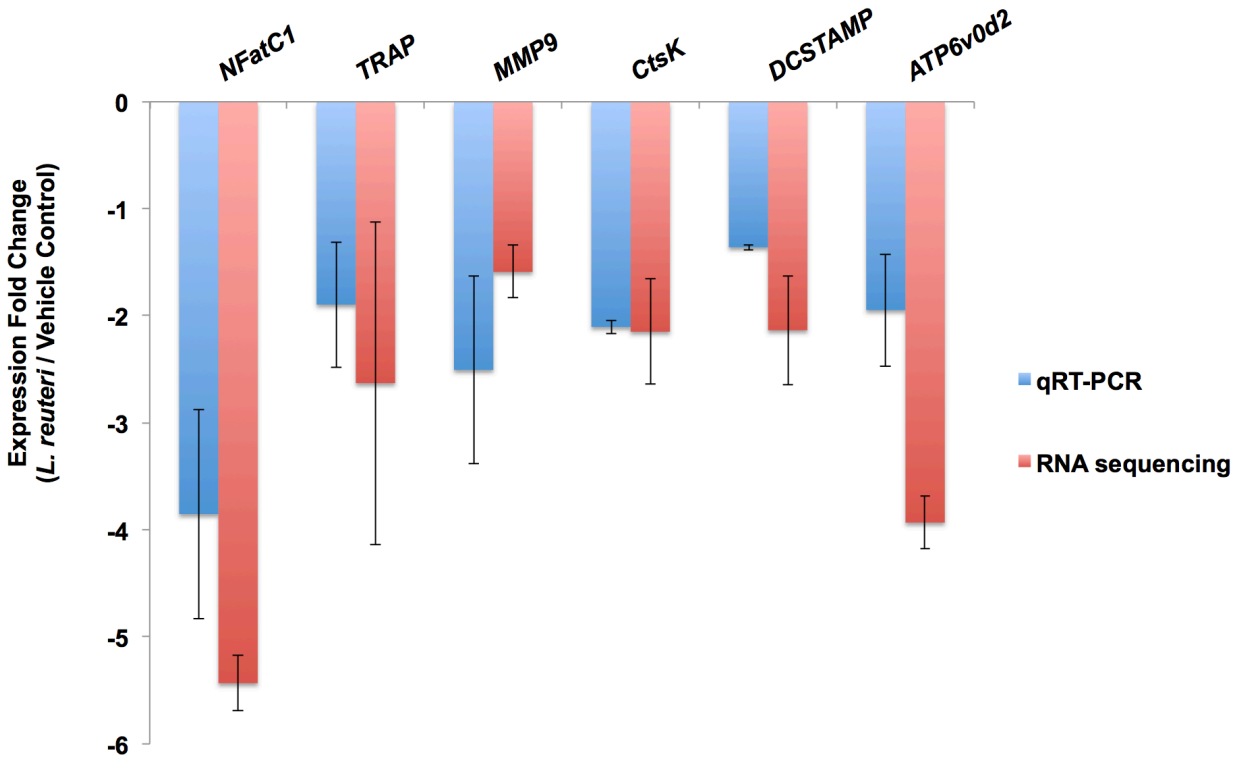

Figure 3.10. Comparison of osteoclastogenesis genes by qPCR and RNA sequencing.

Relative expression levels of genes related to osteoclastogenesis were measured by qPCR and compared to data obtained from the RNA sequencing experiment. In general, the directionality of differential expression for the genes measured was similar between both results.

3.3.8 *Activation of NF-κB and p38 in RAW264.7 cells was inhibited by L. reuteri*

RANKL initiates a cascade of intracellular signaling that culminates in the activation of NF-κB that is essential for osteoclastogenesis [60,61]. Given the importance of NF-κB to osteoclastogenesis and previous studies that demonstrated the ability of *L. reuteri* to suppress NF-κB activation, we next investigated whether *L. reuteri* impacted the NF-κB signaling pathway. Through Western blot analysis, we observed that *L. reuteri* inhibited NF-κB/p65 phosphorylation that was induced by RANKL (Figure 3.11). This was consistent with the

transcriptional analysis that indicated the NF-κB signaling pathway being down-regulated by *L. reuteri*.

Mitogen-activated protein kinases (MAPK) signaling pathways have been shown to be important for various facets of host physiology such as the immune response and cellular metabolism to name a few [62–65]. Additionally, their role in osteoclast differentiation has also been heavily studied [66–70]. To corroborate our transcriptomics findings, we performed Western blot analysis to assess the impact of *L. reuteri* on MAPK signaling. The MAPK p38, ERK, and JNK were activated with RANKL and treated with the vehicle control or *L. reuteri* CCS for 15 minutes. Interestingly, our results suggested that while ERK and JNK were unaffected by *L. reuteri* treatment, p38 activation is inhibited (Figure 3.12). Taken together, our data suggests that *L. reuteri* impacts NF-κB and p38 to suppress RANKL-induced differentiation of RAW264.7 cells.

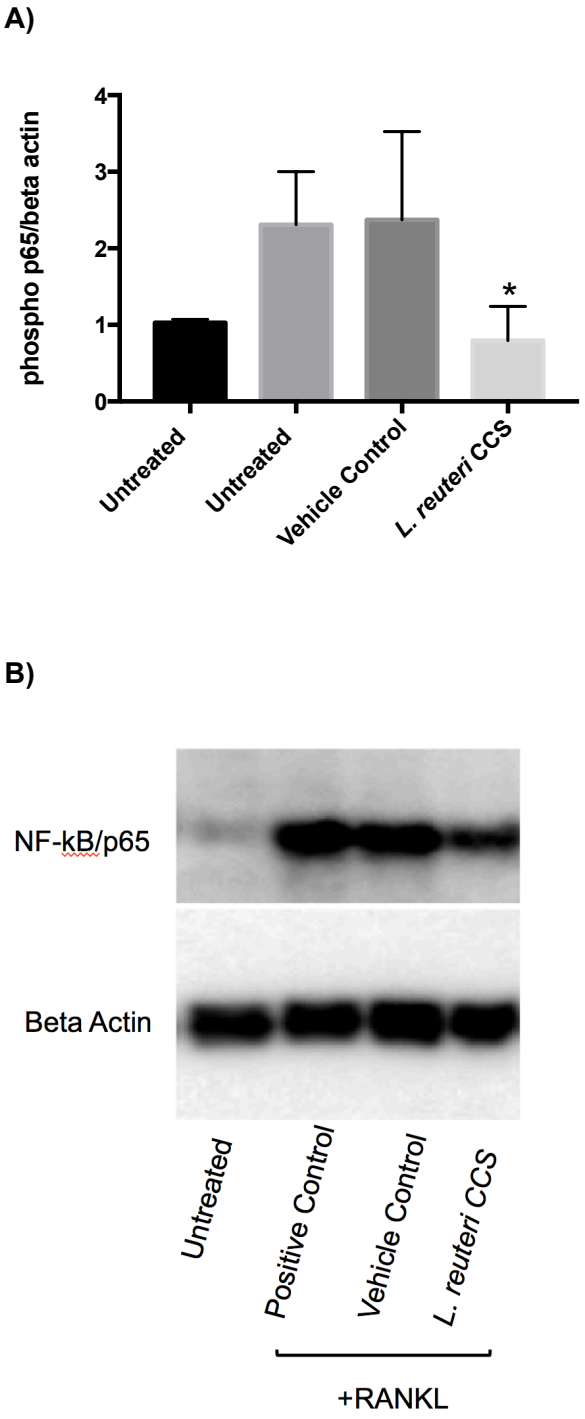

Figure 3.11. Effect of *L. reuteri* on RANKL-induced NF-κB/p65 phosphorylation.

RAW264.7 cells were concurrently treated with RANKL (100ng/ml) and MEM-α or *L. reuteri* CCS for 60 min. Total intracellular contents were prepared and an equal amount of protein was analyzed. Western blot analysis using antibodies to the phosphorylated NF-κB/p65 subunit was

Figure 3.11 (cont'd)

performed. Band intensity was measured by densitometry using the ImageJ software package. Results were normalized to levels of actin. This was performed three times in total and the reported result is a representative experiment with standard error of mean (A), *$p < 0.05$ compared to untreated and MEM-α (vehicle control) conditions as determined by one-way ANOVA.

A)

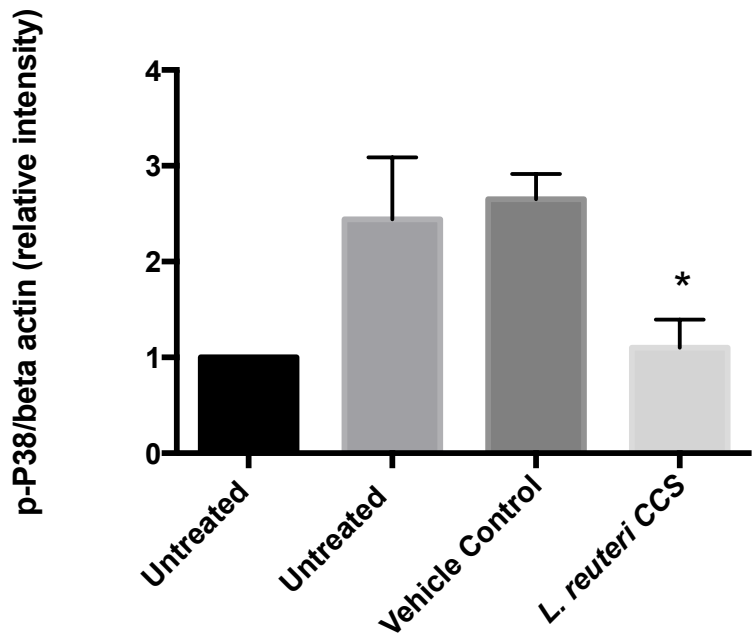

Figure 3.12**.** Impact of *L. reuteri* on MAPK signaling.

RAW264.7 cells were concurrently treated with RANKL (100ng/ml) and MEM-α or *L. reuteri* CCS for 60 min. Total intracellular contents were prepared and an equal amount of protein was analyzed. Western blot analysis using antibodies to the p38, phosphorylated p38, ERK, phosphorylated ERK, JNK, phosphorylated JNK. Band intensity was measured by densitometry using the ImageJ software package. Results were normalized to levels of actin. This was performed three times in total and the reported result is a representative experiment with standard error of mean (A), *$p < 0.05$ compared to untreated and MEM-α (vehicle control) conditions as determined by one-way ANOVA.

Figure 3.12. (cont'd)

B)

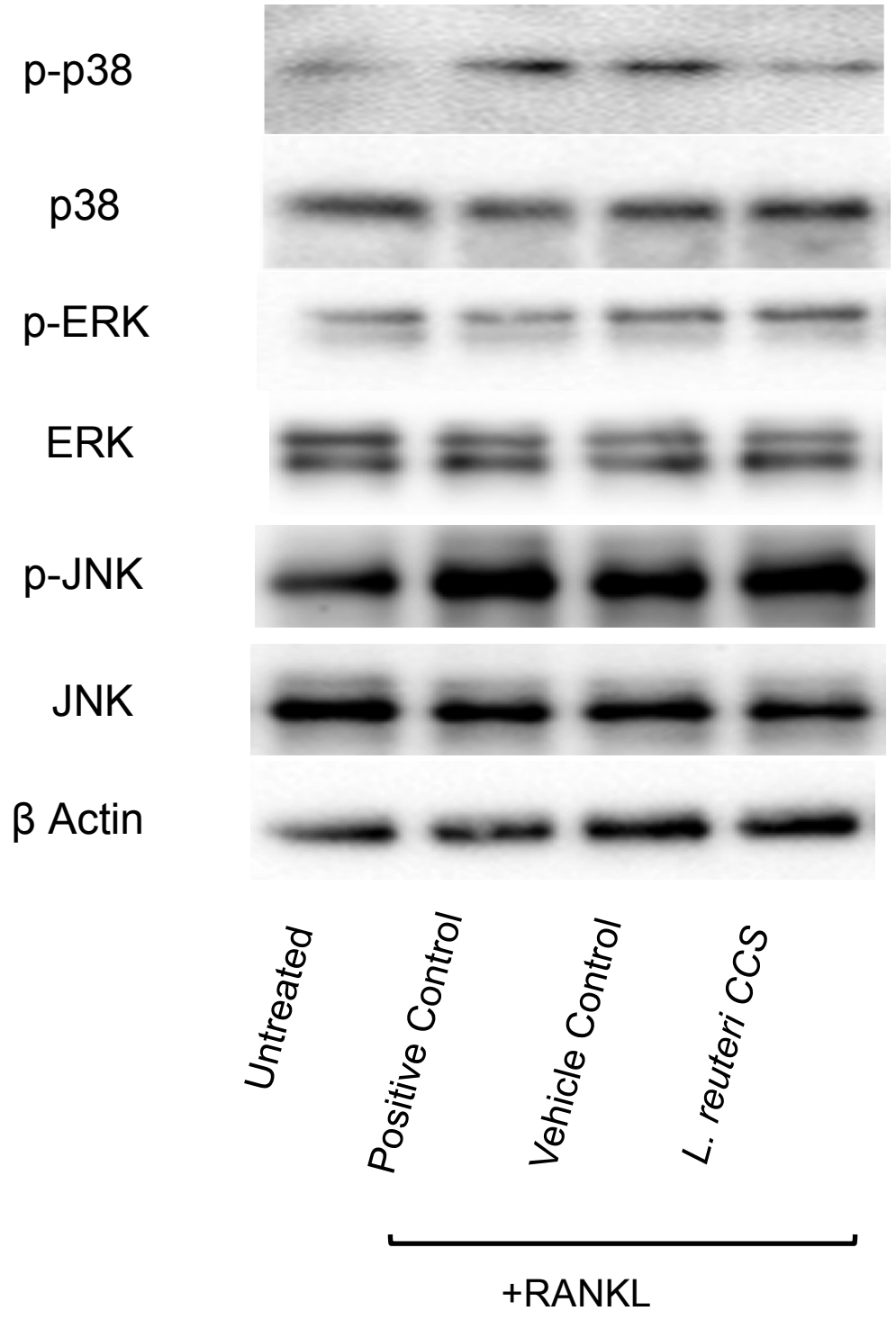

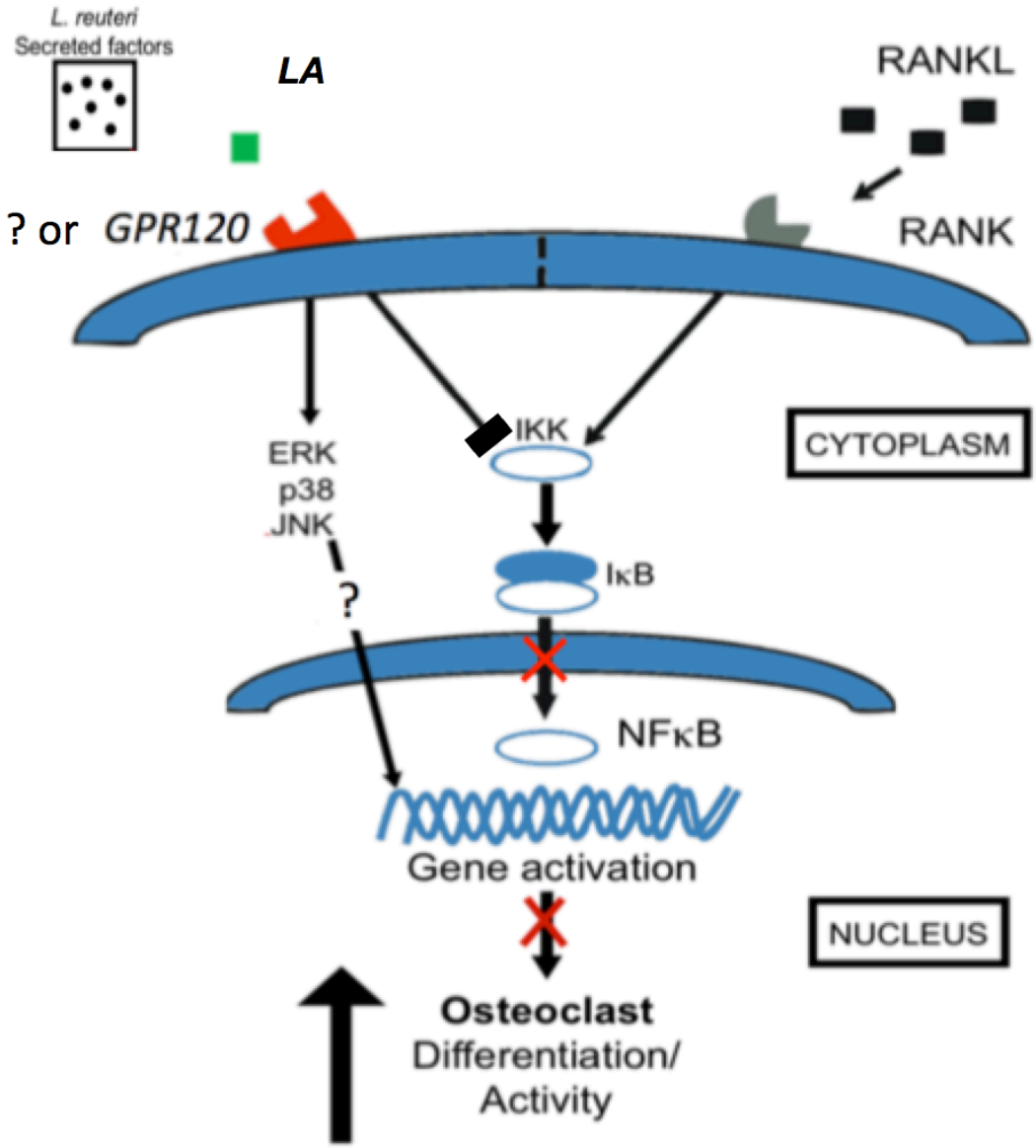

Figure 3.13. Working model of osteoclastogenesis suppression by *L. reuteri* and LA.

RAW264.7 cells are stimulated for osteoclastogenesis by RANKL. *L. reuteri* and LA activated GPR120 or a receptor yet to be identified to suppress osteoclastogenesis. GPR120 receptor antagonism partially inhibited the ability of *L. reuteri* and LA to suppress osteoclastogenesis. MAPK and NF-κB signaling has been shown to be downstream of GPR120 signaling and we demonstrated that *L. reuteri* impacts several arms of these pathways.

3.4 *Discussion*

Osteoporosis remains a growing problem worldwide. According to the International Osteoporosis Foundation, over 200 million people have low bone mass and are at increased risk for sustaining bone fractures. With advancements in research and evidence based medicine, many studies have highlighted the benefits to bone health ranging from lifestyle changes to novel medications targeting the immune and endocrine systems. While we have benefitted from these studies, a few things are becoming clearer as we continue to learn about bone. The pathogenesis of bone diseases are multifactorial, spanning influences from various organ systems that are interconnected, and continual research efforts the interaction between different systems in the body are required for the development of new treatment options that are more efficacious and cost effective.

In recent studies, an emphasis has been placed on the role that probiotics play in regulating bone health. Not only do they inhibit bone loss in localized inflammatory reactions such as bone infections or periodontitis, but they have also been shown to regulate bone mass from a distal site such as the gut [18,20,71]. Despite establishing this link between gut bacteria and bone health, very little is known mechanistically regarding how bacteria interact with bone.

Our results indicated that *L. reuteri* targeted an early stage of osteoclastogenesis using the *in vitro* RAW264.7 cell assay since a single treatment with *L. reuteri* at the beginning of the experiment was able to suppress osteoclastogenesis by 75%. The fact that *L. reuteri* was unable to suppress osteoclastogenesis when added to culture after the initiation of the assay suggested that an early stage of osteoclastogenesis signaling was targeted by *L. reuteri*. However, phenotypic changes were not apparent until days 5 and 7 where *L. reuteri* treatment resulted in an accumulation of fused polykaryons. A majority of the changes in the

transcriptional profile took place later in the assay (day 3 and 5) as very few genes were differentially regulated by *L. reuteri* at the day 1 timepoint. Together, the results indicated that early stimulation by *L. reuteri* did not impact early phenotypic or transcriptional changes in osteoclastogenesis, but sufficiently suppressed osteoclastogenesis and arrested them in a state of fused polykaryons. As a result, we focused our attention on early signaling pathways involved in osteoclastogenesis. The analysis of NF-κB and MAPK signaling activation suggested that these pathways were impacted by *L. reuteri* and is a possible explanation to why not many transcriptional changes were occurring in the beginning (Table 3.1).

The next issue we wanted to address was whether this inhibition of osteoclastogenesis by *L. reuteri* was a direct or indirect effect. It has been shown that osteoclast differentiation can be impacted indirectly by preventing the interaction between RANKL and its receptor, RANK [72]. However, the time course study suggested that *L. reuteri* does not interact with RANKL as an early pulse of RAW264.7 cells with CCS was sufficient to prevent osteoclast formation (Figure 3.3). Our investigations with LA, a long chain fatty acid produced by *L. reuteri*, demonstrated its impact on osteoclastogenesis in two ways (Figure 3.5). Using commercially bought LA, we obtained a dose-dependent inhibition of osteoclastogenesis. Additionally, CCS isolated from a mutant strain of *L. reuteri* incapable of producing LA was not as effective in suppressing osteoclastogenesis. Taken together, these results indicate that exogenous LA directly impacts osteoclastogenesis and its presence in *L. reuteri* contributes to its suppression of osteoclast differentiation. However, *L. reuteri* still maintained partial inhibition of osteoclastogenesis despite the absence of LA suggesting that other bacterial product(s) contribute to this process.

While LA production is not exclusive to *L. reuteri*, its presence in bacteria and potential for bone health suggests an evolutionary relationship that may elucidate the purpose of receptors that detect fatty acids of different carbon chain lengths. G-protein-coupled receptors (GPCR)

signaling systems have been evolutionarily conserved over time [73–75]. Its importance in regulating diseases such as cancer, obesity, and development has been the topic of much research [49,50,76,77]. More recently, the roles of the long chain fatty acid receptors, GPR40 and GPR120, have been shown to be important in bone health and regulating osteoclastogenesis [51,53,78,79]. Although studies have demonstrated the potential impact of long chain fatty acids on bone health, LA has yet to be investigated in the same context and remains a promising candidate as a novel therapeutic [80,81]. In our studies, we established that GPR120, but not GPR40, was important for the suppression of osteoclastogenesis by *L. reuteri* or LA. Future studies directed at testing the impact of LA on *in vivo* osteoclastogenesis and bone health will be crucial for determining whether it can potentially be a novel therapeutic for bone health.

In the present study, we have established that early signaling events in osteoclastogenesis are targeted by *L. reuteri*. Additionally, we have uncovered a role for the fatty acid LA in osteoclastogenesis. In addition to suppressing osteoclastogenesis, we also demonstrated that *L. reuteri* inhibited osteoclast function as bone resorption was decreased on plates coated with calcium and phosphate. In a working model, we propose that *L. reuteri* impacts osteoclast differentiation by targeting P38 and NF-κB activation through a receptor that has yet to be discovered. However, LA produced by *L. reuteri* is important for this inhibition and signaling through GPR120 also plays an important role (Figure 3.13).

With the emergence of microbiome research, the importance of studies identifying and understanding how bioactive compounds are beneficial to health remains a priority. With this knowledge in hand, we come one step closer towards deciphering the mystery of how microbes in the gut regulate bone health.

BIBLIOGRAPHY

BIBLIOGRAPHY

1. Asagiri, M. & Takayanagi, H. The molecular understanding of osteoclast differentiation. *Bone* **40,** 251–64 (2007).

2. Hirayama, T., Danks, L., Sabokbar, a & Athanasou, N. a. Osteoclast formation and activity in the pathogenesis of osteoporosis in rheumatoid arthritis. *Rheumatology (Oxford).* **41,** 1232–1239 (2002).

3. Cenci, S. *et al.* Estrogen deficiency induces bone loss by enhancing T-cell production of TNF-alpha. *J. Clin. Invest.* **106,** 1229–37 (2000).

4. Algate, K., Haynes, D. R., Bartold, P. M., Crotti, T. N. & Cantley, M. D. The effects of tumour necrosis factor-α on bone cells involved in periodontal alveolar bone loss; osteoclasts, osteoblasts and osteocytes. *J. Periodontal Res.* (2015). doi:10.1111/jre.12339

5. Kimble, R. B., Srivastava, S., Ross, F. P., Matayoshi, A. & Pacifici, R. Estrogen deficiency increases the ability of stromal cells to support murine osteoclastogenesis via an interleukin-1and tumor necrosis factor- mediated stimulation of macrophage colony-stimulating factor production. *J Biol Chem* **271,** 28890–7. (1996).

6. Feng, X. Regulatory roles and molecular signaling of TNF family members in osteoclasts. *Gene* **350,** 1–13 (2005).

7. Srivastava, S. *et al.* Estrogen decreases TNF gene expression by blocking JNK activity and the resulting production of c-Jun and JunD. *J. Clin. Invest.* **104,** 503–513 (1999).

8. Weitzmann, M. N. The Role of Inflammatory Cytokines, the RANKL/OPG Axis, and the Immunoskeletal Interface in Physiological Bone Turnover and Osteoporosis. *Scientifica (Cairo).* **2013,** 125705 (2013).

9. Most, W., Van der Wee-Pals, L., Ederveen, A., Papapoulos, S. & Löwik, C. Ovariectomy and orchidectomy induce a transient increase in the osteoclastogenic potential of bone marrow cells in the mouse. *Bone* **20,** 27–30 (1997).

10. Bellido, T. *et al.* Regulation of interleukin-6, osteoclastogenesis, and bone mass by androgens: The role of the androgen receptor. *J. Clin. Invest.* **95,** 2886–2895 (1995).

11. Morelli, L. & Capurso, L. FAO/WHO Guidelines on Probiotics. *J. Clin. Gastroenterol.* **46,** S1–S2 (2012).

12. Narva, M. *et al.* Effects of Long-Term Intervention with *Lactobacillus helveticus*-Fermented Milk on Bone Mineral Density and Bone Mineral Content in Growing Rats. *Ann. Nutr. Metab.* **48,** 228–234 (2004).

13. Narva, M. *et al.* Effects of Bioactive Peptide, Valyl-Prolyl-Proline (VPP), and <i>Lactobacillus helveticus</i> Fermented Milk Containing VPP on Bone Loss in Ovariectomized Rats. *Ann. Nutr. Metab.* **51,** 65–74 (2007).

14. Mutuş, R. *et al.* The effect of dietary probiotic supplementation on tibial bone characteristics and strength in broilers. *Poult. Sci.* **85,** 1621–1625 (2006).

15. Chiang, S. S. & Pan, T. M. Antiosteoporotic effects of lactobacillus-fermented soy skim milk on bone mineral density and the microstructure of femoral bone in ovariectomized mice. *J. Agric. Food Chem.* **59,** 7734–7742 (2011).

16. Tomofuji, T. *et al.* Supplementation of broccoli or Bifidobacterium longum-fermented broccoli suppresses serum lipid peroxidation and osteoclast differentiation on alveolar bone surface in rats fed a high-cholesterol diet. *Nutr. Res.* **32,** 301–307 (2012).

17. McCabe, L. R., Irwin, R., Schaefer, L. & Britton, R. A. Probiotic use decreases intestinal inflammation and increases bone density in healthy male but not female mice. *J. Cell. Physiol.* **228,** 1793–8 (2013).

18. Britton, R. A. *et al.* Probiotic L. reuteri Treatment Prevents Bone Loss in a Menopausal Ovariectomized Mouse Model. *Journal of Cellular Physiology* **229,** 1822–1830 (2014).

19. Collins, F. L. *et al.* Lactobacillus reuteri 6475 Increases Bone Density in Intact Females Only under an Inflammatory Setting. *PLoS One* **11,** e0153180 (2016).

20. Ohlsson, C. *et al.* Probiotics Protect Mice from Ovariectomy-Induced Cortical Bone Loss. *PLoS One* **9,** e92368 (2014).

21. Rahman, M. M., Bhattacharya, A. & Fernandes, G. Conjugated linoleic acid inhibits osteoclast differentiation of RAW264.7 cells by modulating RANKL signaling. *J. Lipid Res.* **47,** 1739–1748 (2006).

22. Ewaschuk, J. B., Walker, J. W., Diaz, H. & Madsen, K. L. Bioproduction of Conjugated Linoleic Acid by Probiotic Bacteria Occurs In Vitro and In Vivo in Mice1,2. *J. Nutr.* **136,** 1483–1487 (2006).

23. Jones, S. E. *et al.* Cyclopropane fatty acid synthase mutants of probiotic human-derived lactobacillus reuteri are defective in TNF inhibition. *Gut Microbes* **2,** 69–79 (2011).

24. Kimble, R. B., Bain, S. & Pacifici, R. The functional block of TNF but not of IL-6 prevents bone loss in ovariectomized mice. *J. Bone Miner. Res.* **12,** 935–941 (1997).

25. Srivastava, S. *et al.* Estrogen decreases TNF gene expression by blocking JNK activity and the resulting production of c-Jun and JunD. *J. Clin. Invest.* **104,** 503–13 (1999).

26. Weitzmann, M. N. & Pacifici, R. Estrogen regulation of immune cell bone interactions. *Ann. N. Y. Acad. Sci.* **1068,** 256–274 (2006).

27. Cornish, J. *et al.* Modulation of osteoclastogenesis by fatty acids. *Endocrinology* **149,** 5688–5695 (2008).

28. Drosatos-Tampakaki, Z. *et al.* Palmitic acid and DGAT1 deficiency enhance osteoclastogenesis, while oleic acid-induced triglyceride formation prevents it. *J. Bone Miner. Res.* **29,** 1183–1195 (2014).

29. Rahman, M. M., Halade, G. V, Williams, P. J. & Fernandes, G. t10c12-CLA maintains higher bone mineral density during aging by modulating osteoclastogenesis and bone marrow adiposity. *J. Cell. Physiol.* **226,** 2406–14 (2011).

30. Zwart, S. R., Pierson, D., Mehta, S., Gonda, S. & Smith, S. M. Capacity of omega-3 fatty acids or eicosapentaenoic acid to counteract weightlessness-induced bone loss by inhibiting NF-kappaB activation: from cells to bed rest to astronauts. *J. bone Miner. Res.* **25,** 1049–1057 (2010).

31. Anders, S. *et al.* Count-based differential expression analysis of RNA sequencing data using R and Bioconductor. *Nat. Protoc.* **8,** 1765–1786 (2013).

32. Luo, W., Friedman, M. S., Shedden, K., Hankenson, K. D. & Woolf, P. J. GAGE: generally applicable gene set enrichment for pathway analysis. *BMC Bioinformatics* **10,** 161 (2009).

33. Pfaffl, M. W. A new mathematical model for relative quantification in real-time RT-PCR. *Nucleic Acids Res.* **29,** e45 (2001).

34. Girish, V., Vijayalakshmi, a. Affordable Image Analysis using NIH Image / ImageJ. *Indian J. Cancer* **41,** 47 (2004).

35. Yang, M. *et al.* Osteoclast stimulatory transmembrane protein (OC-STAMP), a novel protein induced by RANKL that promotes osteoclast differentiation. *J. Cell. Physiol.* **215,** 497–505 (2008).

36. Yagi, M. *et al.* DC-STAMP is essential for cell-cell fusion in osteoclasts and foreign body giant cells. *J. Exp. Med.* **202,** 345–51 (2005).

37. Cuetara, B. L. V, Crotti, T. N., O'Donoghue, A. J. & McHugh, K. P. Cloning and characterization of osteoclast precursors from the RAW264.7 cell line. *In Vitro Cell. Dev. Biol. Anim.* **42,** 182–8 (2006).

38. Ikeda, K. & Takeshita, S. The role of osteoclast differentiation and function in skeletal homeostasis. *J. Biochem.* **159,** mvv112 (2015).

39. Teitelbaum, S. L., Tondravi, M. M. & Ross, F. P. Osteoclasts, macrophages, and the molecular mechanisms of bone resorption. *J. Leukoc. Biol.* **61,** 381–388 (1997).

40. Zhang, R. *et al.* Bone Resorption by Osteoclasts. *Science (80-.).* **289,** 1504–1508 (2000).

41. Weinberg, J. B., Hobbs, M. M. & Misukonis, M. A. Recombinant human gamma-interferon induces human monocyte polykaryon formation. *Proc. Natl. Acad. Sci. U. S. A.* **81,** 4554–7 (1984).

42. Kwon, J.-O., Jin, W. J., Kim, B., Kim, H.-H. & Lee, Z. H. Myristoleic acid inhibits osteoclast formation and bone resorption by suppressing the RANKL activation of Src and Pyk2. *Eur. J. Pharmacol.* **768,** 189–98 (2015).

43. Aharon, R. & Bar-Shavit, Z. Involvement of aquaporin 9 in osteoclast differentiation. *J. Biol. Chem.* **281,** 19305–19309 (2006).

44. Boyle, W. J., Simonet, W. S. & Lacey, D. L. Osteoclast differentiation and activation. *Nature* **423,** 337–42 (2003).

45. Brodbeck, W. G. & Anderson, J. M. Giant cell formation and function. *Curr. Opin. Hematol.* **16,** 53–57 (2009).

46. Miyamoto, H. *et al.* An essential role for STAT6-STAT1 protein signaling in promoting macrophage cell-cell fusion. *J. Biol. Chem.* **287,** 32479–32484 (2012).

47. Kim, H.-J., Yoon, H.-J., Kim, S.-Y. & Yoon, Y.-R. A medium-chain fatty acid, capric acid, inhibits RANKL-induced osteoclast differentiation via the suppression of NF-κB signaling and blocks cytoskeletal organization and survival in mature osteoclasts. *Mol. Cells* **37,** 598–604 (2014).

48. Kasonga, A. E., Deepak, V., Kruger, M. C. & Coetzee, M. Arachidonic acid and docosahexaenoic acid suppress osteoclast formation and activity in human CD14+ monocytes, in vitro. *PLoS One* **10,** e0125145 (2015).

49. Oh, D. Y. *et al.* A Gpr120-selective agonist improves insulin resistance and chronic inflammation in obese mice. *Nat. Med.* **20,** 942–7 (2014).

50. Oh, D. Y. *et al.* GPR120 Is an Omega-3 Fatty Acid Receptor Mediating Potent Anti-inflammatory and Insulin-Sensitizing Effects. *Cell* **142,** 687–698 (2010).

51. Kim, H. J. *et al.* G Protein-Coupled Receptor 120 Signaling Negatively Regulates Osteoclast Differentiation, Survival, and Function. *J. Cell. Physiol.* 844–851 (2015). doi:10.1002/jcp.25133

52. Covington, D. K., Briscoe, C. A., Brown, A. J. & Jayawickreme, C. K. The G-protein-coupled receptor 40 family (GPR40-GPR43) and its role in nutrient sensing. *Biochem Soc Trans* **34,** 770–773 (2006).

53. Wauquier, F. *et al.* The free fatty acid receptor G protein-coupled receptor 40 (GPR40) protects from bone loss through inhibition of osteoclast differentiation. *J. Biol. Chem.* **288,** 6542–51 (2013).

54. Lesclous, P. *et al.* Histamine mediates osteoclastic resorption only during the acute phase of bone loss in ovariectomized rats. *Exp. Physiol.* **91,** 561–70 (2006).

55. Thomas, C. M. *et al.* Histamine derived from probiotic lactobacillus reuteri suppresses tnf via modulation of pka and erk signaling. *PLoS One* **7,** (2012).

56. Love, M. I., Huber, W. & Anders, S. Moderated estimation of fold change and dispersion for RNA-seq data with DESeq2. *Genome Biol.* **15,** 550 (2014).

57. Zhang, Q. *et al.* cDNA microarray analysis of the differentially expressed genes involved in murine pre-osteoclast RAW264.7 cells proliferation stimulated by dexamethasone. *Life Sci.* **82,** 135–48 (2008).

58. Yang, G. *et al.* Functional grouping of osteoclast genes revealed through microarray analysis. *Biochem. Biophys. Res. Commun.* **366,** 352–359 (2008).

59. Iyer, C. *et al.* Probiotic Lactobacillus reuteri promotes TNF-induced apoptosis in human myeloid leukemia-derived cells by modulation of NF-κB and MAPK signalling. *Cell. Microbiol.* **10,** 1442–1452 (2008).

60. Strait, K., Li, Y., Dillehay, D. L. & Weitzmann, M. N. Suppression of NF-kappaB activation blocks osteoclastic bone resorption during estrogen deficiency. *Int. J. Mol. Med.* **21,** 521–5 (2008).

61. Boyce, B. F., Xiu, Y., Li, J., Xing, L. & Yao, Z. NF-κB-Mediated Regulation of Osteoclastogenesis. *Endocrinol. Metab. (Seoul, Korea)* **30,** 35–44 (2015).

62. Eriksson, M., Taskinen, M. & Leppä, S. Mitogen Activated Protein Kinase-Dependent Activation of c-Jun and c-Fos is required for Neuronal differentiation but not for Growth and Stress Reposne in PC12 cells. *J. Cell. Physiol.* **207,** 12–22 (2006).

63. Li, C. Y., Yang, L. C., Guo, K., Wang, Y. P. & Li, Y. G. Mitogen-activated protein kinase phosphatase-1: A critical phosphatase manipulating mitogen-activated protein kinase signaling in cardiovascular disease (Review). *Int. J. Mol. Med.* **35,** 1095–1102 (2015).

64. Arthur, J. S. & Ley, S. C. Mitogen-activated protein kinases in innate immunity. *Nat Rev Immunol* **13,** 679–692 (2013).

65. Alam, H., Gu, B. & Lee, M. G. Histone methylation modifiers in cellular signaling pathways. *Cell. Mol. Life Sci.* **72,** 4577–4592 (2015).

66. Sharma, S. M. *et al.* MITF and PU.1 recruit p38 MAPK and NFATc1 to target genes during osteoclast differentiation. *J. Biol. Chem.* **282,** 15921–15929 (2007).

67. Huang, H. *et al.* Osteoclast differentiation requires TAK1 and MKK6 for NFATc1 induction and NF-kappaB transactivation by RANKL. *Cell Death Differ.* **13,** 1879–1891 (2006).

68. Ihn, H. J. *et al.* Inhibitory effects of KP-A159, a thiazolopyridine derivative, on osteoclast differentiation, function, and inflammatory bone loss via suppression of RANKL-Induced MAP Kinase signaling pathway. *PLoS One* **10,** 1–13 (2015).

69. Nie, S. *et al.* Salicortin inhibits osteoclast differentiation and bone resorption by down-regulating JNK and NF-κB/NFATc1 signaling pathways. *Biochem. Biophys. Res. Commun.* **470,** 61–67 (2016).

70. Chen, N., Gao, R.-F., Yuan, F.-L. & Zhao, M.-D. Recombinant Human Endostatin Suppresses Mouse Osteoclast Formation by Inhibiting the NF-κB and MAPKs Signaling Pathways. *Front. Pharmacol.* **7,** 1–10 (2016).

71. Maekawa, T. & Hajishengallis, G. Topical treatment with probiotic *Lactobacillus brevis* CD2 inhibits experimental periodontal inflammation and bone loss. *J. Periodontal Res.* **49,** 785–791 (2014).

72. Zhao, H. *et al.* Osteoprotegerin exposure at different stages of osteoclastogenesis differentially affects osteoclast formation and function. *Cytotechnology* (2015). doi:10.1007/s10616-015-9892-7

73. Krishnan, A. & Schiöth, H. B. The role of G protein-coupled receptors in the early evolution of neurotransmission and the nervous system. *J. Exp. Biol.* **218,** 562–571 (2015).

74. Corrêa-Oliveira, R., Fachi, J. L., Vieira, A., Sato, F. T. & Vinolo, M. A. R. Regulation of immune cell function by short-chain fatty acids. *Clin. Transl. Immunol.* **5,** e73 (2016).

75. Mushegian, A., Gurevich, V. V. & Gurevich, E. V. The origin and evolution of G protein-coupled receptor kinases. *PLoS One* **7,** 1–12 (2012).

76. Marivin, A. *et al.* Dominant-negative Gα subunits are a mechanism of dysregulated heterotrimeric G protein signaling in human disease. *Sci. Signal.* **9,** ra37–ra37 (2016).

77. Yu, O. M. & Brown, J. H. G Protein-Coupled Receptor and RhoA-Stimulated Transcriptional Responses: Links to Inflammation, Differentiation, and Cell Proliferation. *Mol. Pharmacol.* **88,** 171–180 (2015).

78. Philippe, C., Wauquier, F., Lyan, B., Coxam, V. & Wittrant, Y. GPR40, a free fatty acid receptor, differentially impacts osteoblast behavior depending on differentiation stage and environment. *Mol. Cell. Biochem.* **412,** 197–208 (2016).

79. Ahn, S. H. *et al.* Free Fatty Acid Receptor 4 (GPR120) Stimulates Bone Formation and Suppresses Bone Resorption in the Presence of Elevated n -3 Fatty Acid Levels. *Endocrinology* **4,** en.2015–1855 (2016).

80. Bonnet, N. & Ferrari, S. L. Effects of long-term supplementation with omega-3 fatty acids on longitudinal changes in bone mass and microstructure in mice. *J. Nutr. Biochem.* **22,** 665–672 (2011).

81. Chen, T. Y. *et al.* Endogenous n-3 polyunsaturated fatty acids (PUFAs) mitigate ovariectomy-induced bone loss by attenuating bone marrow adipogenesis in FAT1 transgenic mice. *Drug Des. Devel. Ther.* **7,** 545–552 (2013).

CHAPTER 4. ROLE OF THE GUT MICROBIOTA IN BONE HEALTH

4.1 *Introduction*

In the past two decades, we have witnessed a dramatic increase in studies characterizing how the microbiota, or the collection of microorganisms colonizing at different host sites, contributes to health and disease. At birth, humans become exposed to microorganisms that establish colonization at various sites such as the skin, mouth, gastrointestinal (GI) tract, and the vaginal epithelium. This intimate relationship between the host and their microbial counterparts has led many to believe that they provide various benefits to health and ultimately survival. Prior to the advent of culture-independent characterization methods, it was difficult to study the role of the microbiota in health and disease due to limitations in culturing many of the members in these communities. However, advancements in sequencing technology coupled with the development of animal disease models have greatly aided attempts to understand roles played by different members of the microbiome. This has lead to multiple hallmark studies linking the importance of the microbiota and various diseases with examples that include obesity, diabetes, and atherosclerosis [1–4].

Of the many functions attributable to the microbiota, one would be its role in the development and modulation of the immune system. For example, germ free (GF) mice have decreased gut lymphoid tissue development as well as altered microvilli architecture [5,6]. Moreover, expression levels of pattern recognition receptors (e.g. Toll, NOD-like) important for detecting microbes and antimicrobial peptides (e.g. Reg3γ) are also decreased in GF mice strongly highlighting how the microbiota impacts the functional role of the immune system [6,7]. In animal disease models, the ability to mount an immune response is also hindered in GF animals and restored upon conventionalization (i.e. restoration of microbiota from an animal raised under standard laboratory conditions) [8,9]. However, these responses appear to be microbe specific as only selective colonization by some organisms protect against *Shigella flexneri*

enteric infection [8]. Taken together, these results suggest a complex communication network between the gut and the microbes it encounters to regulate health.

Recently, more emphasis has been placed on the role of the microbiota in skeletal health. The rationale for this is due to the known impact of the microbiota on multiple facets of the immune system, the importance of the immune system in bone remodeling, and the gut that serves as a messenger between the two. Bone remodeling, which is composed of the coupled processes of bone formation and bone resorption, undergoes various phases throughout life. In early human life, bone formation outweighs bone resorption and contributes to increased bone deposition until a plateau is reached around the mid twenties [10]. Then, a shift in favor of bone resorption takes place with bone loss gradually increasing over time. Different pathologies can accelerate bone loss by impacting the processes of bone formation and bone resorption, which are carried out by the osteoblast and osteoclast, respectively. Under many different pathological bone conditions, the primary driver of bone loss is due to increased osteoclastic bone resorption that is often times mediated by immune signaling [11,12].

Osteoclasts originate from a hematopoietic stem cell lineage and many studies have demonstrated its interaction and regulation by immune cells such and B and T cells [13–15]. These cells are shown to drive the formation of osteoclasts from their monocyte precursors [16]. In addition to impacting the local immune response in the gut, the microbiota has also been shown to regulate the immune response and hematopoiesis at distant sites such as the bone marrow compartment [17]. Thus, we and others hypothesize that the gut microbiota can be impacting bone health through its regulation of the immune system [18–20].

Despite relatively few studies assessing the impact of the microbiota on skeletal health, data from previous studies suggested that bone density is highly regulated by the presence of the microbiota. These early studies revolved around the use of GF mouse models. By comparing female GF mice and conventionalized (CONV-D) mice in the C57bl/6 genetic background, it was demonstrated that the gut microbiota decreased bone mass [18]. A link was

established between an expansion in osteoclast precursor cells, CD4+ T cells, and serum serotonin levels in the CONV-D mice with decreased bone mass. These results were consistent with other studies showing that increased immune cell populations and serotonin levels are important driving factors in the development of osteoporosis [21–23]. Conversely, Schwarzer et al. demonstrated that various bone parameters were actually decreased in GF BALB/c animals in comparison to WT mice [24]. In more recent studies, the presence of the microbiota was required in order for bone loss to occur during estrogen deficiency [20].

Although these studies indicated that bone density is highly regulated by the presence of the microbiota, they presented conflicting results and did not resolve the roles that specific microbial community member(s) play in determining bone health. In this study, we set out to identify specific bacterial species that impact bone health by colonizing GF Swiss Webster (SW) mice with microbial communities from diverse fecal donors and characterizing the impact of these communities on bone health. Contrary to results published by Sjögren et al., our results demonstrated that the colonization of GF mice does not lead to a decrease in bone mass. Studies were performed in both the Swiss Webster and C57bl/6 genetic backgrounds. Through comparative 16S rRNA gene analysis, we identified separate and distinct clustering of microbial communities based upon mouse genetic background. Our sequencing depth permitted genus level identification of microbes and enabled us to develop a catalog of microbes (based off of operational taxonomic units (OTUs)) while characterizing their effect on different bone parameters. What still remains to be elucidated is the role that specific microbial community member(s) play in determining bone health and these results serve as the foundation for future studies aimed at discovering how bacteria modulate bone health.

4.2 *Materials and Methods*

4.2.1 *Germ Free Mouse Husbandry*

The Institutional Animal Care and Use Committee (IACUC) at Baylor College of Medicine approved all the protocols performed in this study. GF wild-type (WT) mice in the Swiss Webster and C57bl/6 genetic background were generated by the Baylor College of Medicine GF mouse facility. Germ-free mice were housed in flexible film isolators (Class Biologically Clean, Madison, WI) supplied with HEPA-filtered air. Room light cycle was 12:12 light:dark. Mice were given autoclaved food (5V5R, LabDiet, St. Louis, MO) and sterile tap water. Germ-free status was verified through collection of composite mouse and isolator environmental samples which were subjected to aerobic, anaerobic, and fungal culture. Gram stained smears of these samples were also visually examined. Isolators were tested weekly during initial validation and twice monthly once established. Mice used in this study were confirmed free of all bacteria, fungi, and metazoans by these methods.

Viral infection status was verified by quarterly serology for excluded murine pathogens. Mice in the facility are specific pathogen free (SPF) for the following excluded viruses: sendai virus, pneumonia virus of mice, mouse hepatitis virus, minute virus of mice, Theiler's murine encephalomyelitis virus, reovirus, lymphocytic choriomeningitis, ectromelia virus, K virus, polyoma virus, mouse adenovirus, rotavirus, mouse cytomegalovirus, hantavirus, mouse parvovirus, and mouse norovirus.

The exclusion list for the SPF facility include bacteria and metazoans, which we know aren't present in germ-free: *Mycoplasma pulmonis*, *Helicobacter*, *Pseudomonas*, *Campylobacter*, *Salmonella*, *Citrobacter*, helminth intestinal parasites (pinworms) including *Aspicularis tetraptera*

and *Syphacia obvelata*, and ectoparasites (fur mites) including *Radfordia affinis*, *Myobia musculi*, and *Myocoptes musculinus.*

4.2.2 *Preparation of Cecal and Fecal Samples and inoculation of the GF animals*

Cecal contents were collected from conventionally-raised Swiss Webster and C57bl/6 mice following euthanasia with 5% isoflurane until breathing cessation. Confirmation of euthanasia was executed by cervical dislocation and/or decapitation. Cecal contents were expression from the cecum into a 1.7 mL eppendorf tube and transferred into the anaerobic chamber for further processing. Human fecal samples were collected and stored at -80 °C as previously described [25]. Survey data indicated that one volunteer was a vegetarian and the other volunteer was an omnivore. Samples from the omnivorous donor came from two time points: one shortly after broad-spectrum antibiotic treatment and the other a year following antibiotic treatment to allow for the recovery of the microbiota. Prior to use, cecal and fecal samples were resuspended in 25% w/v phosphate buffered saline that was pre-reduced overnight in an anaerobic chamber. Samples were vortexed for 5 minutes at 2500 revolutions per minute (rpm) on a plate shaker followed by a centrifugation step for 5 minutes at 200 X g rpm to facilitate the removal of the larger particles. 100uL of the supernatant portion was used to gavage each GF animal for conventionalization. All the remaining material was saved and stored in 20% glycerol at -80 °C. Surveying identified one as a vegetarian and the other as an omnivore. The omnivore donated samples at two time points. One came shortly after broad-spectrum antibiotic treatment and the other was a year following that to allow for the recovery of the microbiota.

4.2.3 *Gavage and Sample Collection*

At four weeks of age, GF mice were conventionalized with mouse cecal contents or human fecal samples (as indicated in results) by intragastric gavage. At various times throughout the studies, fecal samples were collected as mice defecated and stored at -80°C. Calcein (10 mg/kg,

intraperitoneally) was injected 7 days and 2 days before euthanasia to evaluate the dynamics of bone formation. Mice were euthanized with 5% isoflurane for one minute following breathing cessation. Confirmation of euthanasia was executed by cervical dislocation and/or decapitation. Retro-orbital bleeding was performed for blood collection and serum separation was achieved by centrifugation at 4°C at 7500rpm for 10 minutes. Serum samples were stored at -80°C. Intestinal sections were collected quickly after euthanasia and stored at -80°C. Cecal contents were expressed from the cecum into a 1.7mL eppendorf tube for storage at -80°C. Femurs were fixed in 10% paraformaldehyde for 3 days and then stored in 70% ethanol at 4°C until micro-computed tomography imaging. Following imaging, femurs were paraffin embedded for histomorphometry.

4.2.4 *Micro Computed Tomography (μCT) Analysis of Bone*

μCT was performed as described in [26]. Briefly, femurs stored in 70% ethanol were scanned using a Scanco μCT-40 sytem (Scanco Medical AG, Brüttsellen, Switzerland) located in the Micro-CT Core at Baylor College of Medicine. Scans were reconstructed at a 16μm isotropic voxel size. Analysis of trabecular (cancellous) bone was performed by manually contouring a region composed of 75 slices (=1.2mm) in the distal metaphyseal region of the femur. Parameters that include bone volume fraction (BVF as defined by bone volume per total volume analyzed (BV/TV)), tissue mineral density (TMD), trabecular thickness (Tb. Th.), trabecular number (Tb. N.), and trabecular spacing (Tb. Sp.) were measured using the Scanco software using a threshold value of 250. The length of the femur was measured between the medial condyle and the top of the femoral head. Analysis of cortical bone parameters was executed using an automated thresholding algorithm that is part of the Scanco software package. The region of interest captured a distance spanning 50 slices (=0.8mm) between the midshaft of the femur towards the distal femur and was measured with a threshold value of 220 using the software package.

4.2.5 *Static and Dynamic Histomorphometry*

Fixed femurs (n = 4-6 per group) were processed as previously described [27,28]. Briefly, fixed femurs were paraffin embedded, sectioned, and analyzed by microscopy. Calcein (100 µl of 20 mg/ml dissolved in sterile saline) was supplemented by gavage at 7 days and 2 days prior to the end of experiment. This incorporation into growing bone allowed for bone formation rate (BFR) and mineral apposition rate (MAR) measurements through quantitating the amount of calcein along the bone surface. The distances between the calcein lines and length along the bone surface were used to measure the MAR and BFR, respectively. A commercially available kit (Catalog number 387A, Sigma, St. Louis, MO) was used to quantitate tartrate resistant alkaline phosphatase (TRAP) activity, a measure of osteoclasts present, from sectioned trabecular bone.

4.2.6 *Quantitative Real Time PCR (qRT-PCR)*

RNA extraction was performed with TRI Reagent (Cat. NO. TR 118, Molecular Research Center). Synthesis of cDNA was performed with Superscript III Reverse Transcriptase (Cat. No. 8080093, Thermo Fisher Scientific). A total of 1 µg of RNA was reverse transcribed. Briefly, an Eppendorf Mastercycler EP S was preheated to 65 °C. The mixture containing RNA, 100 ng of random hexamers, (Cat. No.C1181, Promega) and 1 µl of 10nM dNTPs (Cat. No. 18427088) was placed into the thermocycler for 5 mins. Following 1 min on ice, a mixture containing the reverse transcriptase and RNaseOUT was added to complete the cDNA synthesis. A cycle of 10 min at 25°C, 50 min at 50°C, and then 85°C for 5 min was used. The cDNA was used immediately or stored at -20°C. The qPCR reactions reactions contained 1 µl of cDNA, 1 µl of each forward and reverse primer (10 µM), 7 µl of nuclease free water, and 10 µl of SYBR Green PCR Master Mix (Cat. No. 170-8882, BioRad,inc.). A 2-step PCR amplification protocol was used with acquisition at the annealing and melting curve steps. The protocol included an initial denaturation at 95°C for 30 s, followed by 40 cycles of denaturing at 95°C for 10 s, annealing at

51°C for 20 s. A melting curve was performed at the end at 95°C for 15 s and ramping up from 60°C to 95°C at a rate of +0.2°C/sec. Data analysis was performed according to the method described by Pfaffl [29]. The primer sequences used are as follows: HPRT Forward 5' GCTATAAATTCTTTGCTGACCTGCT 3', HPRT Reverse 5' AATTACTTTTATGTCCCCTGTTGACTG 3', TNF-α Forward 5' AGGCTGCCCCGACTACGT 3', TNF-α Reverse 5' GACTTTCTCCTGGTATGAGATAGCAA 3', IL-1 Forward 5' TCCCCGTCCCTATCGACAAAC 3', IL-1 Reverse 5' GCGGTGATGTGGCATTTTCTG 3', IL-6 Forward 5' ATCCAGTTGCCTTCTTGGGACTGA 3', IL-6 Reverse 5' TAAGCCTCCGACTTGTGAAGTGGT 3', 5-HTT Forward 5' ATTTCCGTTGGTGTTTCAGG 3', 5-HTT Reverse 5' CGTCTGTCATCTGCATCCCT 3', IFNγ Forward 5' GGCTGTCCCTGAAAGAAAGC 3', IFNγ Reverse 5' GAGCGAGTTATTTGTCATTCGG 3', IL-17 Forward 5' TGAGCTTCCCAGATCACAGA 3', IL-17 Reverse 5' TCCAGAAGGCCCTCAGACTA 3', IL-10 Forward 5' GGTTGCCAAGCCTTATCGGA 3', IL-10 Reverse 5' ACCTGCTCCACTGCCTTGCT 3'.

4.2.7 *Flow Cytometry*

Bone marrow cells were flushed and collected from femurs (n = 8-10 per group). $1*10^6$ cells were plated in a 96-well plate. The staining was performed as described in Collins et al. [30]. Briefly, cells were blocked with Fc block (Bectin Dickinson Pharmingen) for 15 min and then stained with antibodies to CD3 (Cat. No. 56-0032, eBioscience), CD4 (Cat No. 11-0041, eBioscience), CD8a (Cat No. 35-0081, eBioscience), GR1/Lys-6G (Cat. No. 53-5931, eBioscience), and CD11b (Cat. No.12-0113, eBioscience) for 30 min. Then, cells were fixed and data was acquired using the Bectin Dickinson LSRII flow cytometer. Data analysis was performed using the FlowJo software package (FlowJo, LLC).

4.2.8 *Osteoclast Outgrowth Assay*

Primary bone marrow cells were isolated from femurs and $4.5X10^5$ cells were plated per well in a 48 well plate (Corning) format. The plated cells were maintained in αMEM (Invitrogen) + 10% FBS (Gibco) containing 1% penicillin/streptomycin (Invitrogen). To induce osteoclast differentiation, cells were stimulated with 30 ng/ml of RANKL (R&D systems) and 2 ng/ml of M-CSF (R&D systems). The complete growth medium was replenished every 2 days. After 4 days, the cells were fixed and stained for tartrate-resistant acid phosphatase (TRAP) according to the manufacturer's protocol (Sigma Aldrich). Cells staining for TRAP and multinucleated (>3) were considered osteoclasts.

4.2.9 *DNA extraction from mouse fecal samples, 16S rRNA gene amplication, and sequencing*

For 16S rRNA gene sequencing, DNA was extracted by bead beating followed by the use of the QIAGEN DNEasy Tissue Kit as described in [27]. PCR Amplification of the V4 region of the 16S rRNA gene was performed with Phusion High Fidelity DNA Polymerase (New England Biolabs) using previously described primers and a protocol [25,31]. PCR reactions were performed in duplicate. Each reaction was composed of 4µl of template, 1X Phusion High Fidelity Buffer, 200 µM dNTPs (Invitrogen), 10nM of forward and reverse primers, 0.2 units of Phusion DNA Polymerase, and PCR grade water adjusting the final volume to 20µl. A 3-step PCR amplification cycle was used and included an initial denaturation at 98°C for 30 s, followed by 30 cycles of denaturing at 98°C for 10 s, annealing at 51°C for 20 s, and extension at 72°C for 1 min. Replicates were pooled and cleaned using the Agencourt AMPure XP kit (Beckman Coulter). DNA sample concentrations were measured using Quant-iT (Life Technologies) and pooled at equimolar ratios. Sequencing was performed on an Ilumina MiSeq platform.

4.2.10 *Microbial Community Analysis*

The MiSeq pipeline in Mothur was used to process sequence data [32]. The MiSeq pipeline for Mothur (essentially as described [33] and the MiSEQ SOP version 28 March 2013 (http://www.mothur.org/wiki/MiSeq_SOP)) was used to process sequence data. Following alignment of forward and reverse reads, sequences were quality-trimmed and aligned to the Silva 16S rRNA gene reference database formatted for mothur. Sequences were then trimmed to overlap the same region of the 16S rRNA gene, pre-clustered to clusters with ≥99 % identity, and potentially chimeric sequences were identified and removed using the mothur-impelementation of uchime. Sequences were classified according to the mothur-formatted ribosomal database project version 9 (August 2013) using the Bayesian classifier in Mothur, and those sequences classified as Eukarya, Archaea, Chloroplast, Mitochondria or unknown were removed. The sequence data was then filtered to remove any sequences present only once in the data set. After building a distance matrix from the remaining sequences with the default parameters in mothur, sequences were clustered into operational taxonomic units (OTUs) with ≥97 % using the average-neighbor algorithm in mothur. Taxonomic assignments for each OTU are the majority consensus taxonomic assignment for each sequence within the OTU. Prior to analysis with the phyloseq package of R, additional filtering of the OTU table was done to remove rare OTUs. Namely, those OTUs present in less than 3 samples and/or that contained less than 25 sequences were removed. These filtering steps reduced the number of OTUs from 6,306 to 923 but only decreased the number of sequences per sample by a mean of 0.7 ± 0.4% (range, 0.1-2.3%). Analysis and visualization of microbiome communities was conducted in R utilizing the phyloseq package to import sample data and calculate alpha- and beta-diversity metrics [34].

4.2.11 *Statistical analyses*

The results presented are as means+/- SEM. An unpaired *t* test was used to assess differences between groups. The cutoff for significance was $p \leq 0.05$. One-way ANOVA analysis was applied when more than 2 groups were being compared. For example, a one-way ANOVA was applied between subjects to compare the effect of different microbiotas on bone volume fraction. For microbial community analysis, significance of categorical variables were determined using the non-parametric Mann-Whitney test for two category comparisons or the Kruskal-Wallis test for three or more categories. Principal coordinate (PCoA) plots employed the Monte Carlo permutation test to estimate *p* values [35]. All *p* values were adjusted for multiple comparisons by taking into account the false discovery rate [36].

4.3 *Results*

4.3.1 *Conventionalization with a human microbiota does not decrease bone mass in GF mice*

In an attempt to start identifying specific microbes that affect bone health, we investigated the impact of different human microbial communities in GF mice. Mice colonized by a human microbiota, also known as humanized microbiota mice, have been used as a model to identify human derived microbes with potential therapeutic benefits that may be more translatable to humans [31].

To do this, 4-week old GF Swiss Webster mice were humanized by intragastric gavage with fecal microbial communities from human volunteers (Figure 4.1, top panel). In total, 4 different human microbial communities were used for colonization (Table 4.1). Following 12 weeks of colonization, bone mass from the distal femur was measured and we found that there was no

significant difference in the BVF between GF mice or mice colonized with our collection of human microbiotas (Figure 4.2, $p = 0.61$). To test whether this lack of impact to bone was specific to human microbiotas, an additional group was conventionalized with cecal contents from a WT Swiss Webster mouse and no significant phenotypic difference was observed (Figure 4.2).

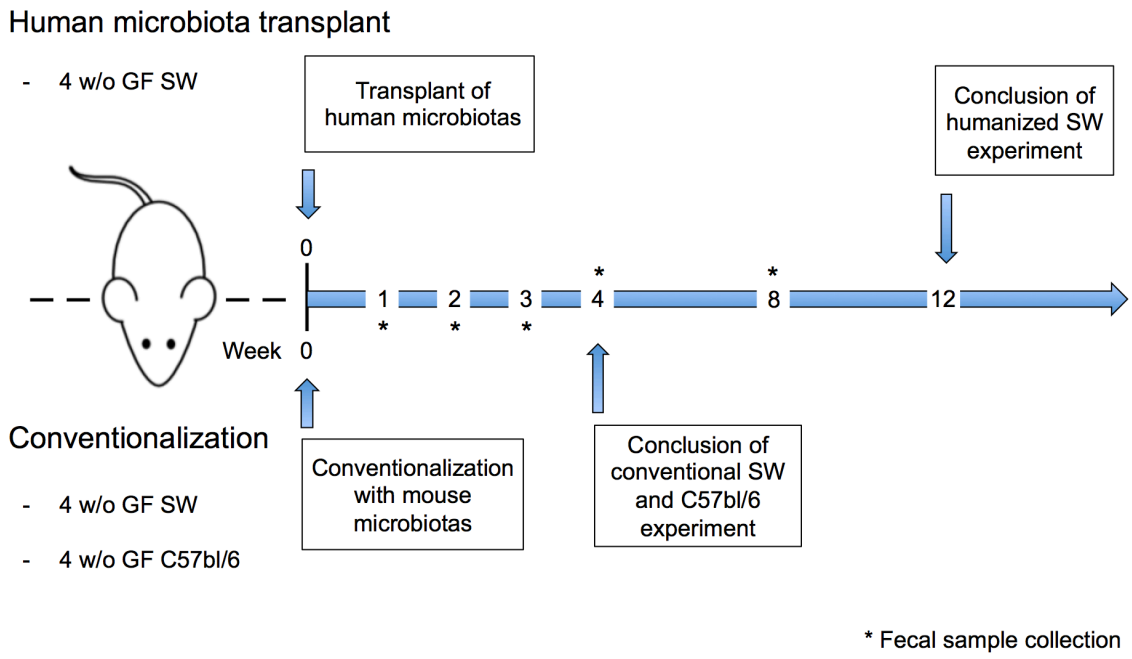

Figure 4.1. Experimental layout for human microbiota and conventionalization mouse studies.

4-wk-old (w/o) germ free (GF) mice from the Swiss Webster genetic background were colonized with various human microbiotas (top half) for 12 weeks. In a separate study (bottom half), 4 w/o mice from the Swiss Webster and C57bl/6 genetic backgrounds were colonized with a conventional mouse microbiota.

Table 4.1. Description of human microbiotas

Microbiota source	Description
FS17	Fecal sample collected from healthy human vegetarian
FS18	Fecal sample collected from healthy human omnivore
FS18abx	Fecal sample collected from human omnivore following broad-spectrum antibiotic treatment
FS17 + *L. reuteri*	FS17 supplemented with *Lactobacillus reuteri* 6475

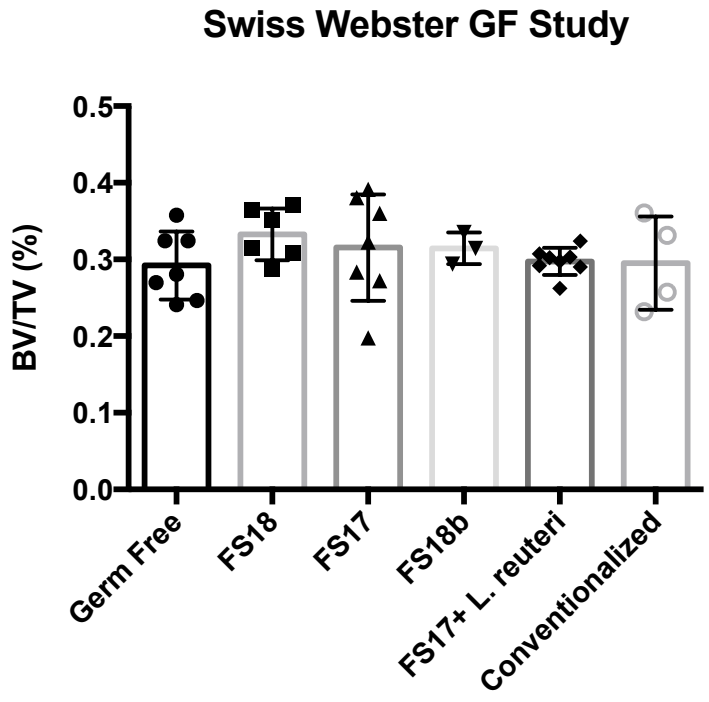

Figure 4.2. Trabecular bone volume fraction (BVF) of GF Swiss Webster mice after colonization with different human microbiotas.

Female GF Swiss Webster mice were colonized with different human microbiotas for 8 weeks. The GF and Conventionalized groups served as controls. The results are shown as mean ± SEM (n= 3-8).

4.3.2 *Presence of a normal mouse gut microbiota does not impact bone mass in female Swiss Webster or C57bl/6 mice*

It was previously demonstrated that reconstitution of the microbiota in GF C57bl/6 mice decreases bone mass [18]. To test whether the difference we observed (Figure 4.2) was due to a difference in the composition of human microbiotas, the duration of the experiment, or the difference in mouse genetic background, we conventionalized 4-week old female GF mice with microbiotas prepared from cecals contents of mice raised in the BCM mouse facility. This was performed in both the Swiss Webster and C57bl/6 genetic backgrounds. The sex and genetic backgrounds of the donors were matched to their recipients (i.e. Female GF Swiss Webster was colonized with a fecal sample from a female WT Swiss Webster). Following 4 weeks of colonization, we compared the BVF of the distal femur between GF and CONV-D mice and observed that there was no significant difference between the two groups (Figure 4.3a, $p = 0.15$; 4.3b, $p = 0.14$). Consistent with the BVF results, other bone parameters such as TMD, Tb. Th., Tb. N., and Tb. Sp. were the same between GF and CONV-D mice (Table 4.2). A comparison of the cortical volume and thickness from the midshaft of the femur also demonstrated no difference between the two groups. Trabecular μCT images comparing GF and CONV-D mice were consistent with quantitative measurements suggesting no difference between the two groups (Figure 4.3c).

A)

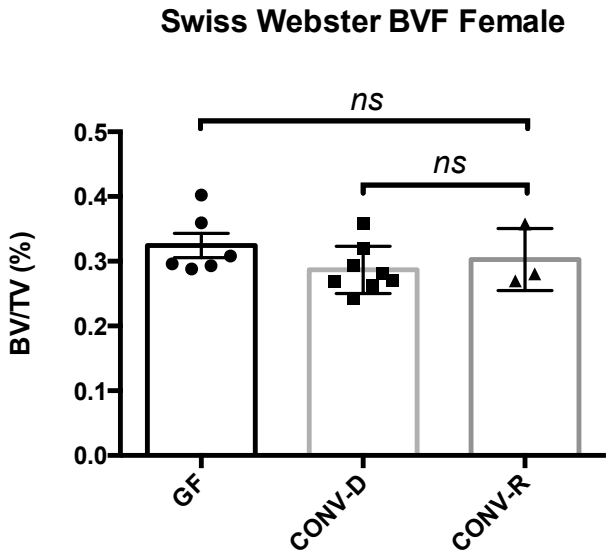

Figure 4.3**.** Conventionalization of female GF Swiss Webster and C57bl/6 mice does not impact bone density.

GF Swiss Webster (A) and C57bl/6 mice (B) were colonized with conventional mouse microbiota for 4 weeks. The GF group served as the control. No differences were observed in BVF between when conventionalized mice were compared to their GF counterparts. This supported the µCT measurements where gross discernible differences were absent. The results are shown as mean ± SEM (n= 3-10).

Figure 4.3. (cont'd)

B)

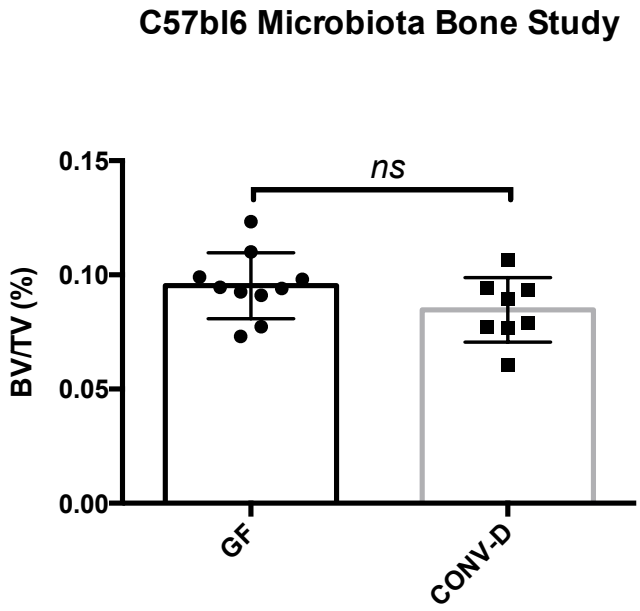

C)

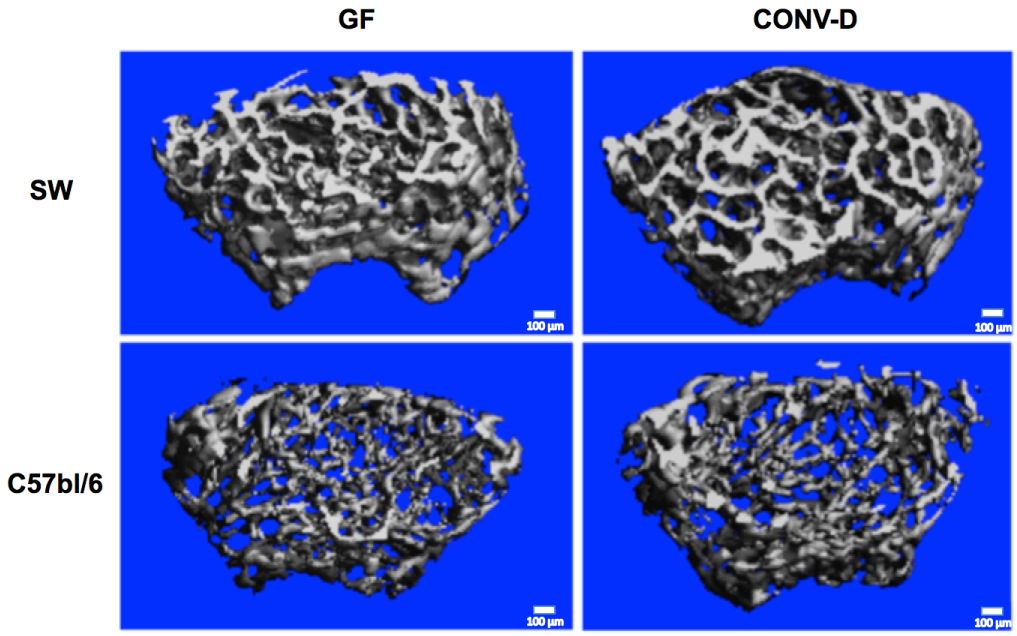

Table 4.2. Trabecular and Cortical Bone Parameters for Swiss Webster Mice

Trabecular	GF	CONV-D	P-value
BV/TV (%)	0.32 ± 0.05	0.29 ± 0.04	0.14
BMD (mg/cm^3)	269.73 ± 32.74	253.17 ± 28.75	0.33
Tb. Th. (μm)	56.31 ± 5.79	53.85 ± 5.21	0.42
Tb. N. (mm^{-1})	5.71 ± 0.21	5.31 ± 0.16	0.15
Tb. Sp. (μm)	149.85 ± 5.77	160.55 ± 6.51	0.26
Cortical			
Ct. Volume (mm^3)	0.55 ± 0.01	0.56 ± 0.01	0.38
Ct.Thickness (μm)	162.38 ± 2.63	166.88 ± 2.18	0.21

4.3.3 *Presence of a normal mouse gut microbiota does not impact bone mass in male Swiss Webster mice*

Sex differences have been shown to impact various facets of bone metabolism [37–39]. To begin understanding whether sex plays a role in determining the impact of the microbiota on bone health, we conventionalized 4-week old male GF Swiss Webster mice. Similar to their female counterparts, the presence of a microbiota did not impact the BVF (Figure 4.4, $p = 0.9253$).

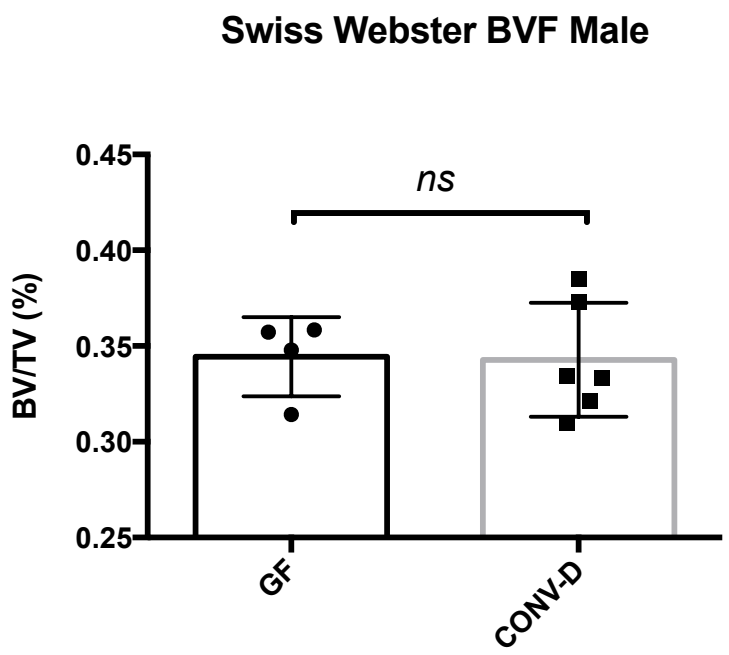

Figure 4.4. Conventionalization of male GF Swiss Webster mice does not lead to bone loss.

Male GF Swiss Webster mice were conventionalized with a mouse microbiota. The results are shown as mean ± SEM (n= 4-6).

4.3.4 *Histomorphometric analysis of the distal femur*

Histomorphometry was performed on the distal femur in order to measure static and dynamic bone parameters. We observed no significant differences between the number of osteoclasts per trabecular surface between GF and CONV-D Swiss Webster mice. Consistent with the bone results thus far, no significant differences were observed when we compared mineralizing surface per trabecular bone surface, bone formation rate, and mineral apposition rate (Figure 4.5, Table 4.3).

Table 4.3. Histomorphometry of Trabecular Bone in Distal Femur

	GF	CONV-D	P-value
OCL/Bone Surface (%)	12.91 ± 4.01	16.41 ± 5.51	0.25
MS/BS (%)	0.11 ± 0.01	0.1 ± 0.01	0.4
BFR (μm/d)	0.19 ± 0.03	0.11 ± 0.04	0.21
MAR ($\mu m^3/\mu m^2/d$)	1.41 ± 0.54	1.04 ± 0.39	0.31

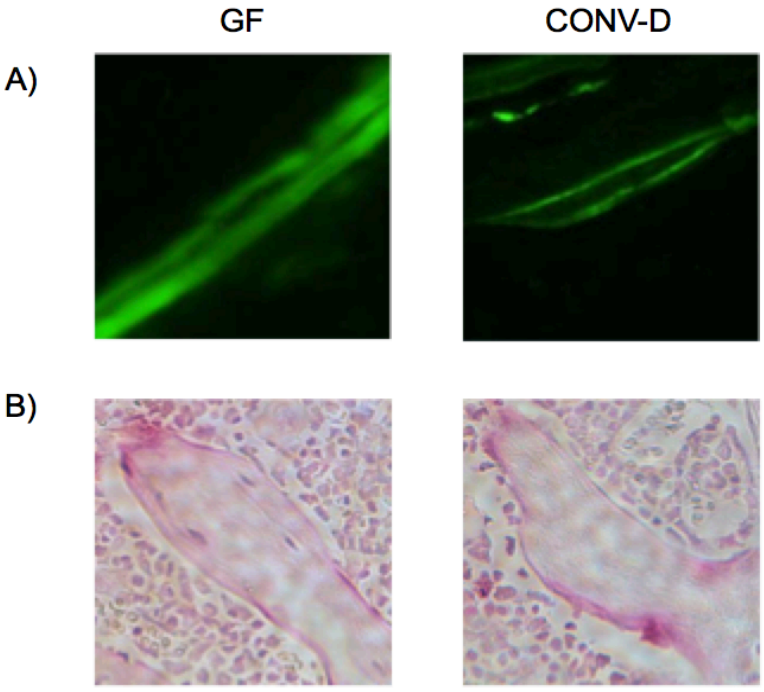

Figure 4.5**.** Conventionalization does not impact MAR or TRAP staining of metaphyseal region of femur.

Images are representative from multiple images taken for each specimen of each animal group (n = 8). (A) Calcein incorporation illustrates the amount of mineral apposition over a span of 5 days. (B) TRAP staining of metaphyseal region where osteoclasts stain purple.

4.3.5 *Flow cytometry and osteoclast outgrowth between GF and CONV-D mice*

An imbalance favoring osteoclastic bone resorption has often times lead to pathological bone loss with one of the underlying causes being the promotion of osteoclast formation by T cells [22,40]. Previously, it was shown that the gut microbiota leads to decreased bone mass and correlated with an increased $CD4^+$ and $CD8^+$ T cell populations as well as osteoclast precursor cells [18]. To investigate whether the gut microbiota impacts immune cell populations in the bone marrow and osteoclastogenesis in the Swiss Webster genetic background, we measured the different T cell populations and amount of osteoclast precursor cells under the presence or absence of a microbiota.

A)

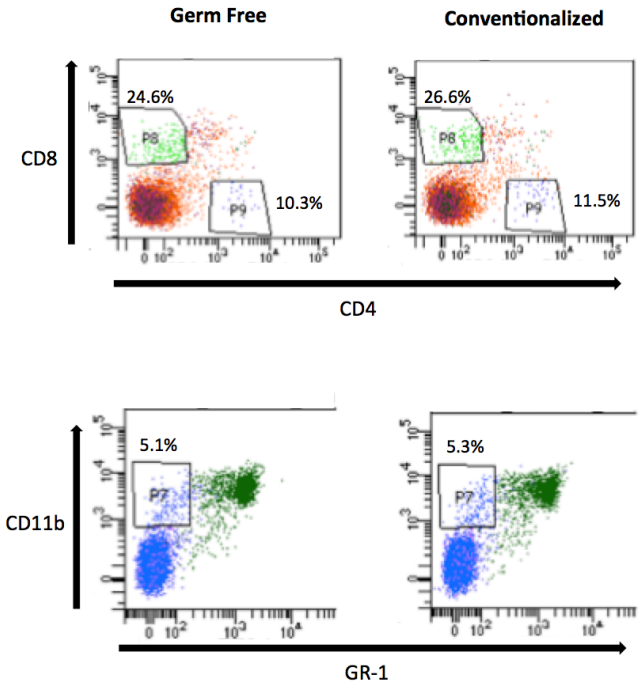

B)

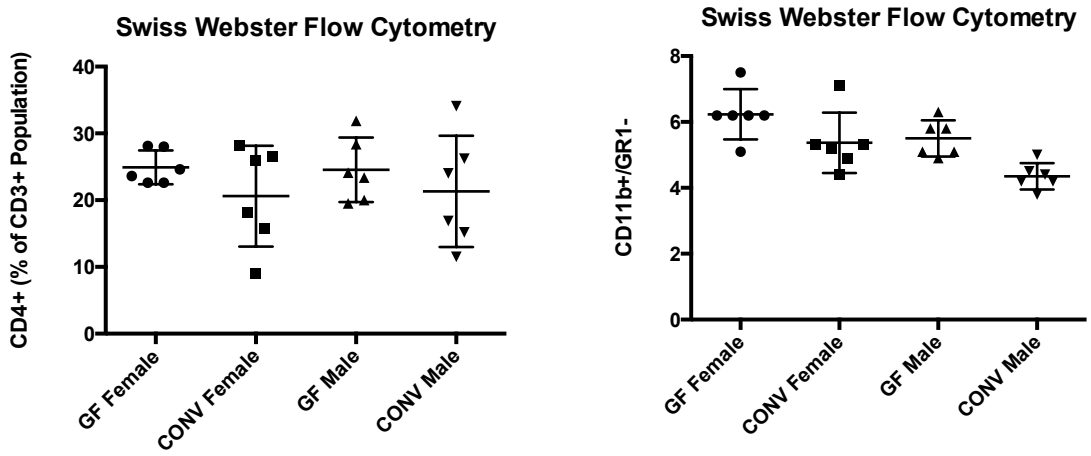

Figure 4.6. Conventionalization of GF Swiss Webster mice resulted in no changes in bone marrow cell populations.

Bone marrow cells were flushed from 8-wk-old mice and stained for antibodies to quantify T cell populations (CD3, CD4, and CD8) and osteoclast precursors (CD11b+/GR1-) by flow cytometry.

Figure 4.6. (cont'd)

(A) Representative image of flow cytometry plots of cell percentages (of total CD3+ population for T cells and total bone marrow population for osteoclast precursors) and (B) quantitation of the different cell populations.

Flow cytometric analyses indicate that conventionalization of GF mice in the Swiss Webster genetic background does not impact the bone marrow T cell populations (Figure 4.6). Osteoclast differentiation was measured by quantitating the amount of giant multinucleated cells that stained positive for TRAP following stimulation with RANKL and M-CSF for 4 days. Consistent with there being no change in the T cell and osteoclast precursor population, no significant difference in osteoclast outgrowth was detected in conventionalized mice when compared to their GF counterparts (Figure 4.7). Osteoclast size and number of nuclei has been shown to correlate with bone resorption potential [41,42]. After partitioning our results into osteoclasts that contained either greater than or less than 5 nuclei, we observed no discernible differences between the GF and CONV-D group (Figure 4.8).

A)

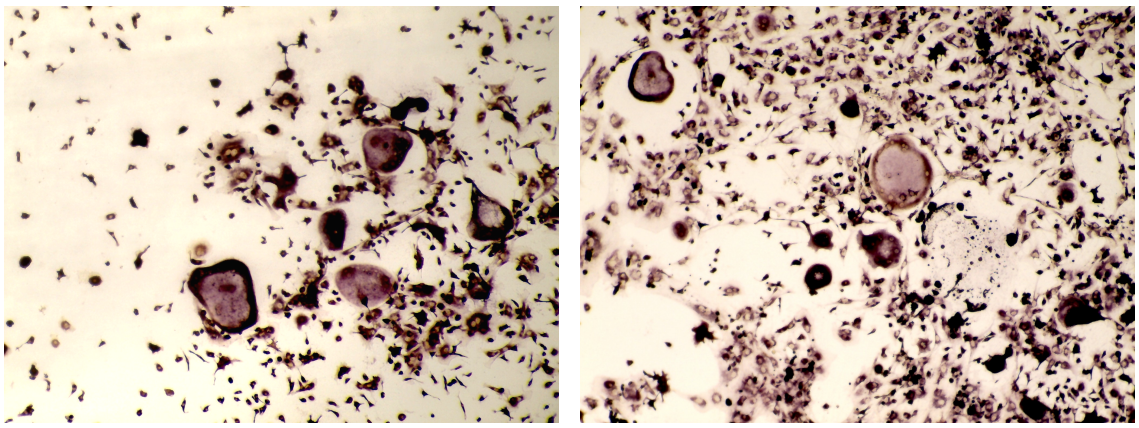

B)

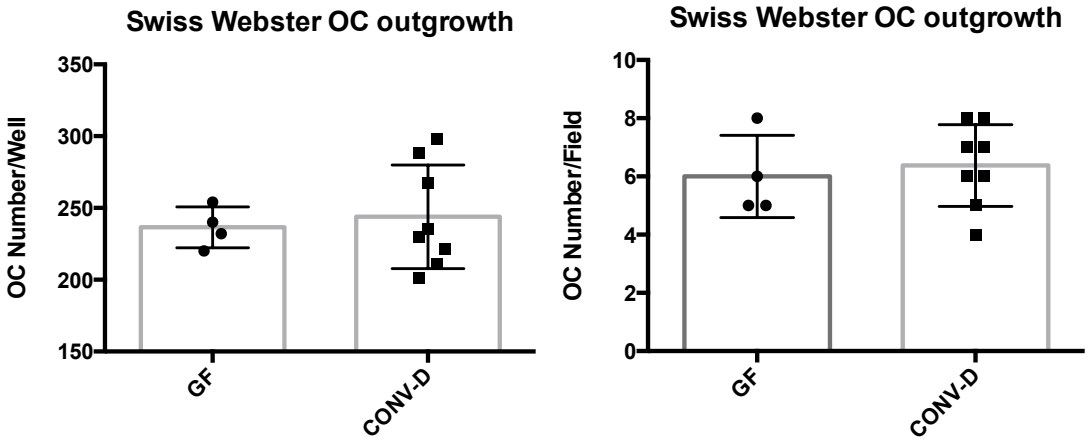

Figure 4.7. Osteoclast outgrowth from bone marrow cells of GF Swiss Webster and conventionalized (CONV-D) mice.

Bone marrow cells are flushed from the femurs of 8-wk-old GF and CONV-D mice and stimulated for differentiation with RANKL and M-CSF. $TRAP^{+}$ cells were quantitated after 4 days of culture. (A) Representative images of GF and CONV-D conditions. (B) Total osteoclast numbers per well and per field were quantitated. Values are provided as mean ± SEM.

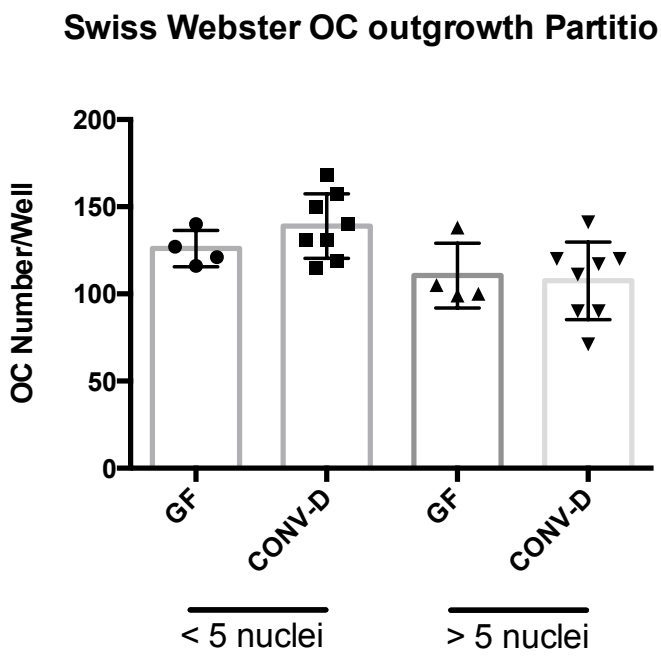

Figure 4.8**.** Partitioning of osteoclast outgrowth from bone marrow cells of GF Swiss Webster and conventionalized (CONV-D) mice.

Bone marrow cells are flushed from the femurs of 8-wk-old GF and CONV-D mice and stimulated for differentiation with RANKL and M-CSF. $TRAP^{+}$ cells were quantitated after 4 days of culture. Total osteoclast numbers in each well were quantitated and separated into populations that had >3 nuclei and >5 nuclei. Values are provided as mean ± SEM.

4.3.6 *Analysis of inflammatory markers from the gut and serum*

Increased levels of various inflammatory cytokines have been shown to promote osteoclastogenesis and bone loss in human and animal studies [43–45]. To investigate whether the production of certain cytokines is regulated by the presence of a gut microbiota, we compared the expression levels between GF and conventionalized mice by performing qRT-PCR on the genes TNF-α, IL-1β, IL-6, SERT (Serotonin reuptake transporter), IFN-γ, IL-17A, and IL-10 from

colonic mRNA. With the exception of IL-17A mRNA expression being increased and IL-10 being decreased, no other genes that were examined were differentially regulated by the reconstituting the gut microbiota in GF mice (Figure 4.9a). Accordingly, TNF-α levels in the serums were not affected by conventionalization (Figure 4.9b).

A)

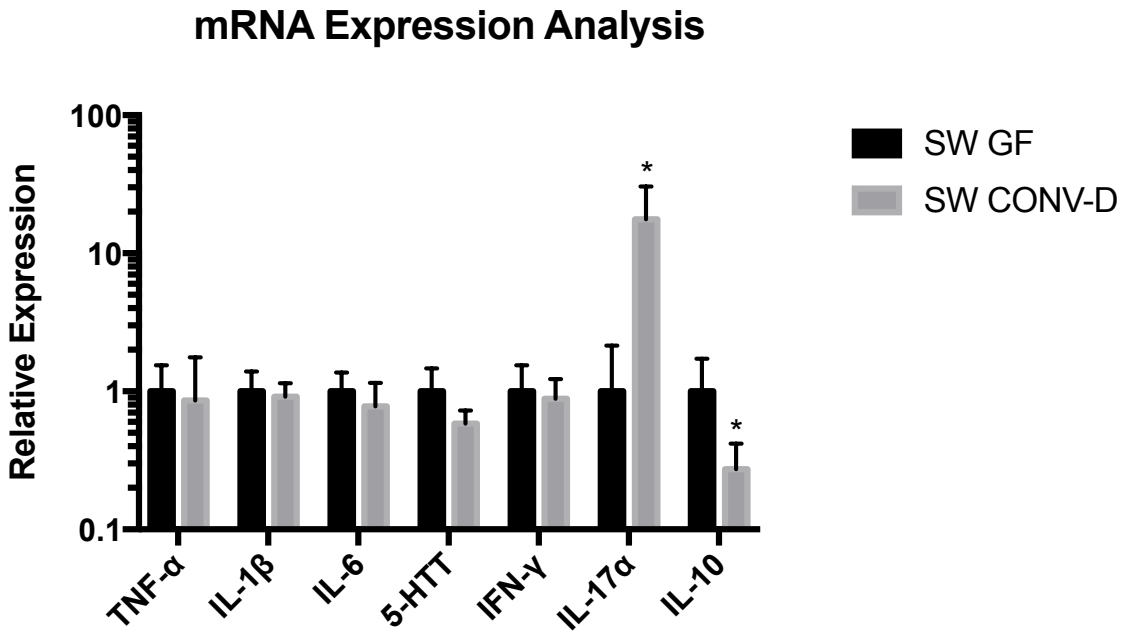

Figure 4.9. Expression analysis of the colon and serum analysis of TNF-α.

(A) The expression level of IL-17α was up-regulated and IL-10 was down-regulated due to conventionalization. (B) Serum levels of TNF-α were unaffected following conventionalization. *$p < 0.05$ with respect to SW GF, Student's *t* test.

Figure 4.9. (cont'd)

B)

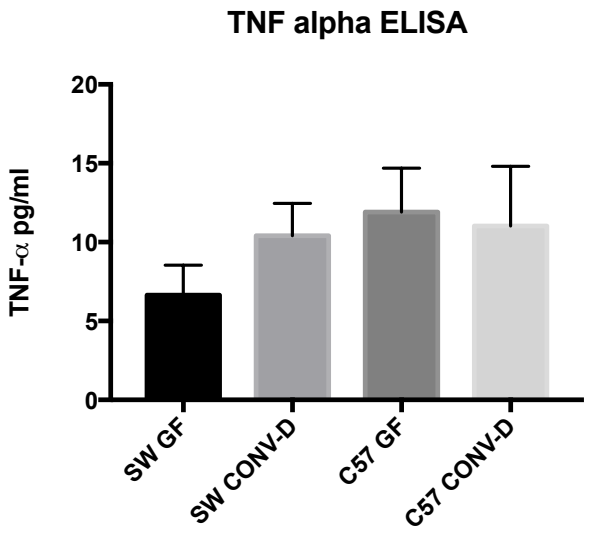

4.3.7 *Fecal microbial community analysis*

Previous studies with the administration of exogenous sources of microbes like probiotics suggest that they are beneficial to bone health [27,46–48]. However, what still needs to be elucidated is the role that indigenous microbes play to impact this bone health. To begin developing a catalog of bacteria with potential impact on bone health, we analyzed the microbial communities present in the fecal samples of mice in our treatment groups by analysis of the V4 hypervariable region of the 16S rRNA gene. The data set included 4,373,773 high-quality sequences. Following the removal of singletons and clustering based off of 97% similarity, 471 OTUs were identified across all samples (n=52) with an average rarefaction depth of 14920 reads per sample. The cutoff value for inclusion in downstream analyses was representing at least 0.01% abundance for that particular community.

Alpha and beta diversity measures reflect a high efficiency of microbiota transfer as most of the species that were identified by sequencing of the inocula were shown to be present in the corresponding recipient CONV-D mice. Conventionalization of female C57bl/6 and Swiss Webster mice identified the presence of 178 OTUs (178/182) and 296 (296/315) present in the original inocula, respectively (Figure 4.10a, Table 4.5). Comparing conventionalized mice of the C57bl/6 genetic background with those of the Swiss Webster group identified that 154 OTUs were shared between the two while 31 OTUs were unique to C57bl/6 mice and 168 OTUs were unique to Swiss Webster mice (Table 4.4 and Table 4.5). Results from the humanized mouse groups demonstrated a lower amount of detected OTUs with the average for groups FS17, FS18, and FS18abx being 133 OTUs (Table 4.4). Interestingly enough, the numbers of OTUs in the starting inocula for these groups were lower in comparison to the mouse conventionalized groups.

A)

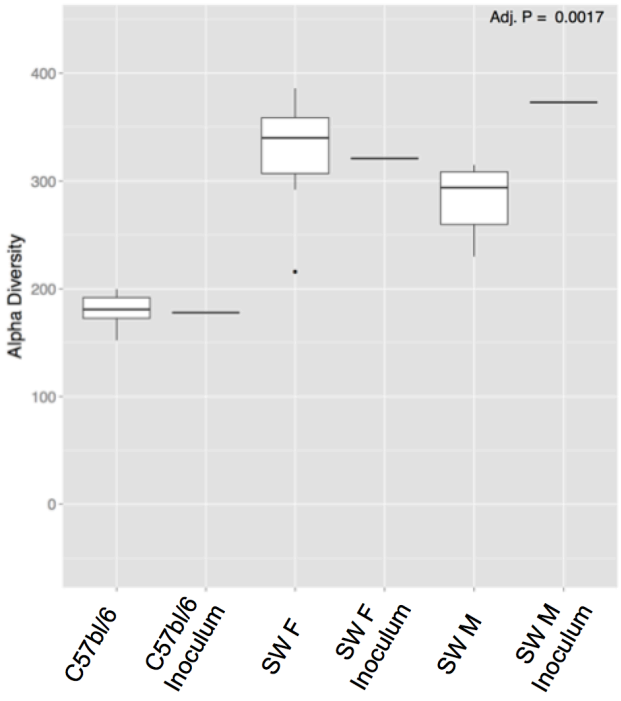

B)

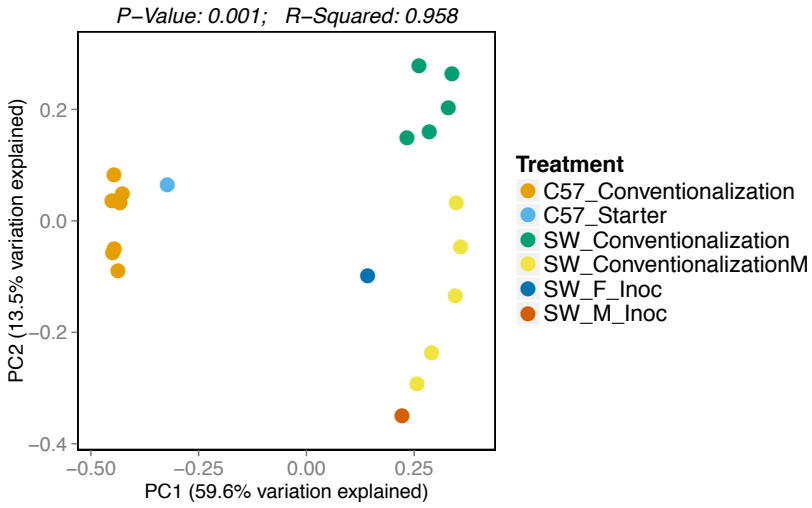

Figure 4.10. Alpha and beta diversity measures for conventionalized mice indicate higher diversity in SW mice and distinct clustering.

Figure 4.10 (cont'd)

The comparison of OTUs (A) in starting inocula and conventionalized mice suggests a high level of colonization and efficient microbiota transfer. In a PCoA plot (B), the conventionalized mice cluster together according to mouse genetic background and starting inocula.

Table 4.4. Abundances of OTUs for each mouse group.

Values are reported as means within that group and as a percentage of the total community.

Taxa	C57_CONV-D	FS17	FS18	FS18_Ab	SW_Conv-D_Female	SW_Conv-D_Male
Otu00001	46.59	0	0	0	2.3	3.75
Otu00002	0	0	0	0	5.98	8.53
Otu00003	0	1.78	0.08	0.01	0.58	2.6
Otu00004	0	0	0	0	6.1	5.66
Otu00005	0	0	0	0	3.91	3.91
Otu00006	0	0	0	0	3.86	1.67
Otu00007	0	0	0	0	1.86	2.11
Otu00008	0	0	0	0	0.56	0.68
Otu00009	0.31	0.01	0	0	2.86	0.49
Otu00010	0.9	0	0	0	0.51	1.47
Otu00011	1.81	0	0.12	0	1.37	0.91
Otu00012	2.03	0.01	0.03	0	1.02	0.86
Otu00013	1	0	0	0	0.65	0.15

Table 4.4. (cont'd)

Otu00014	2.61	0.01	0	0	0.09	0.26
Otu00015	1.37	23.34	16.31	0	0.24	0.03
Otu00016	0.45	0.33	0.11	0	1.84	2.21
Otu00017	0	0.01	0	0	0.85	1.22
Otu00018	1.89	0	0	0	0.32	0.03
Otu00019	0	0	0	0	1.4	0.9
Otu00020	0	0.02	0.25	14.26	0.01	0.05
Otu00021	0	0.81	0.06	0	0.58	0.54
Otu00022	0	0	0	0	1.43	0.43
Otu00023	0	0	0	0	1	2.21
Otu00024	0.46	0	0.03	0.42	0.41	0.43
Otu00026	0	0	0	0	1.81	1.06
Otu00027	0	0	0	0	3.07	1.11
Otu00028	0	0	0	0	0.28	5.45
Otu00029	0	0	0	0	0.45	0.08
Otu00030	0.44	0	0	0	0.55	0.2
Otu00031	3.08	0	0	0	4.21	7.06
Otu00032	0	0.52	0.19	0.34	0.07	0.04
Otu00033	0	0	0	0	0.91	0.5

Table 4.4. (cont'd)

Otu00034	0.18	0	0	0	0.19	0.56
Otu00035	0	0	0.3	0.2	0.65	0.09
Otu00036	0	0.01	0	0	0.23	0.74
Otu00037	0	0	0	0	0.82	0.84
Otu00038	0	2.55	0	0	0.01	0
Otu00039	0	0	0	0	0.74	0.23
Otu00040	0.21	0.01	0.09	0	0.07	0.03
Otu00041	0.12	0	0	0	0.16	0.03
Otu00042	0	0	0	0	0.75	0.54
Otu00043	0	0	0	0	0.22	0.38
Otu00044	0	0.01	0	0	1.47	1.04
Otu00045	0	0.09	0.01	0	0	0
Otu00046	0.71	0	0	0	0.41	0.15
Otu00047	0	0	0	0	0.93	1.07
Otu00048	1.15	0	0	0	0.35	0.02
Otu00049	0	0.02	0	0	0	0.02
Otu00051	0	0	0	0	1.89	0.09
Otu00052	0	0	0	0	2.02	1.07
Otu00053	0.61	0	0	0	0.5	0.34
Otu00054	0	0.07	0.1	1.12	0.07	0.01

Table 4.4. (cont'd)

Otu00055	0	0	0	0	0.05	1.38
Otu00056	0.16	0	0	0	2.74	0.89
Otu00057	0.19	0	0	0	0.37	0.3
Otu00058	0	0	0	0	1.7	0.61
Otu00059	0.18	0	0	0	0.13	0.66
Otu00060	0	0	0.01	0	0.45	0.92
Otu00061	0.06	0	0	0	0.28	0.17
Otu00062	0.39	0	0	0	0.45	0.17
Otu00063	0	0	0	0	0.39	0.4
Otu00064	0.61	0	0	0	0.76	0.49
Otu00065	0	0	0	0	3.83	1.07
Otu00066	0	0	0	0	0	0.86
Otu00067	0	0.11	0.51	0.01	0	0
Otu00068	0.16	0	0	0	0.36	0.32
Otu00069	0.54	0	0	0	0.04	0.1
Otu00070	0	0	2.08	0.08	0	0
Otu00071	0	0.21	2.39	1.02	0	0.01
Otu00072	0.01	0.22	0	0	0.11	0.62
Otu00073	0.18	0	0	0.03	0.09	0.05
Otu00074	0	0	0.01	0	0.39	0.71

Table 4.4. (cont'd)

Otu00075	0.18	0	0	0	0.1	0.09
Otu00076	0.05	0	0	0	0.15	0.07
Otu00077	0.24	0	0	0	0.15	0.19
Otu00078	0	0	0.01	0	0	0.01
Otu00080	0	0	0	0.01	0	0
Otu00081	0	0	0	0	0.15	0.49
Otu00082	0.49	0.01	0.1	0.25	0.21	0.18
Otu00083	0.08	0	0	0	0.07	0.07
Otu00084	0.22	0	0	0	0.22	0.14
Otu00085	2.19	0	0	0	0.98	0.27
Otu00086	0.48	0.07	2.77	64.36	0.01	4.72
Otu00087	0	0	0.02	0.19	0	0
Otu00088	0.32	0	0	0	0.17	0.03
Otu00089	0.23	0	0	0	0.28	0
Otu00090	0	0	0	0	4.46	1.09
Otu00091	0	0	0	0	0.08	0.08
Otu00092	0	0	0	0	0.05	0.08
Otu00093	0.63	0	0	0	0.28	0.12
Otu00094	0.16	0	0	0	0.14	0.06
Otu00095	0	0	0	0	0.1	0.19

Table 4.4. (cont'd)

Otu00096	0.52	0	0.1	0	0.09	0.32
Otu00097	0	0	0	0	0	0.03
Otu00098	0	0.04	0	0	0	0
Otu00099	0	3.7	1.27	1.03	0	0
Otu00100	0	0	0	0	0.31	0.22
Otu00101	0	0	0	0	0	0.56
Otu00102	0.14	0	0	0	0.17	0.12
Otu00103	0	14.46	5.26	0	0	0
Otu00104	0	0	0.01	0	0.19	0.01
Otu00105	0	0	0	0	1.18	1.19
Otu00106	0.14	0.01	0.07	0	0.38	1.04
Otu00108	0	0	0.11	0.77	0	0
Otu00109	0	0	0	0	0.09	0.01
Otu00110	0	0.03	0	0	0	0
Otu00111	0.18	0	0	0	0.23	0.12
Otu00112	0.04	0	0.03	0	0.12	0.08
Otu00113	0	0	0.03	0.01	0	0
Otu00114	0	0	0	0	0	0
Otu00115	0	0	0	0	0.16	0

Table 4.4. (cont'd)

Otu00116	0	0	0	0	0.05	0.05
Otu00117	0.3	0	0	0	0.07	0.03
Otu00118	0	0	0	0	0.12	0.14
Otu00119	0	0	0	0	0.13	0.09
Otu00120	0.07	0	0	0	0.06	0.04
Otu00123	0	2.45	17.63	0	0	0
Otu00124	0	0.04	0	0	0.08	0.02
Otu00125	0	0	0	0	0.92	0.39
Otu00127	0.29	0	0	0	0.05	0.06
Otu00128	1.45	0	0.01	0	0	1.34
Otu00129	0.06	0	0	0	0.05	0.05
Otu00130	0.05	0.01	0	0.01	0.06	0.02
Otu00131	0	0	0	0	0.67	0.35
Otu00132	0.54	0	0	0	0.03	0.06
Otu00133	0	0	0	0	0.06	0.11
Otu00134	0.2	0	0	0	0.03	0.04
Otu00135	0.37	0	0	0	0.14	0.08
Otu00136	0.06	0.76	1.76	0	0.33	1.19
Otu00137	0	0	0	0	0	0.78

Table 4.4. (cont'd)

Otu00138	0	0	0	0	0	0
Otu00139	0	0	0	0	0.03	0.02
Otu00140	0	0	0	0	0.02	0
Otu00141	0.05	0	0	0	0.13	0
Otu00143	0	4.66	4.69	0	0	0
Otu00144	0	0.49	0	0	0.01	0.01
Otu00145	0.09	0	0	0	0	0
Otu00147	0.01	0	0	0	0	0
Otu00148	0	0	0	0	0	0.01
Otu00149	0	0.29	0	0	0	0
Otu00150	0.08	0	0	0	0.01	0.03
Otu00152	0.16	0	0	0	0.01	0.02
Otu00153	0.48	0	0	0	0.02	0.04
Otu00154	0.16	0	0	0	0.04	0.11
Otu00155	0.03	0	0	0	0.02	0.02
Otu00156	0	0	0	0	0.01	0
Otu00157	0	0	0.6	14.24	0	0
Otu00158	0	0.17	1.76	0	0	0
Otu00159	0.04	0	0.03	0	0.06	0.05
Otu00161	0	0	0	0	0.01	0.02

Table 4.4. (cont'd)

Otu00162	0	0	0	0	0.03	0
Otu00163	0	0	0	0	0.12	0.13
Otu00164	0	0	0.02	0	0	0
Otu00165	0.07	0	0	0	0.07	0.02
Otu00166	0.34	0.27	0.97	0	0.07	0.06
Otu00168	0	0.01	0.06	0	0	0
Otu00169	0	0	0	0	0.71	0.34
Otu00170	6.25	0	0	0	0	0
Otu00171	0	0	0	0	0.02	0.01
Otu00173	0.03	0	0	0	0.04	0.04
Otu00174	0.15	1.21	0	0	0.1	0.08
Otu00175	0.18	0	0	0	0.03	0.04
Otu00176	0	0	0	0	0.17	0.03
Otu00178	0	0.48	0.03	0.01	0	0
Otu00179	0	0	0	0	0.08	0.2
Otu00180	0.01	0	0	0	0.01	0.01
Otu00181	0	0	0	0	0.02	0.02
Otu00182	0.07	0	0	0	0.05	0.06
Otu00183	0.07	0	0	0	0.05	0.08
Otu00184	0.04	0	0	0	0.02	0.02

Table 4.4. (cont'd)

Otu00185	0.02	0	0	0	0.05	0.01
Otu00186	2.19	0	0	0	0	0
Otu00187	0.01	0	0.09	0	0.1	0.06
Otu00188	0.06	0	0	0	0.02	0.02
Otu00189	0.03	0	0	0	0.06	0.02
Otu00190	0.51	0	0	0	0.05	0.19
Otu00191	0.25	0	0	0	0.06	0.07
Otu00192	0	0	0	0	0.54	0.02
Otu00194	0	5.27	0.01	0	0	0
Otu00195	0.02	0	0	0	0.03	0.09
Otu00196	0.03	0	0	0	0.05	0.14
Otu00197	0	0.01	0.04	0	0	0.01
Otu00198	0	0	0	0	0.2	0.03
Otu00199	0.09	0	0	0	0.03	0.06
Otu00200	0	0.54	0.04	0	0.08	0.05
Otu00201	0.02	0	0	0	0.2	0.06
Otu00202	0.03	0	0	0	0.07	0.04
Otu00203	0.19	0	0	0	0.01	0.03
Otu00204	0.01	0	0	0	0.04	0
Otu00205	0	0.01	0.01	0	0	0.79

Table 4.4. (cont'd)

Otu00206	0	0	0	0	0.01	0.02
Otu00207	0	0	0	0	0.09	0.05
Otu00209	0.11	0	0	0	0.07	0.16
Otu00210	0	2.59	4.46	0	0	0
Otu00211	0	0	0	0	0.01	0
Otu00212	0	0	0	0	0	0
Otu00213	0	0	0	0	0	0
Otu00214	0	0	0	0	0.17	0.7
Otu00215	0	0	0	0	0.02	0.02
Otu00216	0	0.6	0.71	0	0	0
Otu00219	0	0	0	0	0.03	0.01
Otu00220	0	0	0	0	0.59	0.04
Otu00221	0.82	0	0	0	0.2	0.13
Otu00222	0	0	0	0	0	0.42
Otu00223	0	0	0	0	0.02	0.04
Otu00224	0	0	0	0	0.52	0
Otu00226	0	0	0	0	0.18	0.01
Otu00228	0	0	0	0	0.05	0.41
Otu00230	0	1.11	4.15	0	0	0
Otu00231	0	0	0	0	0.04	0

Table 4.4. (cont'd)

Otu00232	0.01	0	0	0	0.02	0.01
Otu00233	0	15.02	0	0	0	0
Otu00234	0	0	0	0	0.05	0.02
Otu00235	0	0	0	0	0.08	0.16
Otu00237	0.01	0	0	0	0.01	0
Otu00238	0.08	0	0	0	0.05	0.05
Otu00239	0	0.75	0	0	0	0
Otu00240	0	0	0	0	0.1	0.18
Otu00242	0	0	0	0	0	0
Otu00243	0	0	0	0	0.01	0
Otu00244	0	0	0	0	0.01	0.04
Otu00245	0	0	0	0	0.01	0.07
Otu00246	0.14	0	0	0	0.09	0.03
Otu00251	0.06	0	0	0	0.02	0
Otu00252	0	0	0	0	0	0
Otu00254	0	0	0	0	0.13	0.05
Otu00255	0	0	0	0	0.27	0.22
Otu00257	0	0	0	0	0	0
Otu00258	0.06	0	0	0	0	0

Table 4.4. (cont'd)

Otu00259	0	0	0	0	0	0
Otu00260	0.02	0	0	0	0.03	0.02
Otu00262	0	0	0	0	0.05	0.02
Otu00263	0.17	0	0	0	0	0.02
Otu00264	0.03	0	0	0	0	0.02
Otu00265	0	0	0	0	0	0
Otu00267	0.12	0	0	0	0.09	0.02
Otu00268	0	0	0	0	0.08	0.01
Otu00269	0.23	0	0	0	0	0.03
Otu00272	0	0	0	0	0.04	0.01
Otu00273	0	0	0	0	0.01	0
Otu00274	0.32	0	0	0	0.2	0.13
Otu00276	1.18	0	0	0	0	0
Otu00278	0	0	0	0	0.04	0.01
Otu00279	0	0	0	0	0.08	0.04
Otu00280	0	0.01	0.01	0	0.08	0.06
Otu00282	0.03	0	0.12	0	0.02	0.01
Otu00283	0	0	0	0	0.01	0.04
Otu00285	0	0	0	0	0	0
Otu00287	0.02	0	0	0	0.02	0.03

Table 4.4. (cont'd)

Otu00293	0.05	0	0	0	0.04	0.02
Otu00298	0	0.26	0	0	0	0
Otu00299	0	0	0	0	0.01	0.03
Otu00301	0	0	0	0	0.01	0
Otu00302	0	0	0	0	0.01	0
Otu00304	0.22	0	0	0	0.03	0
Otu00306	0	0	0	0	0	0
Otu00307	0	0	0.1	0	0	0
Otu00308	0.03	0	0	0	0.03	0.01
Otu00309	0	0	0	0	0	0
Otu00312	0.01	0.03	0.09	0	0.01	0.01
Otu00313	0	0.68	5.69	0	0	0
Otu00315	0	0	0.63	0.02	0	0
Otu00317	0.29	0	0.01	0	0.06	0.05
Otu00318	0	0	0	0.04	0	0
Otu00319	0	0	0	0	0.15	0.08
Otu00321	0	0	0	0	0.03	0.01
Otu00322	0	0	0	0	0.09	0
Otu00326	0	0	0	0	0.01	0.02
Otu00328	0	0.26	2.12	0	0	0

Table 4.4. (cont'd)

Otu00329	0	0.01	0.12	0	0	0
Otu00330	0	1.51	9.85	0	0	0
Otu00332	0	0	0	0	0.06	0.02
Otu00333	0	0.05	0	0	0	0
Otu00334	0.09	0	0	0	0.05	0.02
Otu00335	0	0.03	0	0	0	0
Otu00336	0.14	0	0	0	0.02	0.03
Otu00338	0	0	0	0	0.02	0.02
Otu00340	0	0	0	0	0	0.02
Otu00341	0.03	0	0	0	0.04	0.05
Otu00342	0.09	0	0	0	0.03	0.05
Otu00343	0	0	0	0	0.03	0.04
Otu00344	0.12	0	0	0	0	0
Otu00345	0	0.02	0	0	0.01	0.01
Otu00346	0	0	0	0	0	0
Otu00348	0	0	0	0	0	0.02
Otu00349	0	0.58	0	0	0	0
Otu00350	0	0	0	0	0.06	0.02
Otu00351	0	0	0	0	0.04	0.02
Otu00352	0	0.55	1.81	0	0	0

Table 4.4. (cont'd)

Otu00353	0	0	0	0	0.01	0
Otu00356	0.03	0	0	0	0.02	0
Otu00357	0	0	0.06	0	0.02	0.03
Otu00358	0	0.03	0.03	0	0	0
Otu00359	0	0	0	0	0.04	0.02
Otu00360	0	0	0	0	0.12	0.06
Otu00361	0.28	0	0	0	0.01	0.01
Otu00362	0	2.33	0.43	0	0	0
Otu00366	0.01	0	0	0	0.03	0.05
Otu00367	0	0	0.03	0	0	0
Otu00369	0.06	0	0	0	0.05	0.05
Otu00370	0.06	0	0	0	0.01	0.01
Otu00371	0	0	0	0	0.01	0.01
Otu00375	0	0	0	0	0.05	0.01
Otu00380	0.07	0	0	0	0.03	0.01
Otu00381	0	0	0	0	0.07	0.05
Otu00384	0	0.4	1.14	0	0	0
Otu00385	0.06	0	0	0	0.04	0.02
Otu00387	0	0	0	0	0	0
Otu00391	0.04	0	0	0.53	0	0

Table 4.4. (cont'd)

Otu00395	0	0	0	0	0.05	0.02
Otu00396	0	0	0	0	0.03	0.02
Otu00398	0	0	0	0	0	0.03
Otu00399	0	0	0	0	0.09	0.02
Otu00402	0.17	0	0	0	0.03	0
Otu00404	0	0	0	0	0.07	0.1
Otu00405	0.02	0	0	0	0.03	0.01
Otu00409	0	0	0	0	0.03	0
Otu00411	0	0	0	0	0.02	0
Otu00412	0.01	0	0	0	0.04	0.03
Otu00413	0	0	0	0	0.05	0
Otu00415	0	0.04	0.03	0	0	0
Otu00417	0.03	0	0	0	0.02	0.02
Otu00418	0.11	0	0	0	0.03	0.01
Otu00419	0	0	0	0	0.01	0.03
Otu00420	0	0.03	0.01	0	0	0
Otu00421	0	0.79	0.6	0	0	0
Otu00422	0	1.19	0.01	0	0	0
Otu00430	0	0	0	0	0.01	0.01
Otu00432	0.38	0	0	0	0.03	0

Table 4.4. (cont'd)

Otu00435	0	0	0	0	0.01	0.01
Otu00437	0	0.07	0	0	0	0
Otu00440	0	0	0	0	0	0
Otu00441	0	0.49	0.6	0	0	0
Otu00443	0	0	0	0.03	0	0
Otu00445	0	0	0	0	0.01	0.02
Otu00446	0.05	0	0	0	0	0
Otu00448	0	0	2.74	0	0	0
Otu00457	0.06	0	0	0	0.02	0.01
Otu00458	0	0	0	0	0	0.04
Otu00460	0	0	0	0	0	0.08
Otu00462	0	1.58	0	0	0	0
Otu00469	0.01	0	0	0	0.02	0.02
Otu00471	0.01	0	0	0	0.01	0.01
Otu00472	0	0	0	0	0.04	0.01
Otu00473	0.08	0	0	0	0.01	0.01
Otu00475	0.01	0	0	0	0.02	0
Otu00476	0.01	0	0	0	0.01	0.01
Otu00479	0	0	0	0	0.01	0.22
Otu00480	0.33	0	0	0	0.02	0.03

Table 4.4. (cont'd)

Otu00481	0	0.13	0	0	0	0
Otu00487	1.05	0	0	0	0	0
Otu00488	0	0	0	0	0.02	0.01
Otu00499	0	0	0	0	0.01	0
Otu00501	0	0	0	0	0.02	0
Otu00505	0	1.39	0.05	0	0	0
Otu00506	0	0	0	0	0.01	0.01
Otu00508	0	0	0	0	0.01	0
Otu00509	0.01	0	0	0	0.01	0.01
Otu00510	0	0	0	0	0	0
Otu00511	0	0	0	0	0.02	0.01
Otu00512	0	0	0	0	0.21	0.02
Otu00515	0	0	0	0	0.01	0
Otu00516	0	0	0	0	0.03	0
Otu00519	0	0	0.01	0	0	0
Otu00520	0	0	0	0	0.01	0.03
Otu00522	0	0	0	0	0.01	0.01
Otu00526	0.03	0	0	0	0.03	0
Otu00530	0.07	0	0	0	0.05	0.04
Otu00539	0	0	0.02	0	0	0

Table 4.4. (cont'd)

Otu00541	0.02	0	0	0	0.03	0.03
Otu00542	0	0.02	0.09	0.01	0	0
Otu00546	0	0	0	0	0.03	0.04
Otu00548	0	0	0	0	0.05	0
Otu00554	0	0	0	0	0	0.02
Otu00555	0.01	0	0	0	0.01	0
Otu00560	0.04	0	0	0	0.01	0
Otu00570	0	0	0	0	0.03	0.01
Otu00572	0	0.02	0	0	0.01	0.01
Otu00577	0.01	0	0	0	0	0
Otu00578	0	0	0	0.01	0	0
Otu00579	0	0.05	0.56	0	0	0
Otu00580	0	0.34	0.03	0	0	0
Otu00591	0	0	0	0	0.01	0.01
Otu00593	0.01	0	0	0	0.05	0
Otu00594	0.03	0	0	0	0.01	0.02
Otu00595	0	0.01	0.19	0	0	0
Otu00600	0	0	0	0	0	0.01
Otu00601	0	0	0	0	0.01	0
Otu00603	0.15	0	0	0	0.01	0

Table 4.4. (cont'd)

Otu00606	0.03	0	0	0	0.01	0.01
Otu00608	0	0	0	0	0.04	0.03
Otu00609	0	0	0	0	0.04	0.03
Otu00613	0.03	0	0	0	0.01	0
Otu00623	0	0	0.52	0.07	0	0
Otu00625	0	0	0	0	0	0
Otu00626	0.01	0	0	0	0.01	0.01
Otu00634	0.01	0	0	0	0.01	0
Otu00636	0.05	0	0	0	0.03	0
Otu00637	0	0.01	0	0	0	0
Otu00654	0	0	0	0	0.02	0
Otu00657	0.24	0	0	0	0.01	0.01
Otu00661	0	0	0	0	0	0
Otu00667	0	0	0	0	0	0
Otu00668	0.03	0	0	0	0.01	0.02
Otu00676	0.09	0	0	0	0	0
Otu00677	0	0.62	0.66	0	0	0
Otu00679	0	0	0	0	0.02	0
Otu00681	0	0	0	0	0.04	0.03
Otu00682	0.01	0	0	0	0.01	0.01

Table 4.4. (cont'd)

Otu00684	0	0.11	0	0	0.01	0.04
Otu00685	0	0	0	0	0.02	0.05
Otu00691	0.04	0	0	0	0.02	0.01
Otu00700	0.02	0	0	0	0	0
Otu00703	0	0.12	0.18	0.01	0	0
Otu00725	0	0	0	0	0.07	0
Otu00730	0	0	0	0	0	0.01
Otu00739	0.03	0	0	0	0.01	0
Otu00740	0.06	0	0	0	0	0
Otu00741	0.02	0	0	0	0.01	0.03
Otu00742	0	0	0	0.59	0	0
Otu00773	0	0	0.08	0	0.01	0
Otu00779	0	0	0	0	0.01	0
Otu00782	0	0	0	0	0.07	0.15
Otu00785	0	0	0.03	0	0	0
Otu00809	0.13	0	0	0	0	0
Otu00810	0	0	0.4	0	0	0
Otu00818	0	0	0	0	0	0
Otu00822	0	0	0	0	0	0
Otu00830	0	0	0	0	0.01	0

Table 4.4. (cont'd)

Otu00833	0	0	0	0	0.03	0.01
Otu00835	0.01	0	0	0	0.02	0.01
Otu00859	0	0	0	0	0	0
Otu00861	0.03	0	0	0	0	0
Otu00864	0	0	0	0	0.01	0.06
Otu00873	0	0	0	0	0.03	0
Otu00878	0.09	0	0	0	0.01	0
Otu00880	0.05	0	0	0	0.01	0
Otu00891	0	0.27	0.15	0.01	0	0
Otu00894	0.02	0	0	0	0.01	0.01
Otu00902	0.04	0	0	0	0.02	0.01
Otu00930	0.05	0	0	0	0.01	0
Otu00973	0.08	0	0	0	0.01	0
Otu00994	0	0	0	0	0.04	0.02
Otu00998	0.02	0	0	0	0.01	0
Otu01030	0	0	0	0	0.03	0
Otu01033	0	0	0	0	0.02	0.01
Otu01043	0	0	0	0	0.02	0
Otu01114	0	0	0.32	0	0	0
Otu01120	0.08	0	0	0	0	0

Table 4.4. (cont'd)

Otu01158	0.02	0	0	0	0	0
Otu01340	0	0	0	0	0.01	0
Otu01372	0.02	0	0	0	0	0
Otu01395	0.08	0	0	0	0	0.02
Otu01432	0.18	0	0	0	0	0
Otu01445	0	0	0	0	0	0
Otu01460	0.03	0	0	0	0.01	0.02
Otu01464	0.08	0	0	0	0	0
Otu02071	0.04	0	0	0	0	0
Otu02174	0	0	0	0	0	0
Otu02236	0.05	0	0	0	0	0
Otu02277	0.14	0	0	0	0	0
Otu02288	0.09	0	0	0	0	0
Otu03141	0	0	0	0	0	0
Otu03149	0	0	0.03	0	0	0
Otu03156	0.03	0	0	0	0	0
Otu03157	0	0	0	0	0	0.08
Otu03158	0	0	0	0	0.04	0

Table 4.5. OTU taxonomy table.

OTU	Taxonomy
Otu00001	Bacteria(100);"Bacteroidetes"(100);"Bacteroidia"(100);"Bacteroidales"(100);Bacteroidaceae(100);Bacteroides(100);
Otu00002	Bacteria(100);"Bacteroidetes"(100);"Bacteroidia"(93);"Bacteroidales"(93);"Porphyromonadaceae"(92);unclassified(92);
Otu00003	Bacteria(100);"Bacteroidetes"(100);"Bacteroidia"(100);"Bacteroidales"(100);"Porphyromonadaceae"(100);unclassified(100);
Otu00004	Bacteria(100);"Bacteroidetes"(100);"Bacteroidia"(100);"Bacteroidales"(100);"Porphyromonadaceae"(100);unclassified(100);
Otu00005	Bacteria(100);"Verrucomicrobia"(100);Verrucomicrobiae(100);Verrucomicrobiales(100);Verrucomicrobiaceae(100);Akkermansia(100);
Otu00006	Bacteria(100);Firmicutes(100);Erysipelotrichia(100);Erysipelotrichales(100);Erysipelotrichaceae(100);Turicibacter(100);
Otu00007	Bacteria(100);"Bacteroidetes"(100);"Bacteroidia"(100);"Bacteroidales"(100);"Porphyromonadaceae"(100);unclassified(100);
Otu00008	Bacteria(100);"Bacteroidetes"(100);"Bacteroidia"(100);"Bacteroidales"(100);"Rikenellaceae"(100);Alistipes(100);
Otu00009	Bacteria(100);Firmicutes(100);Clostridia(100);Clostridiales(100);Lachnospiraceae(100);unclassified(100);
Otu00010	Bacteria(100);"Bacteroidetes"(100);unclassified(100);unclassified(100);unclassified(100);unclassified(100);
Otu00011	Bacteria(100);Firmicutes(100);Clostridia(100);Clostridiales(100);Lachnospiraceae(100);unclassified(100);
Otu00012	Bacteria(100);Firmicutes(100);Bacilli(100);Lactobacillales(100);Lactobacillaceae(100);Lactobacillus(100);
Otu00013	Bacteria(100);"Bacteroidetes"(100);"Bacteroidia"(100);"Bacteroidales"(100);"Rikenellaceae"(100);Alistipes(100);
Otu00014	Bacteria(100);"Bacteroidetes"(100);"Bacteroidia"(100);"Bacteroidales"(100);Bacteroidaceae(100);Bacteroides(100);
Otu00015	Bacteria(100);"Bacteroidetes"(100);"Bacteroidia"(100);"Bacteroidales"(100);"Porphyromonadaceae"(100);unclassified(100);
Otu00016	Bacteria(100);Firmicutes(100);Clostridia(100);Clostridiales(100);Ruminococcaceae(100);unclassified(100);
Otu00017	Bacteria(100);Firmicutes(100);Clostridia(100);Clostridiales(100);Lachnospiraceae(100);unclassified(100);
Otu00018	Bacteria(100);Firmicutes(100);Clostridia(100);Clostridiales(100);Ruminococcaceae(100);unclassified(75);
Otu00019	Bacteria(100);Firmicutes(100);Erysipelotrichia(100);Erysipelotrichales(100);Erysipelotrichaceae(100);Allobaculum(97);
Otu00020	Bacteria(100);"Bacteroidetes"(100);"Bacteroidia"(100);"Bacteroidales"(100);"Porphyromonadaceae"(100);Odoribacter(100);

Table 4.5. (cont'd)

Otu00021	Bacteria(100);Firmicutes(100);Clostridia(100);Clostridiales(100);Lachnospiraceae(100);unclassified(100);
Otu00022	Bacteria(100);Firmicutes(100);Clostridia(100);Clostridiales(100);Lachnospiraceae(100);unclassified(100);
Otu00023	Bacteria(100);"Bacteroidetes"(100);"Bacteroidia"(100);"Bacteroidales"(100);"Rikenellaceae"(100);Alistipes(100);
Otu00024	Bacteria(100);"Bacteroidetes"(100);"Bacteroidia"(100);"Bacteroidales"(100);"Rikenellaceae"(100);Alistipes(100);
Otu00026	Bacteria(100);Firmicutes(100);Clostridia(100);Clostridiales(100);Lachnospiraceae(100);Clostridium_XlVa(78);
Otu00027	Bacteria(100);Firmicutes(100);Clostridia(100);Clostridiales(100);Lachnospiraceae(100);unclassified(100);
Otu00028	Bacteria(100);"Bacteroidetes"(100);"Bacteroidia"(100);"Bacteroidales"(100);"Prevotellaceae"(93);unclassified(93);
Otu00029	Bacteria(100);Firmicutes(100);Clostridia(100);Clostridiales(100);Lachnospiraceae(100);unclassified(100);
Otu00030	Bacteria(100);"Deferribacteres"(100);Deferribacteres(100);Deferribacterales(100);Deferribacteraceae(100);Mucispirillum(100);
Otu00031	Bacteria(100);"Tenericutes"(100);Mollicutes(100);Anaeroplasmatales(100);Anaeroplasmataceae(100);Anaeroplasma(100);
Otu00032	Bacteria(100);"Bacteroidetes"(100);"Bacteroidia"(100);"Bacteroidales"(100);"Porphyromonadaceae"(100);unclassified(100);
Otu00033	Bacteria(100);"Bacteroidetes"(100);"Bacteroidia"(99);"Bacteroidales"(99);"Porphyromonadaceae"(99);Barnesiella(99);
Otu00034	Bacteria(100);Firmicutes(100);Clostridia(100);Clostridiales(100);Lachnospiraceae(100);unclassified(100);
Otu00035	Bacteria(100);Firmicutes(100);Clostridia(100);Clostridiales(100);Peptostreptococcaceae(100);Clostridium_XI(96);
Otu00036	Bacteria(100);Firmicutes(100);Clostridia(100);Clostridiales(100);Ruminococcaceae(100);unclassified(99);
Otu00037	Bacteria(100);"Bacteroidetes"(100);"Bacteroidia"(100);"Bacteroidales"(100);"Porphyromonadaceae"(99);unclassified(99);
Otu00038	Bacteria(100);"Bacteroidetes"(100);"Bacteroidia"(100);"Bacteroidales"(100);"Porphyromonadaceae"(100);unclassified(100);
Otu00039	Bacteria(100);"Bacteroidetes"(100);"Bacteroidia"(100);"Bacteroidales"(100);"Porphyromonadaceae"(100);unclassified(93);
Otu00040	Bacteria(100);Firmicutes(100);Clostridia(100);Clostridiales(100);Ruminococcaceae(100);unclassified(100);
Otu00041	Bacteria(100);"Bacteroidetes"(100);"Bacteroidia"(100);"Bacteroidales"(100);"Porphyromonadaceae"(100);unclassified(100);

Table 4.5. (cont'd)

Otu00042	Bacteria(100);Firmicutes(100);Clostridia(100);Clostridiales(100);Lachnospiraceae(100);Roseburia(95);
Otu00043	Bacteria(100);Firmicutes(100);Clostridia(100);Clostridiales(100);Lachnospiraceae(100);unclassified(100);
Otu00044	Bacteria(100);Firmicutes(100);Clostridia(100);Clostridiales(100);Lachnospiraceae(100);unclassified(100);
Otu00045	Bacteria(100);Firmicutes(100);Bacilli(100);Lactobacillales(100);Lactobacillaceae(100);Lactobacillus(99);
Otu00046	Bacteria(100);"Bacteroidetes"(100);"Bacteroidia"(100);"Bacteroidales"(100);"Rikenellaceae"(100);Alistipes(100);
Otu00047	Bacteria(100);"Bacteroidetes"(100);"Bacteroidia"(100);"Bacteroidales"(100);"Porphyromonadaceae"(100);Barnesiella(99);
Otu00048	Bacteria(100);"Bacteroidetes"(99);unclassified(99);unclassified(99);unclassified(99);unclassified(99);
Otu00049	Bacteria(100);"Proteobacteria"(100);Deltaproteobacteria(99);Desulfovibrionales(99);unclassified(99);unclassified(99);
Otu00051	Bacteria(100);Firmicutes(100);Clostridia(100);Clostridiales(100);Ruminococcaceae(100);Oscillibacter(99);
Otu00052	Bacteria(100);"Bacteroidetes"(100);"Bacteroidia"(100);"Bacteroidales"(100);Bacteroidaceae(100);Bacteroides(100);
Otu00053	Bacteria(100);Firmicutes(100);Bacilli(100);Lactobacillales(100);Lactobacillaceae(100);Lactobacillus(100);
Otu00054	Bacteria(100);"Bacteroidetes"(100);"Bacteroidia"(100);"Bacteroidales"(100);"Porphyromonadaceae"(99);Barnesiella(54);
Otu00055	Bacteria(100);"Bacteroidetes"(100);"Bacteroidia"(100);"Bacteroidales"(100);"Porphyromonadaceae"(100);unclassified(99);
Otu00056	Bacteria(100);"Bacteroidetes"(100);"Bacteroidia"(100);"Bacteroidales"(100);"Porphyromonadaceae"(100);Odoribacter(100);
Otu00057	Bacteria(100);"Bacteroidetes"(100);unclassified(100);unclassified(100);unclassified(100);unclassified(100);
Otu00058	Bacteria(100);"Bacteroidetes"(100);"Bacteroidia"(98);"Bacteroidales"(98);"Porphyromonadaceae"(96);unclassified(96);
Otu00059	Bacteria(100);"Proteobacteria"(100);Gammaproteobacteria(100);Pseudomonadales(100);Pseudomonadaceae(100);Pseudomonas(100);
Otu00060	Bacteria(100);Firmicutes(100);Clostridia(100);Clostridiales(100);Lachnospiraceae(100);unclassified(100);
Otu00061	Bacteria(100);Firmicutes(100);Clostridia(100);Clostridiales(100);Ruminococcaceae(100);Oscillibacter(100);
Otu00062	Bacteria(100);Firmicutes(100);Clostridia(100);Clostridiales(100);Lachnospiraceae(100);unclassified(100);

Table 4.5. (cont'd)

Otu00063	Bacteria(100);Firmicutes(99);Erysipelotrichia(96);Erysipelotrichales(96);Erysipelotrichaceae(96);unclassified(96);
Otu00064	Bacteria(100);"Bacteroidetes"(100);"Bacteroidia"(100);"Bacteroidales"(100);"Porphyromonadaceae"(100);unclassified(100);
Otu00065	Bacteria(100);Firmicutes(100);Bacilli(100);Lactobacillales(92);Enterococcaceae(91);Enterococcus(88);
Otu00066	Bacteria(100);Firmicutes(100);Bacilli(100);Lactobacillales(100);Lactobacillaceae(100);Lactobacillus(100);
Otu00067	Bacteria(100);Firmicutes(100);Clostridia(100);Clostridiales(100);Lachnospiraceae(99);unclassified(99);
Otu00068	Bacteria(100);"Bacteroidetes"(100);"Bacteroidia"(100);"Bacteroidales"(100);"Porphyromonadaceae"(100);unclassified(98);
Otu00069	Bacteria(100);Firmicutes(100);Clostridia(100);Clostridiales(100);Ruminococcaceae(100);unclassified(83);
Otu00070	Bacteria(100);"Bacteroidetes"(100);"Bacteroidia"(100);"Bacteroidales"(100);"Porphyromonadaceae"(100);unclassified(100);
Otu00071	Bacteria(100);Firmicutes(100);Clostridia(100);Clostridiales(100);Lachnospiraceae(100);unclassified(100);
Otu00072	Bacteria(100);"Proteobacteria"(100);Betaproteobacteria(100);Burkholderiales(100);Sutterellaceae(100);Parasutterella(100);
Otu00073	Bacteria(100);Firmicutes(100);Erysipelotrichia(100);Erysipelotrichales(100);Erysipelotrichaceae(100);unclassified(100);
Otu00074	Bacteria(100);Firmicutes(100);Clostridia(100);Clostridiales(100);Lachnospiraceae(100);unclassified(100);
Otu00075	Bacteria(100);Firmicutes(100);Clostridia(100);Clostridiales(100);Ruminococcaceae(100);unclassified(100);
Otu00076	Bacteria(100);Firmicutes(100);Clostridia(100);Clostridiales(100);Lachnospiraceae(59);unclassified(59);
Otu00077	Bacteria(100);Firmicutes(100);Clostridia(100);Clostridiales(100);Lachnospiraceae(100);unclassified(100);
Otu00078	Bacteria(100);"Bacteroidetes"(100);"Bacteroidia"(100);"Bacteroidales"(100);"Rikenellaceae"(100);Alistipes(100);
Otu00080	Bacteria(100);"Bacteroidetes"(100);"Bacteroidia"(100);"Bacteroidales"(100);Bacteroidaceae(100);Bacteroides(100);
Otu00081	Bacteria(100);"Bacteroidetes"(100);"Bacteroidia"(100);"Bacteroidales"(100);"Porphyromonadaceae"(100);Parabacteroides(100);
Otu00082	Bacteria(100);Firmicutes(100);Clostridia(99);Clostridiales(99);unclassified(99);unclassified(99);
Otu00083	Bacteria(100);Firmicutes(100);Clostridia(100);Clostridiales(100);Ruminococcaceae(100);unclassified(63);

Table 4.5. (cont'd)

Otu00084	Bacteria(100);Firmicutes(100);Clostridia(100);Clostridiales(100);unclassified(100);unclassified(100);
Otu00085	Bacteria(100);Firmicutes(100);Clostridia(100);Clostridiales(100);Lachnospiraceae(100);Clostridium_XlVb(100);
Otu00086	Bacteria(100);Firmicutes(100);Clostridia(100);Clostridiales(100);Lachnospiraceae(100);Clostridium_XlVa(93);
Otu00087	Bacteria(100);"Bacteroidetes"(100);"Bacteroidia"(100);"Bacteroidales"(100);"Porphyromonadaceae"(100);unclassified(100);
Otu00088	Bacteria(100);Firmicutes(100);Clostridia(100);Clostridiales(100);Lachnospiraceae(100);Clostridium_XlVb(100);
Otu00089	Bacteria(100);"Proteobacteria"(100);Gammaproteobacteria(100);"Enterobacteriales"(100);Enterobacteriaceae(100);unclassified(100);
Otu00090	Bacteria(100);Firmicutes(100);Clostridia(100);Clostridiales(100);Lachnospiraceae(100);Clostridium_XlVa(94);
Otu00091	Bacteria(100);Firmicutes(100);Clostridia(100);Clostridiales(100);Clostridiaceae_1(100);Clostridium_sensu_stricto(100);
Otu00092	Bacteria(100);Firmicutes(100);Erysipelotrichia(100);Erysipelotrichales(100);Erysipelotrichaceae(100);Clostridium_XVIII(100);
Otu00093	Bacteria(100);"Bacteroidetes"(100);"Bacteroidia"(100);"Bacteroidales"(100);"Porphyromonadaceae"(100);Odoribacter(100);
Otu00094	Bacteria(100);Firmicutes(100);Clostridia(100);Clostridiales(100);Ruminococcaceae(99);unclassified(99);
Otu00095	Bacteria(100);"Actinobacteria"(100);Actinobacteria(100);Bifidobacteriales(100);Bifidobacteriaceae(100);Bifidobacterium(100);
Otu00096	Bacteria(100);Firmicutes(100);Clostridia(100);Clostridiales(100);Lachnospiraceae(100);unclassified(100);
Otu00097	Bacteria(100);unclassified(100);unclassified(100);unclassified(100);unclassified(100);unclassified(100);
Otu00098	Bacteria(100);Firmicutes(100);Clostridia(100);Clostridiales(100);Ruminococcaceae(100);Clostridium_IV(80);
Otu00099	Bacteria(100);Firmicutes(100);Clostridia(100);Clostridiales(100);Lachnospiraceae(100);unclassified(100);
Otu00100	Bacteria(100);"Bacteroidetes"(100);"Bacteroidia"(100);"Bacteroidales"(100);unclassified(98);unclassified(98);
Otu00101	Bacteria(100);Firmicutes(100);Clostridia(100);Clostridiales(100);Lachnospiraceae(100);unclassified(98);
Otu00102	Bacteria(100);Firmicutes(100);Clostridia(99);Clostridiales(99);unclassified(99);unclassified(99);
Otu00103	Bacteria(100);Firmicutes(100);Clostridia(100);Clostridiales(100);Ruminococcaceae(100);unclassified(100);

Table 4.5. (cont'd)

Otu00104	Bacteria(100);Firmicutes(100);Clostridia(100);Clostridiales(100);Lachnospiraceae(100);unclassified(100);
Otu00105	Bacteria(100);"Proteobacteria"(100);Betaproteobacteria(100);unclassified(100);unclassified(100);unclassified(100);
Otu00106	Bacteria(100);Firmicutes(99);Clostridia(99);Clostridiales(99);unclassified(99);unclassified(99);
Otu00108	Bacteria(100);Firmicutes(100);Clostridia(100);Clostridiales(100);Lachnospiraceae(100);Clostridium_XlVa(97);
Otu00109	Bacteria(100);Firmicutes(100);Clostridia(100);Clostridiales(100);Ruminococcaceae(100);unclassified(82);
Otu00110	Bacteria(100);"Proteobacteria"(100);Gammaproteobacteria(100);Oceanospirillales(100);Halomonadaceae(100);Halomonas(100);
Otu00111	Bacteria(100);"Bacteroidetes"(100);"Bacteroidia"(100);"Bacteroidales"(100);Bacteroidaceae(100);Bacteroides(100);
Otu00112	Bacteria(100);unclassified(100);unclassified(100);unclassified(100);unclassified(100);unclassified(100);
Otu00113	Bacteria(100);Firmicutes(99);unclassified(99);unclassified(99);unclassified(99);unclassified(99);
Otu00114	Bacteria(100);Firmicutes(100);Clostridia(100);Clostridiales(100);Ruminococcaceae(100);Clostridium_IV(95);
Otu00115	Bacteria(100);Firmicutes(100);Clostridia(100);Clostridiales(100);Lachnospiraceae(100);unclassified(100);
Otu00116	Bacteria(100);"Bacteroidetes"(100);"Bacteroidia"(100);"Bacteroidales"(100);"Porphyromonadaceae"(100);unclassified(100);
Otu00117	Bacteria(100);Firmicutes(100);Clostridia(100);Clostridiales(100);Ruminococcaceae(97);unclassified(97);
Otu00118	Bacteria(100);Firmicutes(100);Clostridia(100);Clostridiales(100);Ruminococcaceae(100);unclassified(61);
Otu00119	Bacteria(100);"Bacteroidetes"(100);"Bacteroidia"(100);"Bacteroidales"(100);Bacteroidaceae(100);Bacteroides(100);
Otu00120	Bacteria(100);"Bacteroidetes"(100);unclassified(100);unclassified(100);unclassified(100);unclassified(100);
Otu00123	Bacteria(100);Firmicutes(100);Clostridia(100);Clostridiales(100);unclassified(100);unclassified(100);
Otu00124	Bacteria(100);Firmicutes(100);Clostridia(100);Clostridiales(100);Ruminococcaceae(99);unclassified(99);
Otu00125	Bacteria(100);Firmicutes(100);Clostridia(100);Clostridiales(100);Ruminococcaceae(100);Flavonifractor(100);
Otu00127	Bacteria(100);Firmicutes(100);Clostridia(100);Clostridiales(100);Lachnospiraceae(100);unclassified(100);

Table 4.5. (cont'd)

Otu00128	Bacteria(100);"Bacteroidetes"(100);"Bacteroidia"(100);"Bacteroidales"(100);"Porphyromonadaceae"(100);unclassified(100);
Otu00129	Bacteria(100);Firmicutes(100);Clostridia(100);Clostridiales(100);Lachnospiraceae(100);unclassified(100);
Otu00130	Bacteria(100);Firmicutes(100);Clostridia(100);Clostridiales(100);Lachnospiraceae(100);unclassified(100);
Otu00131	Bacteria(100);Firmicutes(100);Clostridia(100);Clostridiales(100);Lachnospiraceae(100);unclassified(100);
Otu00132	Bacteria(100);Firmicutes(100);Clostridia(100);Clostridiales(100);Lachnospiraceae(99);unclassified(99);
Otu00133	Bacteria(100);Firmicutes(100);Clostridia(100);Clostridiales(100);Lachnospiraceae(100);unclassified(100);
Otu00134	Bacteria(100);Firmicutes(100);Clostridia(100);Clostridiales(98);unclassified(98);unclassified(98);
Otu00135	Bacteria(100);Firmicutes(100);Clostridia(100);Clostridiales(100);Lachnospiraceae(100);Lachnospiracea_incertae_sedis(95);
Otu00136	Bacteria(100);Firmicutes(100);Clostridia(100);Clostridiales(100);Lachnospiraceae(100);Blautia(98);
Otu00137	Bacteria(100);Firmicutes(100);Clostridia(100);Clostridiales(100);Ruminococcaceae(95);unclassified(95);
Otu00138	Bacteria(100);Firmicutes(100);Clostridia(100);Clostridiales(100);Lachnospiraceae(100);unclassified(100);
Otu00139	Bacteria(100);Firmicutes(100);Clostridia(100);Clostridiales(100);Ruminococcaceae(100);Ruminococcus(100);
Otu00140	Bacteria(100);Firmicutes(100);Clostridia(100);Clostridiales(100);unclassified(100);unclassified(100);
Otu00141	Bacteria(100);Firmicutes(100);unclassified(94);unclassified(94);unclassified(94);unclassified(94);
Otu00143	Bacteria(100);Firmicutes(100);Clostridia(100);Clostridiales(100);Ruminococcaceae(100);Pseudoflavonifractor(94);
Otu00144	Bacteria(100);Firmicutes(100);Clostridia(90);Clostridiales(90);unclassified(90);unclassified(90);
Otu00145	Bacteria(100);Firmicutes(100);Bacilli(99);Bacillales(97);Staphylococcaceae(96);Staphylococcus(95);
Otu00147	Bacteria(100);Firmicutes(100);Clostridia(100);Clostridiales(100);Ruminococcaceae(100);unclassified(99);
Otu00148	Bacteria(100);Firmicutes(100);Clostridia(100);Clostridiales(100);Ruminococcaceae(100);Clostridium_IV(97);
Otu00149	Bacteria(100);Firmicutes(100);Clostridia(100);Clostridiales(100);Ruminococcaceae(100);Faecalibacterium(96);

Table 4.5. (cont'd)

Otu00150	Bacteria(100);Firmicutes(100);Clostridia(100);Clostridiales(100);Lachnospiraceae(99);unclassified(99);
Otu00152	Bacteria(100);Firmicutes(100);Clostridia(100);Clostridiales(100);Lachnospiraceae(100);unclassified(100);
Otu00153	Bacteria(100);Firmicutes(100);Clostridia(100);Clostridiales(100);unclassified(95);unclassified(95);
Otu00154	Bacteria(100);"Proteobacteria"(100);Deltaproteobacteria(100);Desulfovibrionales(100);Desulfovibrionaceae(100);Desulfovibrio(98);
Otu00155	Bacteria(100);"Bacteroidetes"(100);"Bacteroidia"(100);"Bacteroidales"(100);"Porphyromonadaceae"(100);unclassified(100);
Otu00156	Bacteria(100);Firmicutes(100);Clostridia(100);Clostridiales(100);Lachnospiraceae(100);unclassified(93);
Otu00157	Bacteria(100);Firmicutes(100);Clostridia(100);Clostridiales(100);Lachnospiraceae(100);unclassified(100);
Otu00158	Bacteria(100);Firmicutes(100);Clostridia(100);Clostridiales(100);unclassified(67);unclassified(67);
Otu00159	Bacteria(100);"Bacteroidetes"(100);"Bacteroidia"(100);"Bacteroidales"(100);"Rikenellaceae"(100);Alistipes(100);
Otu00161	Bacteria(100);Firmicutes(100);Clostridia(100);Clostridiales(100);Lachnospiraceae(100);unclassified(100);
Otu00162	Bacteria(100);"Bacteroidetes"(100);"Sphingobacteria"(100);"Sphingobacteriales"(100);Sphingobacteriaceae(100);Sphingobacterium(100);
Otu00163	Bacteria(100);Firmicutes(100);Clostridia(100);Clostridiales(100);Ruminococcaceae(94);unclassified(94);
Otu00164	Bacteria(100);"Bacteroidetes"(100);"Bacteroidia"(100);"Bacteroidales"(100);"Porphyromonadaceae"(100);Parabacteroides(100);
Otu00165	Bacteria(100);unclassified(100);unclassified(100);unclassified(100);unclassified(100);unclassified(100);
Otu00166	Bacteria(100);Firmicutes(100);Clostridia(100);Clostridiales(100);Lachnospiraceae(100);Dorea(100);
Otu00168	Bacteria(100);Firmicutes(100);Clostridia(100);Clostridiales(100);Ruminococcaceae(100);unclassified(100);
Otu00169	Bacteria(100);Firmicutes(100);Clostridia(100);Clostridiales(100);Lachnospiraceae(100);unclassified(100);
Otu00170	Bacteria(100);"Bacteroidetes"(100);"Bacteroidia"(100);"Bacteroidales"(100);"Porphyromonadaceae"(100);unclassified(100);
Otu00171	Bacteria(100);Firmicutes(100);Clostridia(100);Clostridiales(100);Lachnospiraceae(100);unclassified(100);
Otu00173	Bacteria(100);Firmicutes(100);Erysipelotrichia(100);Erysipelotrichales(100);Erysipelotrichaceae(100);unclassified(100);

Table 4.5. (cont'd)

Otu00174	Bacteria(100);"Bacteroidetes"(100);"Bacteroidia"(100);"Bacteroidales"(100);"Porphyromonadaceae"(99);unclassified(52);
Otu00175	Bacteria(100);Firmicutes(100);Negativicutes(100);Selenomonadales(100);Acidaminococcaceae(100);Phascolarctobacterium(100);
Otu00176	Bacteria(100);Firmicutes(100);Clostridia(100);Clostridiales(100);Lachnospiraceae(100);Johnsonella(100);
Otu00178	Bacteria(100);Firmicutes(100);Clostridia(100);Clostridiales(100);Eubacteriaceae(100);Eubacterium(100);
Otu00179	Bacteria(100);"Bacteroidetes"(100);"Bacteroidia"(100);"Bacteroidales"(100);"Porphyromonadaceae"(100);unclassified(100);
Otu00180	Bacteria(100);"Bacteroidetes"(100);"Bacteroidia"(99);"Bacteroidales"(99);unclassified(99);unclassified(99);
Otu00181	Bacteria(100);"Bacteroidetes"(100);"Bacteroidia"(99);"Bacteroidales"(99);"Porphyromonadaceae"(51);unclassified(51);
Otu00182	Bacteria(100);Firmicutes(100);Clostridia(100);Clostridiales(100);Lachnospiraceae(99);unclassified(99);
Otu00183	Bacteria(100);Firmicutes(100);Clostridia(100);Clostridiales(100);Lachnospiraceae(100);unclassified(100);
Otu00184	Bacteria(100);Firmicutes(100);Clostridia(100);Clostridiales(100);Lachnospiraceae(100);unclassified(100);
Otu00185	Bacteria(100);Firmicutes(100);Clostridia(100);Clostridiales(100);Lachnospiraceae(100);unclassified(100);
Otu00186	Bacteria(100);Firmicutes(100);Clostridia(100);Clostridiales(100);Ruminococcaceae(100);unclassified(99);
Otu00187	Bacteria(100);Firmicutes(100);Clostridia(100);Clostridiales(100);Ruminococcaceae(100);unclassified(100);
Otu00188	Bacteria(100);Firmicutes(100);Clostridia(100);Clostridiales(100);Ruminococcaceae(100);Oscillibacter(96);
Otu00189	Bacteria(100);"Proteobacteria"(100);Gammaproteobacteria(100);Alteromonadales(100);Shewanellaceae(100);Shewanella(100);
Otu00190	Bacteria(100);"Bacteroidetes"(100);"Bacteroidia"(62);"Bacteroidales"(62);unclassified(61);unclassified(61);
Otu00191	Bacteria(100);Firmicutes(100);Clostridia(100);Clostridiales(100);Lachnospiraceae(100);unclassified(100);
Otu00192	Bacteria(100);Firmicutes(100);unclassified(97);unclassified(97);unclassified(97);unclassified(97);
Otu00194	Bacteria(100);Firmicutes(100);Clostridia(100);Clostridiales(100);Ruminococcaceae(100);Oscillibacter(61);
Otu00195	Bacteria(100);Firmicutes(100);Clostridia(100);Clostridiales(100);Lachnospiraceae(100);unclassified(100);

Table 4.5. (cont'd)

Otu00196	Bacteria(100);Firmicutes(100);Clostridia(100);Clostridiales(100);Lachnospiraceae(100);unclassified(100);
Otu00197	Bacteria(100);Firmicutes(100);Clostridia(100);Clostridiales(100);Lachnospiraceae(100);unclassified(100);
Otu00198	Bacteria(100);Firmicutes(100);Clostridia(100);Clostridiales(100);Lachnospiraceae(100);unclassified(100);
Otu00199	Bacteria(100);Firmicutes(100);Clostridia(100);Clostridiales(100);Lachnospiraceae(100);unclassified(100);
Otu00200	Bacteria(100);Firmicutes(100);Clostridia(100);Clostridiales(100);Lachnospiraceae(100);unclassified(100);
Otu00201	Bacteria(100);Firmicutes(100);Clostridia(100);Clostridiales(100);Lachnospiraceae(100);unclassified(100);
Otu00202	Bacteria(100);Firmicutes(100);Clostridia(100);Clostridiales(100);Lachnospiraceae(66);unclassified(66);
Otu00203	Bacteria(100);Firmicutes(100);Clostridia(100);Clostridiales(100);Lachnospiraceae(100);unclassified(100);
Otu00204	Bacteria(100);Firmicutes(100);Clostridia(100);Clostridiales(100);Lachnospiraceae(100);unclassified(100);
Otu00205	Bacteria(100);Firmicutes(100);Clostridia(100);Clostridiales(100);unclassified(96);unclassified(96);
Otu00206	Bacteria(100);Firmicutes(100);Clostridia(100);Clostridiales(100);unclassified(89);unclassified(89);
Otu00207	Bacteria(100);Firmicutes(100);Clostridia(100);Clostridiales(100);unclassified(100);unclassified(100);
Otu00209	Bacteria(100);Firmicutes(100);Clostridia(100);Clostridiales(100);Ruminococcaceae(100);Clostridium_IV(87);
Otu00210	Bacteria(100);Firmicutes(100);Clostridia(100);Clostridiales(100);Lachnospiraceae(100);unclassified(100);
Otu00211	Bacteria(100);Firmicutes(100);Clostridia(100);Clostridiales(100);Lachnospiraceae(100);unclassified(100);
Otu00212	Bacteria(100);"Proteobacteria"(100);Alphaproteobacteria(99);unclassified(99);unclassified(99);unclassified(99);
Otu00213	Bacteria(100);Firmicutes(100);Clostridia(100);Clostridiales(100);Lachnospiraceae(100);unclassified(100);
Otu00214	Bacteria(100);unclassified(100);unclassified(100);unclassified(100);unclassified(100);unclassified(100);
Otu00215	Bacteria(100);"Bacteroidetes"(100);"Bacteroidia"(100);"Bacteroidales"(100);"Porphyromonadaceae"(100);Barnesiella(85);
Otu00216	Bacteria(100);Firmicutes(100);Clostridia(100);Clostridiales(100);Ruminococcaceae(100);unclassified(100);

Table 4.5. (cont'd)

Otu00219	Bacteria(100);Firmicutes(100);Clostridia(100);Clostridiales(100);Lachnospiraceae(100);unclassified(100);
Otu00220	Bacteria(100);"Bacteroidetes"(100);"Bacteroidia"(100);"Bacteroidales"(100);Bacteroidaceae(100);Bacteroides(100);
Otu00221	Bacteria(100);Firmicutes(100);Clostridia(100);Clostridiales(100);Lachnospiraceae(99);unclassified(99);
Otu00222	Bacteria(100);Firmicutes(100);Clostridia(100);Clostridiales(100);Lachnospiraceae(100);Clostridium_XlVb(100);
Otu00223	Bacteria(100);Firmicutes(100);Clostridia(100);Clostridiales(100);Ruminococcaceae(100);unclassified(99);
Otu00224	Bacteria(100);Firmicutes(100);Clostridia(100);Clostridiales(100);Lachnospiraceae(100);unclassified(100);
Otu00226	Bacteria(100);"Bacteroidetes"(100);"Bacteroidia"(100);"Bacteroidales"(100);"Porphyromonadaceae"(100);unclassified(100);
Otu00228	Bacteria(100);Firmicutes(100);Clostridia(100);Clostridiales(55);unclassified(55);unclassified(55);
Otu00230	Bacteria(100);Firmicutes(100);Clostridia(100);Clostridiales(100);Lachnospiraceae(100);unclassified(100);
Otu00231	Bacteria(100);Firmicutes(100);Clostridia(100);Clostridiales(100);Lachnospiraceae(100);unclassified(100);
Otu00232	Bacteria(100);Firmicutes(100);Clostridia(100);Clostridiales(100);Ruminococcaceae(100);Oscillibacter(75);
Otu00233	Bacteria(100);Firmicutes(84);unclassified(84);unclassified(84);unclassified(84);unclassified(84);
Otu00234	Bacteria(100);Firmicutes(100);Clostridia(100);Clostridiales(100);Lachnospiraceae(100);unclassified(100);
Otu00235	Bacteria(100);Firmicutes(100);Clostridia(100);Clostridiales(100);unclassified(91);unclassified(91);
Otu00237	Bacteria(100);Firmicutes(100);Clostridia(100);Clostridiales(100);Ruminococcaceae(100);unclassified(100);
Otu00238	Bacteria(100);Firmicutes(67);unclassified(100);unclassified(100);unclassified(100);unclassified(100);
Otu00239	Bacteria(100);Firmicutes(100);Clostridia(100);Clostridiales(100);Lachnospiraceae(100);unclassified(100);
Otu00240	Bacteria(100);Firmicutes(100);Clostridia(100);Clostridiales(100);Lachnospiraceae(100);unclassified(100);
Otu00242	Bacteria(100);Firmicutes(100);Clostridia(100);Clostridiales(100);unclassified(100);unclassified(100);
Otu00243	Bacteria(100);Firmicutes(100);Clostridia(100);Clostridiales(100);Lachnospiraceae(100);unclassified(100);

Table 4.5. (cont'd)

Otu00244	Bacteria(100);Firmicutes(100);Clostridia(100);Clostridiales(100);Lachnospiraceae(100);unclassified(100);
Otu00245	Bacteria(100);Firmicutes(100);Clostridia(100);Clostridiales(100);unclassified(100);unclassified(100);
Otu00246	Bacteria(100);Firmicutes(100);Clostridia(100);Clostridiales(100);Lachnospiraceae(100);unclassified(97);
Otu00251	Bacteria(100);Firmicutes(100);Clostridia(100);Clostridiales(100);Ruminococcaceae(100);Butyricicoccus(100);
Otu00252	Bacteria(100);"Actinobacteria"(100);Actinobacteria(100);Coriobacteriales(100);Coriobacteriaceae(100);Enterorhabdus(100);
Otu00254	Bacteria(100);Firmicutes(100);Erysipelotrichia(100);Erysipelotrichales(100);Erysipelotrichaceae(100);Holdemania(100);
Otu00255	Bacteria(100);unclassified(100);unclassified(100);unclassified(100);unclassified(100);unclassified(100);
Otu00257	Bacteria(100);unclassified(100);unclassified(100);unclassified(100);unclassified(100);unclassified(100);
Otu00258	Bacteria(100);"Actinobacteria"(100);Actinobacteria(100);Coriobacteriales(100);Coriobacteriaceae(100);Collinsella(100);
Otu00259	Bacteria(100);Firmicutes(100);Clostridia(100);Clostridiales(100);Ruminococcaceae(100);unclassified(100);
Otu00260	Bacteria(100);"Bacteroidetes"(100);"Bacteroidia"(100);"Bacteroidales"(100);"Porphyromonadaceae"(100);unclassified(100);
Otu00262	Bacteria(100);Firmicutes(100);Clostridia(100);Clostridiales(100);Lachnospiraceae(100);unclassified(100);
Otu00263	Bacteria(100);unclassified(99);unclassified(99);unclassified(99);unclassified(99);unclassified(99);
Otu00264	Bacteria(100);Firmicutes(100);Clostridia(100);Clostridiales(100);Lachnospiraceae(100);unclassified(99);
Otu00265	Bacteria(100);Firmicutes(100);Clostridia(100);Clostridiales(100);Lachnospiraceae(96);unclassified(96);
Otu00267	Bacteria(100);Firmicutes(100);Clostridia(100);Clostridiales(100);Lachnospiraceae(61);unclassified(61);
Otu00268	Bacteria(100);Firmicutes(100);Clostridia(100);Clostridiales(100);Lachnospiraceae(100);unclassified(100);
Otu00269	Bacteria(100);Firmicutes(100);Clostridia(100);Clostridiales(100);Ruminococcaceae(100);unclassified(100);
Otu00272	Bacteria(100);Firmicutes(100);Clostridia(92);Clostridiales(92);Lachnospiraceae(92);unclassified(92);
Otu00273	Bacteria(100);Firmicutes(100);Clostridia(100);Clostridiales(100);Lachnospiraceae(100);unclassified(100);

Table 4.5. (cont'd)

Otu00274	Bacteria(100);"Bacteroidetes"(100);"Bacteroidia"(100);"Bacteroidales"(100);"Porphyromonadaceae"(100);unclassified(84);
Otu00276	Bacteria(100);Firmicutes(100);Clostridia(100);Clostridiales(100);Lachnospiraceae(99);unclassified(99);
Otu00278	Bacteria(100);Firmicutes(100);Clostridia(100);Clostridiales(100);Clostridiales_Incertae_Sedis_XIII(98);Anaerovorax(98);
Otu00279	Bacteria(100);Firmicutes(100);Clostridia(100);Clostridiales(100);Lachnospiraceae(100);unclassified(100);
Otu00280	Bacteria(100);Firmicutes(100);Clostridia(100);Clostridiales(100);Lachnospiraceae(100);unclassified(76);
Otu00282	Bacteria(100);Firmicutes(100);Clostridia(100);Clostridiales(100);Ruminococcaceae(100);unclassified(100);
Otu00283	Bacteria(100);Firmicutes(100);Clostridia(100);Clostridiales(100);unclassified(100);unclassified(100);
Otu00285	Bacteria(100);Firmicutes(98);Clostridia(98);Clostridiales(98);Ruminococcaceae(98);unclassified(71);
Otu00287	Bacteria(100);Firmicutes(98);unclassified(98);unclassified(98);unclassified(98);unclassified(98);
Otu00293	Bacteria(100);Firmicutes(100);Clostridia(100);Clostridiales(100);Lachnospiraceae(100);unclassified(100);
Otu00298	Bacteria(100);Firmicutes(100);Clostridia(100);Clostridiales(100);Lachnospiraceae(100);unclassified(100);
Otu00299	Bacteria(100);Firmicutes(100);Bacilli(100);Lactobacillales(100);Streptococcaceae(100);Lactococcus(100);
Otu00301	Bacteria(100);"Bacteroidetes"(100);"Bacteroidia"(100);"Bacteroidales"(100);"Porphyromonadaceae"(100);unclassified(99);
Otu00302	Bacteria(100);Firmicutes(100);Clostridia(100);Clostridiales(100);Lachnospiraceae(100);Blautia(76);
Otu00304	Bacteria(100);"Bacteroidetes"(100);"Bacteroidia"(100);"Bacteroidales"(100);"Rikenellaceae"(100);Alistipes(100);
Otu00306	Bacteria(100);Firmicutes(100);Clostridia(100);Clostridiales(100);unclassified(67);unclassified(67);
Otu00307	Bacteria(100);Firmicutes(100);unclassified(61);unclassified(61);unclassified(61);unclassified(61);
Otu00308	Bacteria(100);"Actinobacteria"(100);Actinobacteria(100);Coriobacteriales(100);Coriobacteriaceae(100);unclassified(100);
Otu00309	Bacteria(100);Firmicutes(100);Clostridia(100);Clostridiales(100);Ruminococcaceae(100);unclassified(100);
Otu00312	Bacteria(100);"Actinobacteria"(100);Actinobacteria(100);Coriobacteriales(100);Coriobacteriaceae(100);Asaccharobacter(80);

Table 4.5. (cont'd)

Otu00313	Bacteria(100);Firmicutes(100);Erysipelotrichia(100);Erysipelotrichales(100);Erysipelotrichaceae(100);unclassified(100);
Otu00315	Bacteria(100);"Bacteroidetes"(100);"Bacteroidia"(100);"Bacteroidales"(100);"Porphyromonadaceae"(100);unclassified(100);
Otu00317	Bacteria(100);Firmicutes(100);Clostridia(100);Clostridiales(100);Lachnospiraceae(100);unclassified(100);
Otu00318	Bacteria(100);"Bacteroidetes"(100);"Bacteroidia"(100);"Bacteroidales"(100);"Porphyromonadaceae"(100);Odoribacter(100);
Otu00319	Bacteria(100);Firmicutes(100);Clostridia(100);Clostridiales(100);Lachnospiraceae(100);Lachnospiracea_incertae_sedis(98);
Otu00321	Bacteria(100);Firmicutes(100);Clostridia(100);Clostridiales(100);Lachnospiraceae(100);unclassified(100);
Otu00322	Bacteria(100);"Bacteroidetes"(100);"Bacteroidia"(100);"Bacteroidales"(100);"Porphyromonadaceae"(100);unclassified(100);
Otu00326	Bacteria(100);Firmicutes(100);Clostridia(100);Clostridiales(100);Lachnospiraceae(100);unclassified(99);
Otu00328	Bacteria(100);Firmicutes(100);Clostridia(100);Clostridiales(100);Ruminococcaceae(99);unclassified(99);
Otu00329	Bacteria(100);Firmicutes(100);Clostridia(100);Clostridiales(100);Lachnospiraceae(100);unclassified(100);
Otu00330	Bacteria(100);Firmicutes(100);Clostridia(100);Clostridiales(100);unclassified(100);unclassified(100);
Otu00332	Bacteria(100);Firmicutes(100);Clostridia(100);Clostridiales(100);Lachnospiraceae(100);unclassified(100);
Otu00333	Bacteria(100);unclassified(100);unclassified(100);unclassified(100);unclassified(100);unclassified(100);
Otu00334	Bacteria(100);Firmicutes(100);Clostridia(100);Clostridiales(100);Ruminococcaceae(100);unclassified(100);
Otu00335	Bacteria(100);Firmicutes(100);unclassified(53);unclassified(53);unclassified(53);unclassified(53);
Otu00336	Bacteria(100);Firmicutes(100);Clostridia(100);Clostridiales(100);unclassified(100);unclassified(100);
Otu00338	Bacteria(100);Firmicutes(100);Clostridia(100);Clostridiales(100);Lachnospiraceae(100);unclassified(100);
Otu00340	Bacteria(100);Firmicutes(100);Clostridia(100);Clostridiales(100);Ruminococcaceae(97);unclassified(97);
Otu00341	Bacteria(100);Firmicutes(100);Clostridia(100);Clostridiales(100);Lachnospiraceae(100);unclassified(99);
Otu00342	Bacteria(100);Firmicutes(100);Clostridia(100);Clostridiales(100);Lachnospiraceae(100);Clostridium_XlVa(67);

Table 4.5. (cont'd)

Otu00343	Bacteria(100);Firmicutes(100);unclassified(100);unclassified(100);unclassified(100);unclassified(100);
Otu00344	Bacteria(100);Firmicutes(100);Clostridia(100);Clostridiales(100);Lachnospiraceae(100);unclassified(100);
Otu00345	Bacteria(100);Firmicutes(100);Clostridia(100);Clostridiales(100);Lachnospiraceae(100);unclassified(100);
Otu00346	Bacteria(100);Firmicutes(100);Bacilli(100);Lactobacillales(100);Streptococcaceae(100);Streptococcus(100);
Otu00348	Bacteria(100);Firmicutes(100);Clostridia(100);Clostridiales(100);Ruminococcaceae(100);unclassified(100);
Otu00349	Bacteria(100);Firmicutes(99);unclassified(99);unclassified(99);unclassified(99);unclassified(99);
Otu00350	Bacteria(100);Firmicutes(100);Erysipelotrichia(100);Erysipelotrichales(100);Erysipelotrichaceae(100);Erysipelotrichaceae_incertae_sedis(100);
Otu00351	Bacteria(100);Firmicutes(100);Clostridia(100);Clostridiales(100);Lachnospiraceae(100);unclassified(100);
Otu00352	Bacteria(100);Firmicutes(100);Clostridia(100);Clostridiales(100);Lachnospiraceae(100);Anaerostipes(97);
Otu00353	Bacteria(100);"Bacteroidetes"(100);"Bacteroidia"(100);"Bacteroidales"(100);Bacteroidaceae(100);Bacteroides(100);
Otu00356	Bacteria(100);"Actinobacteria"(100);Actinobacteria(100);Coriobacteriales(100);Coriobacteriaceae(100);unclassified(100);
Otu00357	Bacteria(100);Firmicutes(100);Clostridia(100);Clostridiales(100);unclassified(100);unclassified(100);
Otu00358	Bacteria(100);Firmicutes(100);Clostridia(100);Clostridiales(100);Ruminococcaceae(100);unclassified(100);
Otu00359	Bacteria(100);Firmicutes(100);Clostridia(100);Clostridiales(100);Ruminococcaceae(100);unclassified(100);
Otu00360	Bacteria(100);Firmicutes(100);Erysipelotrichia(100);Erysipelotrichales(100);Erysipelotrichaceae(100);unclassified(100);
Otu00361	Bacteria(100);Firmicutes(100);Clostridia(100);Clostridiales(100);Lachnospiraceae(100);unclassified(100);
Otu00362	Bacteria(100);Firmicutes(100);Clostridia(100);Clostridiales(100);unclassified(100);unclassified(100);
Otu00366	Bacteria(100);Firmicutes(97);unclassified(97);unclassified(97);unclassified(97);unclassified(97);
Otu00367	Bacteria(100);Firmicutes(100);Clostridia(100);Clostridiales(100);Lachnospiraceae(100);Clostridium_XlVa(98);
Otu00369	Bacteria(100);Firmicutes(100);Clostridia(100);Clostridiales(100);Lachnospiraceae(100);unclassified(98);

Table 4.5. (cont'd)

Otu00370	Bacteria(100);"Bacteroidetes"(100);"Bacteroidia"(100);"Bacteroidales"(100);"Rikenellaceae"(100);Alistipes(100);
Otu00371	Bacteria(100);Firmicutes(100);Clostridia(100);Clostridiales(100);Lachnospiraceae(100);unclassified(100);
Otu00375	Bacteria(100);"Bacteroidetes"(100);"Bacteroidia"(99);"Bacteroidales"(99);"Porphyromonadaceae"(53);unclassified(53);
Otu00380	Bacteria(100);Firmicutes(100);Clostridia(100);Clostridiales(100);Lachnospiraceae(100);unclassified(99);
Otu00381	Bacteria(100);unclassified(100);unclassified(100);unclassified(100);unclassified(100);unclassified(100);
Otu00384	Bacteria(100);Firmicutes(100);Clostridia(100);Clostridiales(100);Ruminococcaceae(100);Oscillibacter(99);
Otu00385	Bacteria(100);Firmicutes(100);Clostridia(100);Clostridiales(100);Ruminococcaceae(100);Oscillibacter(100);
Otu00387	Bacteria(100);Firmicutes(100);Clostridia(100);Clostridiales(100);Lachnospiraceae(99);Lachnospiracea_incertae_sedis(92);
Otu00391	Bacteria(100);Firmicutes(100);Clostridia(100);Clostridiales(100);Ruminococcaceae(100);unclassified(100);
Otu00395	Bacteria(100);Firmicutes(100);Clostridia(100);Clostridiales(100);unclassified(100);unclassified(100);
Otu00396	Bacteria(100);Firmicutes(100);Clostridia(100);Clostridiales(100);Ruminococcaceae(100);unclassified(93);
Otu00398	Bacteria(100);Firmicutes(98);unclassified(98);unclassified(98);unclassified(98);unclassified(98);
Otu00399	Bacteria(100);Firmicutes(100);Clostridia(100);Clostridiales(100);Lachnospiraceae(100);unclassified(100);
Otu00402	Bacteria(100);unclassified(100);unclassified(100);unclassified(100);unclassified(100);unclassified(100);
Otu00404	Bacteria(100);Firmicutes(100);Clostridia(100);Clostridiales(100);unclassified(98);unclassified(98);
Otu00405	Bacteria(100);Firmicutes(100);unclassified(92);unclassified(92);unclassified(92);unclassified(92);
Otu00409	Bacteria(100);Firmicutes(100);Clostridia(100);Clostridiales(100);Lachnospiraceae(98);unclassified(95);
Otu00411	Bacteria(100);"Bacteroidetes"(100);"Bacteroidia"(100);"Bacteroidales"(100);Bacteroidaceae(100);Bacteroides(100);
Otu00412	Bacteria(100);Firmicutes(100);Clostridia(100);Clostridiales(100);Lachnospiraceae(100);unclassified(95);
Otu00413	Bacteria(100);unclassified(100);unclassified(100);unclassified(100);unclassified(100);unclassified(100);

Table 4.5. (cont'd)

Otu00415	Bacteria(100);Firmicutes(100);Clostridia(100);Clostridiales(100);Lachnospiraceae(100);unclassified(100);
Otu00417	Bacteria(100);Firmicutes(100);Clostridia(100);Clostridiales(100);Ruminococcaceae(100);Anaerotruncus(100);
Otu00418	Bacteria(100);Firmicutes(100);Clostridia(99);Clostridiales(99);unclassified(99);unclassified(99);
Otu00419	Bacteria(100);Firmicutes(100);Clostridia(100);Clostridiales(100);Lachnospiraceae(100);unclassified(100);
Otu00420	Bacteria(100);Firmicutes(100);Clostridia(100);Clostridiales(100);Lachnospiraceae(100);Coprococcus(100);
Otu00421	Bacteria(100);Firmicutes(100);Clostridia(100);Clostridiales(100);Lachnospiraceae(100);Blautia(100);
Otu00422	Bacteria(100);Firmicutes(100);Clostridia(100);Clostridiales(100);Lachnospiraceae(100);unclassified(100);
Otu00430	Bacteria(100);Firmicutes(100);Clostridia(100);Clostridiales(100);unclassified(100);unclassified(100);
Otu00432	Bacteria(100);Firmicutes(100);Clostridia(100);Clostridiales(100);Lachnospiraceae(100);unclassified(100);
Otu00435	Bacteria(100);Firmicutes(100);unclassified(85);unclassified(85);unclassified(85);unclassified(85);
Otu00437	Bacteria(100);Firmicutes(100);Clostridia(100);Clostridiales(100);Ruminococcaceae(92);unclassified(92);
Otu00440	Bacteria(100);Firmicutes(100);Clostridia(100);Clostridiales(100);Ruminococcaceae(100);unclassified(100);
Otu00441	Bacteria(100);Firmicutes(100);Clostridia(100);Clostridiales(100);Lachnospiraceae(100);unclassified(100);
Otu00443	Bacteria(100);Firmicutes(100);unclassified(100);unclassified(100);unclassified(100);unclassified(100);
Otu00445	Bacteria(100);Firmicutes(100);Clostridia(100);Clostridiales(100);Ruminococcaceae(100);Clostridium_IV(82);
Otu00446	Bacteria(100);Firmicutes(100);Clostridia(100);Clostridiales(100);unclassified(100);unclassified(100);
Otu00448	Bacteria(100);Firmicutes(100);Clostridia(100);Clostridiales(100);unclassified(98);unclassified(98);
Otu00457	Bacteria(100);"Bacteroidetes"(100);"Bacteroidia"(100);"Bacteroidales"(100);"Porphyromonadaceae"(100);unclassified(100);
Otu00458	Bacteria(100);Firmicutes(100);Clostridia(100);Clostridiales(100);Lachnospiraceae(100);unclassified(100);
Otu00460	Bacteria(100);Firmicutes(100);Clostridia(84);Clostridiales(84);unclassified(84);unclassified(84);

Table 4.5. (cont'd)

Otu00462	Bacteria(100);"Bacteroidetes"(100);"Bacteroidia"(100);"Bacteroidales"(100);"Porphyromonadaceae"(100);Barnesiella(82);
Otu00469	Bacteria(100);Firmicutes(100);Clostridia(98);Clostridiales(98);unclassified(98);unclassified(98);
Otu00471	Bacteria(100);Firmicutes(100);Clostridia(100);Clostridiales(100);Ruminococcaceae(100);Faecalibacterium(100);
Otu00472	Bacteria(100);Firmicutes(100);Clostridia(100);Clostridiales(100);Lachnospiraceae(100);Blautia(100);
Otu00473	Bacteria(100);Firmicutes(100);Clostridia(100);Clostridiales(100);Ruminococcaceae(99);Sporobacter(87);
Otu00475	Bacteria(100);Firmicutes(100);Clostridia(100);Clostridiales(100);unclassified(97);unclassified(97);
Otu00476	Bacteria(100);Firmicutes(100);Clostridia(100);Clostridiales(100);Lachnospiraceae(100);unclassified(95);
Otu00479	Bacteria(100);"Bacteroidetes"(100);"Bacteroidia"(100);"Bacteroidales"(100);"Porphyromonadaceae"(100);unclassified(100);
Otu00480	Bacteria(100);Firmicutes(100);Clostridia(100);Clostridiales(100);Lachnospiraceae(100);unclassified(100);
Otu00481	Bacteria(100);"Bacteroidetes"(100);"Bacteroidia"(100);"Bacteroidales"(100);"Porphyromonadaceae"(100);Barnesiella(99);
Otu00487	Bacteria(100);"Bacteroidetes"(100);"Bacteroidia"(100);"Bacteroidales"(100);"Porphyromonadaceae"(100);Parabacteroides(100);
Otu00488	Bacteria(100);"Bacteroidetes"(100);"Bacteroidia"(100);"Bacteroidales"(100);"Porphyromonadaceae"(93);unclassified(93);
Otu00499	Bacteria(100);Firmicutes(100);Clostridia(100);Clostridiales(100);Lachnospiraceae(100);unclassified(100);
Otu00501	Bacteria(100);"Bacteroidetes"(100);"Bacteroidia"(100);"Bacteroidales"(100);"Porphyromonadaceae"(100);unclassified(97);
Otu00505	Bacteria(100);Firmicutes(100);Clostridia(100);Clostridiales(100);Ruminococcaceae(100);Clostridium_IV(100);
Otu00506	Bacteria(100);Firmicutes(100);Clostridia(100);Clostridiales(100);Ruminococcaceae(100);unclassified(100);
Otu00508	Bacteria(100);Firmicutes(100);Clostridia(100);Clostridiales(100);Ruminococcaceae(100);unclassified(100);
Otu00509	Bacteria(100);Firmicutes(100);Clostridia(100);Clostridiales(100);Lachnospiraceae(100);unclassified(100);
Otu00510	Bacteria(100);"Bacteroidetes"(100);"Bacteroidia"(99);"Bacteroidales"(99);"Porphyromonadaceae"(95);unclassified(95);
Otu00511	Bacteria(100);"Bacteroidetes"(100);"Bacteroidia"(100);"Bacteroidales"(100);"Rikenellaceae"(100);Alistipes(100);

Table 4.5. (cont'd)

	Bacteria(100);Firmicutes(100);Clostridia(100);Clostridiales(100);Lachnospiraceae(75);unclassified(75);
Otu00515	Bacteria(100);"Bacteroidetes"(100);"Bacteroidia"(100);"Bacteroidales"(100);"Porphyromonadaceae"(100);unclassified(99);
Otu00516	Bacteria(100);Firmicutes(100);Clostridia(100);Clostridiales(100);Lachnospiraceae(100);unclassified(100);
Otu00519	Bacteria(100);Firmicutes(98);unclassified(93);unclassified(93);unclassified(93);unclassified(93);
Otu00520	Bacteria(100);"Bacteroidetes"(100);"Bacteroidia"(98);"Bacteroidales"(98);"Porphyromonadaceae"(95);unclassified(95);
Otu00522	Bacteria(100);"Bacteroidetes"(100);"Bacteroidia"(100);"Bacteroidales"(100);"Porphyromonadaceae"(100);unclassified(100);
Otu00526	Bacteria(100);unclassified(93);unclassified(93);unclassified(93);unclassified(93);unclassified(93);
Otu00530	Bacteria(100);Firmicutes(100);Clostridia(100);Clostridiales(100);Lachnospiraceae(100);unclassified(55);
Otu00539	Bacteria(100);Firmicutes(100);Erysipelotrichia(100);Erysipelotrichales(100);Erysipelotrichaceae(100);Erysipelotrichaceae_incertae_sedis(100);
Otu00541	Bacteria(100);"Bacteroidetes"(100);"Bacteroidia"(100);"Bacteroidales"(100);"Porphyromonadaceae"(100);Barnesiella(95);
Otu00542	Bacteria(100);Firmicutes(100);Clostridia(100);Clostridiales(100);Ruminococcaceae(99);Butyricicoccus(95);
Otu00546	Bacteria(100);Firmicutes(100);Clostridia(100);Clostridiales(100);Ruminococcaceae(100);unclassified(100);
Otu00548	Bacteria(100);Firmicutes(100);Clostridia(100);Clostridiales(100);Ruminococcaceae(100);unclassified(99);
Otu00554	Bacteria(100);Firmicutes(100);Clostridia(100);Clostridiales(100);Lachnospiraceae(100);unclassified(100);
Otu00555	Bacteria(100);Firmicutes(100);Clostridia(100);Clostridiales(100);Lachnospiraceae(100);unclassified(100);
Otu00560	Bacteria(100);Firmicutes(100);Clostridia(100);Clostridiales(100);unclassified(100);unclassified(100);
Otu00570	Bacteria(100);Firmicutes(100);Clostridia(100);Clostridiales(100);Lachnospiraceae(100);unclassified(76);
Otu00572	Bacteria(100);Firmicutes(100);Clostridia(100);Clostridiales(100);Lachnospiraceae(100);Anaerostipes(95);
Otu00577	Bacteria(100);unclassified(98);unclassified(98);unclassified(98);unclassified(98);unclassified(98);
Otu00578	Bacteria(100);"Bacteroidetes"(100);"Bacteroidia"(100);"Bacteroidales"(100);"Rikenellaceae"(100);Alistipes(100);

Table 4.5. (cont'd)

Otu00579	Bacteria(100);Firmicutes(100);Clostridia(100);Clostridiales(100);Ruminococcaceae(98);unclassified(98);
Otu00580	Bacteria(100);Firmicutes(100);Clostridia(100);Clostridiales(100);Lachnospiraceae(100);unclassified(86);
Otu00591	Bacteria(100);Firmicutes(100);Clostridia(100);Clostridiales(100);Ruminococcaceae(100);unclassified(100);
Otu00593	Bacteria(100);unclassified(100);unclassified(100);unclassified(100);unclassified(100);unclassified(100);
Otu00594	Bacteria(100);Firmicutes(100);Bacilli(100);Lactobacillales(100);unclassified(98);unclassified(98);
Otu00595	Bacteria(100);Firmicutes(100);Clostridia(100);Clostridiales(100);Ruminococcaceae(97);unclassified(97);
Otu00600	Bacteria(100);Firmicutes(100);Clostridia(100);Clostridiales(100);Ruminococcaceae(100);unclassified(100);
Otu00601	Bacteria(100);Firmicutes(100);Clostridia(100);Clostridiales(100);Lachnospiraceae(100);unclassified(100);
Otu00603	Bacteria(100);Firmicutes(100);unclassified(100);unclassified(100);unclassified(100);unclassified(100);
Otu00606	Bacteria(100);Firmicutes(100);Clostridia(100);Clostridiales(100);Lachnospiraceae(100);Clostridium_XlVa(93);
Otu00608	Bacteria(100);"Actinobacteria"(100);Actinobacteria(100);Coriobacteriales(100);Coriobacteriaceae(100);Eggerthella(100);
Otu00609	Bacteria(100);Firmicutes(100);Bacilli(100);unclassified(92);unclassified(92);unclassified(92);
Otu00613	Bacteria(100);"Bacteroidetes"(100);"Bacteroidia"(100);"Bacteroidales"(100);"Porphyromonadaceae"(100);Barnesiella(96);
Otu00623	Bacteria(100);"Bacteroidetes"(100);"Bacteroidia"(100);"Bacteroidales"(100);Bacteroidaceae(100);Bacteroides(100);
Otu00625	Bacteria(100);"Bacteroidetes"(100);"Bacteroidia"(100);"Bacteroidales"(100);"Porphyromonadaceae"(62);unclassified(62);
Otu00626	Bacteria(100);Firmicutes(100);Clostridia(100);Clostridiales(100);Ruminococcaceae(98);unclassified(98);
Otu00634	Bacteria(100);Firmicutes(100);Clostridia(100);Clostridiales(100);unclassified(100);unclassified(100);
Otu00636	Bacteria(100);Firmicutes(100);Clostridia(100);Clostridiales(100);unclassified(100);unclassified(100);
Otu00637	Bacteria(100);Firmicutes(77);Clostridia(77);Clostridiales(77);Ruminococcaceae(77);unclassified(77);
Otu00654	Bacteria(100);Firmicutes(100);Clostridia(100);Clostridiales(100);Lachnospiraceae(100);unclassified(100);

Table 4.5. (cont'd)

Otu00657	Bacteria(100);"Bacteroidetes"(100);"Bacteroidia"(100);"Bacteroidales"(100);"Porphyromonadaceae"(91);unclassified(91);
Otu00661	Bacteria(100);Firmicutes(100);Clostridia(100);Clostridiales(100);Lachnospiraceae(100);unclassified(100);
Otu00667	Bacteria(100);Firmicutes(54);unclassified(100);unclassified(100);unclassified(100);unclassified(100);
Otu00668	Bacteria(100);Firmicutes(100);Bacilli(100);Lactobacillales(100);Carnobacteriaceae(100);Atopostipes(100);
Otu00676	Bacteria(100);Firmicutes(100);Clostridia(100);Clostridiales(100);Ruminococcaceae(96);unclassified(96);
Otu00677	Bacteria(100);"Bacteroidetes"(100);"Bacteroidia"(100);"Bacteroidales"(100);unclassified(100);unclassified(100);
Otu00679	Bacteria(100);Firmicutes(100);Clostridia(100);Clostridiales(100);Lachnospiraceae(100);Blautia(84);
Otu00681	Bacteria(100);"Actinobacteria"(100);Actinobacteria(100);Coriobacteriales(100);Coriobacteriaceae(100);Gordonibacter(100);
Otu00682	Bacteria(100);Firmicutes(100);Clostridia(100);Clostridiales(100);Ruminococcaceae(100);unclassified(100);
Otu00684	Bacteria(100);Firmicutes(100);Clostridia(100);Clostridiales(100);Lachnospiraceae(100);unclassified(100);
Otu00685	Bacteria(100);Firmicutes(100);Clostridia(100);Clostridiales(100);Lachnospiraceae(100);unclassified(100);
Otu00691	Bacteria(100);Firmicutes(100);Clostridia(100);Clostridiales(100);Lachnospiraceae(100);unclassified(100);
Otu00700	Bacteria(100);Firmicutes(100);Clostridia(100);Clostridiales(100);Ruminococcaceae(100);unclassified(100);
Otu00703	Bacteria(100);Firmicutes(100);Clostridia(100);Clostridiales(100);Lachnospiraceae(100);unclassified(100);
Otu00725	Bacteria(100);Firmicutes(100);Clostridia(100);Clostridiales(100);unclassified(76);unclassified(76);
Otu00730	Bacteria(100);"Bacteroidetes"(100);"Bacteroidia"(100);"Bacteroidales"(100);"Porphyromonadaceae"(100);Barnesiella(51);
Otu00739	Bacteria(100);Firmicutes(100);Clostridia(100);Clostridiales(100);Ruminococcaceae(100);Subdoligranulum(81);
Otu00740	Bacteria(100);Firmicutes(100);Clostridia(100);Clostridiales(100);Lachnospiraceae(100);unclassified(100);
Otu00741	Bacteria(100);"Bacteroidetes"(100);"Bacteroidia"(100);"Bacteroidales"(100);Bacteroidaceae(100);Bacteroides(100);
Otu00742	Bacteria(100);unclassified(100);unclassified(100);unclassified(100);unclassified(100);unclassified(100);

Table 4.5. (cont'd)

Otu00773	Bacteria(100);"Bacteroidetes"(100);unclassified(100);unclassified(100);unclassified(100);unclassified(100);
Otu00779	Bacteria(100);unclassified(100);unclassified(100);unclassified(100);unclassified(100);unclassified(100);
Otu00782	Bacteria(100);Firmicutes(100);Clostridia(100);Clostridiales(100);Lachnospiraceae(100);unclassified(100);
Otu00785	Bacteria(100);Firmicutes(100);Clostridia(100);Clostridiales(100);Ruminococcaceae(95);unclassified(95);
Otu00809	Bacteria(100);Firmicutes(100);Negativicutes(100);Selenomonadales(100);Veillonellaceae(100);Megasphaera(100);
Otu00810	Bacteria(100);Firmicutes(100);Clostridia(100);Clostridiales(100);Lachnospiraceae(100);unclassified(100);
Otu00818	Bacteria(100);"Bacteroidetes"(100);"Bacteroidia"(100);"Bacteroidales"(100);Bacteroidaceae(100);Bacteroides(100);
Otu00822	Bacteria(100);Firmicutes(100);Clostridia(96);Clostridiales(62);unclassified(100);unclassified(100);
Otu00830	Bacteria(100);"Bacteroidetes"(100);"Bacteroidia"(100);"Bacteroidales"(100);"Rikenellaceae"(100);Alistipes(100);
Otu00833	Bacteria(100);"Bacteroidetes"(100);"Bacteroidia"(100);"Bacteroidales"(100);"Porphyromonadaceae"(100);Barnesiella(96);
Otu00835	Bacteria(100);Firmicutes(100);Clostridia(100);Clostridiales(100);Ruminococcaceae(100);unclassified(100);
Otu00859	Bacteria(100);"Bacteroidetes"(100);"Bacteroidia"(100);"Bacteroidales"(100);"Porphyromonadaceae"(100);unclassified(100);
Otu00861	Bacteria(100);Firmicutes(100);Clostridia(100);Clostridiales(100);Lachnospiraceae(100);unclassified(100);
Otu00864	Bacteria(100);"Bacteroidetes"(100);"Bacteroidia"(100);"Bacteroidales"(100);"Porphyromonadaceae"(100);Barnesiella(81);
Otu00873	Bacteria(100);"Actinobacteria"(100);Actinobacteria(100);Coriobacteriales(100);Coriobacteriaceae(100);unclassified(100);
Otu00878	Bacteria(100);"Bacteroidetes"(100);"Bacteroidia"(100);"Bacteroidales"(100);"Rikenellaceae"(100);Alistipes(100);
Otu00880	Bacteria(100);Firmicutes(100);Clostridia(100);Clostridiales(100);Lachnospiraceae(100);unclassified(100);
Otu00891	Bacteria(100);Firmicutes(100);Clostridia(100);Clostridiales(100);Ruminococcaceae(100);unclassified(95);
Otu00894	Bacteria(100);Firmicutes(100);Clostridia(100);Clostridiales(100);Lachnospiraceae(100);unclassified(95);
Otu00902	Bacteria(100);Firmicutes(100);Clostridia(100);Clostridiales(100);Ruminococcaceae(100);unclassified(100);

Table 4.5. (cont'd)

Otu00930	Bacteria(100);"Bacteroidetes"(100);"Bacteroidia"(100);"Bacteroidales"(100);"Porphyromonadaceae"(95);unclassified(95);
Otu00973	Bacteria(100);Firmicutes(100);Clostridia(100);Clostridiales(100);unclassified(100);unclassified(100);
Otu00994	Bacteria(100);Firmicutes(100);Clostridia(100);Clostridiales(100);Lachnospiraceae(100);Blautia(100);
Otu00998	Bacteria(100);Firmicutes(100);Clostridia(100);Clostridiales(100);Lachnospiraceae(100);unclassified(100);
Otu01030	Bacteria(100);Firmicutes(89);Bacilli(89);unclassified(89);unclassified(89);unclassified(89);
Otu01033	Bacteria(100);Firmicutes(100);Clostridia(100);Clostridiales(100);Ruminococcaceae(100);unclassified(100);
Otu01043	Bacteria(100);Firmicutes(100);Clostridia(100);Clostridiales(100);Lachnospiraceae(100);unclassified(100);
Otu01114	Bacteria(100);"Bacteroidetes"(100);"Bacteroidia"(100);"Bacteroidales"(100);"Porphyromonadaceae"(100);unclassified(100);
Otu01120	Bacteria(100);Firmicutes(100);Bacilli(100);Lactobacillales(100);Lactobacillaceae(100);Lactobacillus(100);
Otu01158	Bacteria(100);"Bacteroidetes"(100);"Bacteroidia"(100);"Bacteroidales"(100);"Porphyromonadaceae"(100);unclassified(100);
Otu01340	Bacteria(100);"Bacteroidetes"(100);"Bacteroidia"(80);"Bacteroidales"(80);"Porphyromonadaceae"(80);unclassified(80);
Otu01372	Bacteria(100);Firmicutes(100);Clostridia(100);Clostridiales(100);Lachnospiraceae(100);unclassified(100);
Otu01395	Bacteria(100);Firmicutes(100);Clostridia(100);Clostridiales(100);Lachnospiraceae(100);unclassified(100);
Otu01432	Bacteria(100);"Bacteroidetes"(100);"Bacteroidia"(100);"Bacteroidales"(100);"Porphyromonadaceae"(100);unclassified(100);
Otu01445	Bacteria(100);"Bacteroidetes"(100);"Bacteroidia"(100);"Bacteroidales"(100);"Porphyromonadaceae"(100);unclassified(100);
Otu01460	Bacteria(100);"Bacteroidetes"(100);"Bacteroidia"(100);"Bacteroidales"(100);"Porphyromonadaceae"(100);unclassified(100);
Otu01464	Bacteria(100);"Bacteroidetes"(100);"Bacteroidia"(84);"Bacteroidales"(84);unclassified(67);unclassified(67);
Otu02071	Bacteria(100);"Bacteroidetes"(100);"Bacteroidia"(100);"Bacteroidales"(100);"Porphyromonadaceae"(100);unclassified(100);
Otu02174	Bacteria(100);"Bacteroidetes"(100);"Bacteroidia"(100);"Bacteroidales"(100);"Porphyromonadaceae"(67);unclassified(100);
Otu02236	Bacteria(100);Firmicutes(100);Clostridia(100);Clostridiales(100);Ruminococcaceae(100);unclassified(100);

Table 4.5. (cont'd)

Otu02277	Bacteria(100);Firmicutes(100);Clostridia(67);Clostridiales(67);unclassified(67);unclassified(67);
Otu02288	Bacteria(100);Firmicutes(100);Clostridia(100);Clostridiales(100);Lachnospiraceae(100);unclassified(100);
Otu03141	Bacteria(100);"Bacteroidetes"(100);"Bacteroidia"(100);"Bacteroidales"(100);"Porphyromonadaceae"(100);unclassified(100);
Otu03149	Bacteria(100);Firmicutes(100);Clostridia(100);Clostridiales(100);Lachnospiraceae(100);unclassified(100);
Otu03156	Bacteria(100);"Bacteroidetes"(100);"Bacteroidia"(100);"Bacteroidales"(100);"Porphyromonadaceae"(100);unclassified(100);
Otu03157	Bacteria(100);"Bacteroidetes"(100);"Bacteroidia"(100);"Bacteroidales"(100);unclassified(100);unclassified(100);
Otu03158	Bacteria(100);Firmicutes(100);Clostridia(100);Clostridiales(100);Ruminococcaceae(100);unclassified(100);

Sterility of the GF mice was monitored by PCR of the 16S rRNA gene and assessment of cecal size. During the course of the experiment, it was discovered that some GF mice (n = 5, total = 29) were monocolonized with bacteria of the genus Turicibacter (Sanger sequencing, data not shown). Their ecological role and impact on health remain largely unknown, but it has been shown to be a contaminant of GF derivation attempts from the animal vendor Taconic Farms [49]. Interestingly enough, monocolonization with Turicibacter alone is not sufficient to impact the characteristically large cecal size of GF animals (Figure 4.11). Lastly, *Turicibacter* monocolonization does not impact bone density (Figure 4.12).

(A)

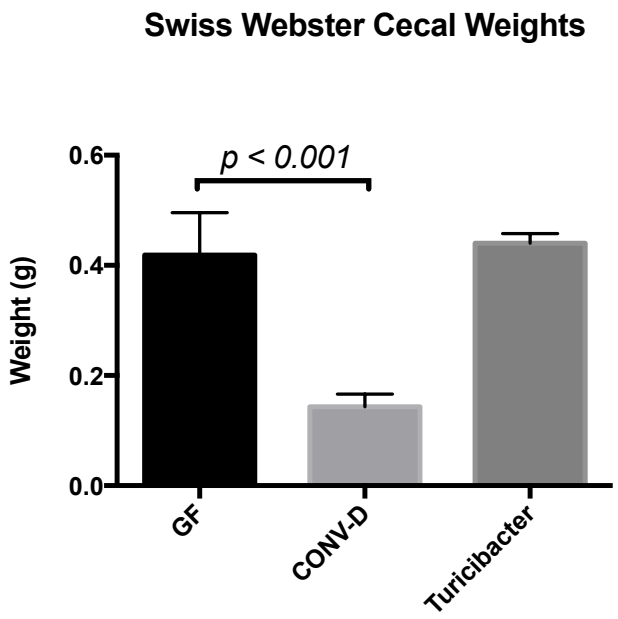

(B)

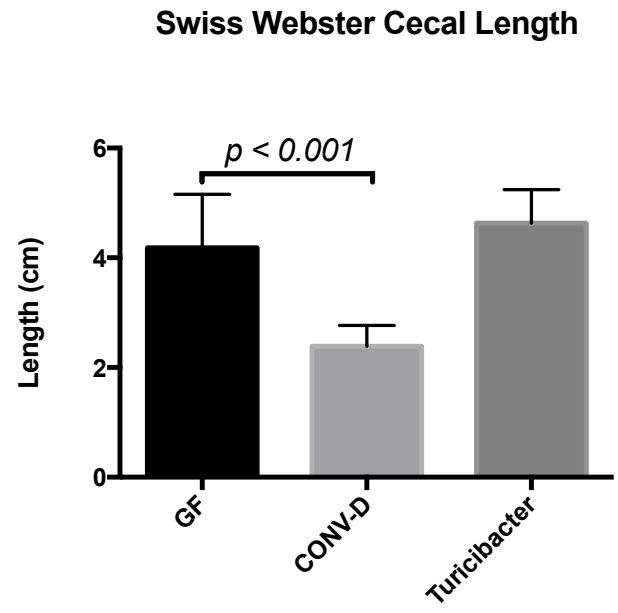

Figure 4.11. Conventionalization of Swiss Webster mice reduces cecal weight and length while *Turicibacter* monocolonization does not.

Figure 4.11. (cont'd)

GF Swiss Webster mice were conventionalized with a mouse microbiota. The weight (A) and length (B) of the cecum were decreased by conventionalization but not with *Turicibacter* colonization. The results are shown as mean ± SEM (n= 3-10). $p < 0.05$ with respect to SW GF, Student's *t* test.

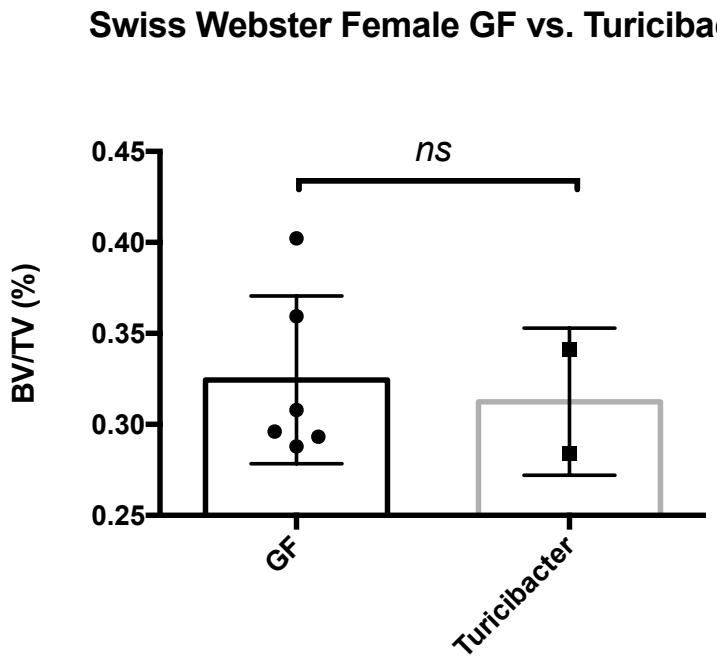

Figure 4.12. Turicibacter colonization did not impact BVF.

GF Swiss Webster mice monocolonization with *Turicibacter*. The results are shown as mean ± SEM.

4.4 *Discussion*

The importance of the gut microbiota and its impact on health is being heavily investigated. Several studies have shown that different microbiota compositions can have pronounced health impacts on a wide range of systems spanning from infectious diseases that seemingly involve a microbial component to those that do not such as mental health [50–52]. In this study, we focused on the impact of the microbiota on bone health with the goal of identifying microbes with therapeutic potential. Overall, our study demonstrated that the introduction of various defined microbiotas to GF animals does not decrease bone mass in a series of animal experiments using two different mouse genetic backgrounds.

It was previously demonstrated that conventionalizing female GF C57bl6/J mice with a normal mouse gut microbiota decreases bone mass [53]. As a result, we were surprised to find that colonizing GF mice with various human microbiotas did not impact bone mass. In subsequent experiments, we tried to test whether this effect was specific to a human microbiota but conventionalization with a mouse microbiota did not impact bone density either.

When comparing our results with published studies, there were some factors that could be accounting for the differences observed. First, the mode of transplantation of the microbiota differed. Both studies conventionalized their mice with cecal contents. However, as reported by Sjogren et al., their conventionalization process was based off of coprophagy following the sprinkling of the cecal contents onto the fur of the mice whereas we conventionalized our animals by intragastric gavage after the cecal contents were prepared and maintained in anaerobic conditions. While it is hard to speculate on whether this ultimately culminated in pronounced differences in community colonization, it cannot be excluded.

Another possibility for the observed differences is that there are inherent differences between the microbiotas used to conventionalize mice manifesting in the lack of an impact on bone mass. It has been well documented that mice purchased from different animal vendors and housed at different mouse facilities foster microbial community colonization that is location specific [54]. Since there was no community analysis performed by Sjogren et al., it is impossible to compare their study with ours with respect to the microbial communities used for the conventionalization study. However, it is worth noting that other recent studies observed no bone loss following colonization of GF animals (Li et al., 2016; Schwarzer et al., 2016). One study actually showed an increase in various parameters of bone health [24] while the other showed no change (Li et al., 2016), which further supports the notion that bone health is highly regulated by the composition of the microbiota.

In addition to bacteria, the presence of other microbes like murine norovirus has also been shown to have notable effects on the development of disease [55,56]. The BCM GF facility performs routine screening in order to monitor the presence of common viruses present. However, this can never rule out the possibility of something else being present that goes undetected. To complicate things further, different genetic backgrounds in mice have also contributed to differences observed on a physiological and immunological level [57,58]. Thus, it highlights the challenges of investigating the impact of the microbiome on disease using various animal models.

Despite the challenge in trying to establish the link between cause and effect regarding the immune response and host-microbe interactions, what is becoming clearer is that health outcomes are greatly affected by both the immunological state of the host and its interaction with microbes. For example, Collins et al. demonstrated the beneficial use of a probiotic to increase bone density in female Balb/c mice that were in a heightened state of inflammation [30].

The same strain of *Lactobacillus reuteri* was shown to effectively increase bone density in WT male mice and in female mice that were estrogen deficient following ovariectomy by decreasing inflammation [27,28]. Taken together, these studies suggest that the beneficial impact on bone health from the probiotic *L. reuteri* takes place under specific conditions such as inflammation or estrogen deficiency in female mice or when homeostasis is perturbed.

While it is difficult to even begin understanding the contributions of sex differences on the microbiota and health, one place to start is by assessing whether there is a sex-specific microbiota. Specifically, do different sexes in the same genetic background harbor the same or different microbiotas? In our studies, there were no statistical significant differences between cecal microbial communities in male and female Swiss Webster mice. However, compositional analysis of the microbial analysis only provides information on what is present or was once present. Additionally, even if the microbial compositions of two communities are different, the functions of these communities may not differ. To gain insight into what that specific community is carrying out functionally, further studies (i.e. metagenomics, transcriptomics, and proteomics) are required.

When investigating the bone-microbiota interaction, it is important to consider both the composition of the microbiota and the specific animal model used to study disease. Our studies, coupled with existing studies, suggest that the gut microbiota may have an important role in regulating bone health. However, it is increasingly important to not only identify what is present in the microbial community but also the specific functions that are carried out. As more studies are directed towards investigating this relationship, our results provide a reference for the discovery of microbes with the potential of impacting bone health. This has the potential to allow for the discovery and characterization of novel therapeutics or next generation probiotics to combat bone disease.

BIBLIOGRAPHY

BIBLIOGRAPHY

1. Turnbaugh, P. J. *et al.* An obesity-associated gut microbiome with increased capacity for energy harvest. *Nature* **444,** 1027–31 (2006).

2. Turnbaugh, P. J. *et al.* LETTERS A core gut microbiome in obese and lean twins. *Nature* **457,** 480–484 (2009).

3. Cani, P. D. *et al.* Changes in gut microbiota control inflammation in obese mice through a mechanism involving GLP-2-driven improvement of gut permeability. *Gut* **58,** 1091–1103 (2009).

4. Koeth, R. a *et al.* Intestinal microbiota metabolism of l-carnitine, a nutrient in red meat, promotes atherosclerosis. *Nat. Med.* **19,** 576–85 (2013).

5. Abrams, G. D., Bauer, H. & Sprinz, H. Influence of the normal flora on mucosal morphology and cellular renewal in the ileum. *Lab Invest* **12,** 355–364 (1963).

6. Bouskra, D. *et al.* Lymphoid tissue genesis induced by commensals through NOD1 regulates intestinal homeostasis. *Nature* **456,** 507–10 (2008).

7. Cash, H. L., Whitham, C. V, Behrendt, C. L. & Hooper, L. V. Symbiotic bacteria direct expression of an intestinal bactericidal lectin. *Science* **313,** 1126–30 (2006).

8. Maier, B. R. & Hentges, D. J. Experimental Shigella infections in laboratory animals. I. Antagonism by human normal flora components in gnotobiotic mice. *Infect. Immun.* **6,** 168–73 (1972).

9. Fernández-Santoscoy, M. *et al.* The Gut Microbiota Reduces Colonization of the Mesenteric Lymph Nodes and IL-12-Independent IFN-γ Production During Salmonella Infection. *Front. Cell. Infect. Microbiol.* **5,** 93 (2015).

10. Riggs, B. L. *et al.* Population-based study of age and sex differences in bone volumetric density, size, geometry, and structure at different skeletal sites. *J. Bone Miner. Res.* **19,** 1945–1954 (2004).

11. Karieb, S. & Fox, S. W. Suppression of T cell-induced osteoclast formation. *Biochem. Biophys. Res. Commun.* **436,** 619–624 (2013).

12. Salamanna, F. *et al.* Peripheral Blood Mononuclear Cells Spontaneous Osteoclastogenesis: Mechanisms Driving the Process and Clinical Relevance in Skeletal Disease. *J. Cell. Physiol.* **231,** 521–530 (2016).

13. Martin, G. H. K. Q. R. Activated T lymphocytes support osteoclast formation in vitro. *Biochem Biophys Res Commun* **265,** 144–150 (1999).

14. Pappalardo, A. & Thompson, K. Activated γδ T cells inhibit osteoclast differentiation and resorptive activity in vitro. *Clin. Exp. Immunol.* **174,** 281–291 (2013).

15. Nakashima, T. & Takayanagi, H. Osteoimmunology: Crosstalk between the immune and bone systems. *J. Clin. Immunol.* **29,** 555–567 (2009).

16. Asagiri, M. & Takayanagi, H. The molecular understanding of osteoclast differentiation. *Bone* **40,** 251–64 (2007).

17. Khosravi, A. *et al.* Gut microbiota promote hematopoiesis to control bacterial infection. *Cell Host Microbe* **15,** 374–381 (2014).

18. Sjögren, K. *et al.* The gut microbiota regulates bone mass in mice. *J. Bone Miner. Res.* **27,** 1357–1367 (2012).

19. Ohlsson, C. & Sjögren, K. Effects of the gut microbiota on bone mass. *Trends Endocrinol. Metab.* **26,** 69–74 (2015).

20. Li, J.-Y. *et al.* Sex steroid deficiency-associated bone loss is microbiota dependent and prevented by probiotics. *J. Clin. Invest.* **126,** 2049–63 (2016).

21. Goltzman, D. LRP5, serotonin, and bone: Complexity, contradictions, and conundrums. *J. Bone Miner. Res.* **26,** 1997–2001 (2011).

22. Cenci, S. *et al.* Estrogen deficiency induces bone loss by enhancing T-cell production of TNF-alpha. *J. Clin. Invest.* **106,** 1229–37 (2000).

23. Pacifici, R. Estrogen deficiency, T cells and bone loss. *Cell. Immunol.* **252,** 68–80 (2008).

24. Schwarzer, M. *et al.* Lactobacillus plantarum strain maintains growth of infant mice during chronic undernutrition. **351,** (2016).

25. Auchtung, J. M., Robinson, C. D. & Britton, R. A. Cultivation of stable, reproducible microbial communities from different fecal donors using minibioreactor arrays (MBRAs). *Microbiome* **3,** 42 (2015).

26. Grafe, I. *et al.* Sclerostin Antibody Treatment Improves the Bone Phenotype of Crtap(-/-) Mice, a Model of Recessive Osteogenesis Imperfecta. *J. Bone Miner. Res.* **xx,** 1–11 (2015).

27. Britton, R. A. *et al.* Probiotic L. reuteri Treatment Prevents Bone Loss in a Menopausal Ovariectomized Mouse Model. *Journal of Cellular Physiology* **229,** 1822–1830 (2014).

28. McCabe, L. R., Irwin, R., Schaefer, L. & Britton, R. A. Probiotic use decreases intestinal inflammation and increases bone density in healthy male but not female mice. *J. Cell. Physiol.* **228,** 1793–8 (2013).

29. Pfaffl, M. W. A new mathematical model for relative quantification in real-time RT-PCR. *Nucleic Acids Res.* **29,** e45 (2001).

30. Collins, F. L. *et al.* Lactobacillus reuteri 6475 Increases Bone Density in Intact Females Only under an Inflammatory Setting. *PLoS One* **11,** e0153180 (2016).

31. Collins, J., Auchtung, J. M., Schaefer, L., Eaton, K. A. & Britton, R. A. Humanized microbiota mice as a model of recurrent Clostridium difficile disease. *Microbiome* **3,** 35 (2015).

32. Schloss, P. D. *et al.* Introducing mothur: Open-source, platform-independent, community-supported software for describing and comparing microbial communities. *Appl. Environ. Microbiol.* **75,** 7537–7541 (2009).

33. Kozich, J. J., Westcott, S. L., Baxter, N. T., Highlander, S. K. & Schloss, P. D. Development of a dual-index sequencing strategy and curation pipeline for analyzing amplicon sequence data on the miseq illumina sequencing platform. *Appl. Environ. Microbiol.* **79,** 5112–5120 (2013).

34. McMurdie, P. J. & Holmes, S. Phyloseq: An R Package for Reproducible Interactive Analysis and Graphics of Microbiome Census Data. *PLoS One* **8,** (2013).

35. Dwass, M. Modified Randomization Tests for Nonparametric Hypotheses. *Ann. Math. Stat.* **28,** 181–187 (1957).

36. Green, G. H. & Diggle, P. J. On the operational characteristics of the Benjamini and Hochberg False Discovery Rate procedure. *Stat. Appl. Genet. Mol. Biol.* **6,** Article27 (2007).

37. Kay, E., Gomez-Garcia, L., Woodfin, A., Scotland, R. S. & Whiteford, J. R. Sexual dimorphisms in leukocyte trafficking in a mouse peritonitis model. *J Leukoc Biol* **98,** 805–817 (2015).

38. Bragdon, B. *et al.* Intrinsic sex-linked variations in osteogenic and adipogenic differentiation potential of bone marrow multipotent stromal cells. *J. Cell. Physiol.* **230,** 296–307 (2015).

39. Zanotti, S., Kalajzic, I., Aguila, H. L. & Canalis, E. Sex and genetic factors determine osteoblastic differentiation potential of murine bone marrow stromal cells. *PLoS One* **9,** 1–13 (2014).

40. Srivastava, S. *et al.* Estrogen decreases osteoclast formation by down-regulating receptor activator of NF-kappa B ligand (RANKL)-induced JNK activation. *J Biol Chem* **276,** 8836–8840 (2001).

41. Piper, K., Boyde, A. & Jones, S. J. The relationship between the number of nuclei of an osteoclast and its resorptive capability in vitro. *Anat. Embryol. (Berl).* **186,** 291–299 (1992).

42. Lees, R. L. & Heersche, J. N. Macrophage colony stimulating factor increases bone resorption in dispersed osteoclast cultures by increasing osteoclast size. *J. Bone Miner. Res.* **14,** 937–45 (1999).

43. Weitzmann, M. N. & Pacifici, R. Estrogen regulation of immune cell bone interactions. *Ann. N. Y. Acad. Sci.* **1068,** 256–274 (2006).

44. Weitzmann, M. N. The Role of Inflammatory Cytokines, the RANKL/OPG Axis, and the Immunoskeletal Interface in Physiological Bone Turnover and Osteoporosis. *Scientifica (Cairo).* **2013,** 125705 (2013).

45. Charatcharoenwitthaya, N., Khosla, S., Atkinson, E. J., McCready, L. K. & Riggs, B. L. Effect of blockade of TNF-alpha and Interleukin-1 action on bone resorption in early postmenopausal women. *J. Bone Miner. Res.* **22,** 724–729 (2007).

46. Narva, M. *et al.* Effects of Long-Term Intervention with *Lactobacillus helveticus*-Fermented Milk on Bone Mineral Density and Bone Mineral Content in Growing Rats. *Ann. Nutr. Metab.* **48,** 228–234 (2004).

47. Mccabe, L. R., Irwin, R., Schaefer, L. & Britton, R. A. Probiotic use decreases intestinal inflammation and increases bone density in healthy male but not female mice. *J. Cell. Physiol.* **228,** 1793–1798 (2013).

48. Ohlsson, C. *et al.* Probiotics Protect Mice from Ovariectomy-Induced Cortical Bone Loss. *PLoS One* **9,** e92368 (2014).

49. Auchtung, T. A. *et al.* Complete Genome Sequence of Turicibacter sp . Strain H121 , Isolated from the Feces of a Contaminated Germ-Free Mouse. **4,** 2015–2016 (2016).

50. Bravo, J. A. *et al.* Ingestion of Lactobacillus strain regulates emotional behavior and central GABA receptor expression in a mouse via the vagus nerve. *Proc. Natl. Acad. Sci. U. S. A.* **108,** 16050–5 (2011).

51. Dinan, T. G. & Cryan, J. F. Microbes, Immunity and Behaviour: Psychoneuroimmunology Meets the Microbiome. *Neuropsychopharmacology* 1–15 (2016). doi:10.1038/npp.2016.103

52. Rogers, G. B. *et al.* From gut dysbiosis to altered brain function and mental illness: mechanisms and pathways. *Mol. Psychiatry* **21,** 1–11 (2016).

53. Sjögren, K. *et al.* The gut microbiota regulates bone mass in mice. *J. Bone Miner. Res.* **27,** 1357–1367 (2012).

54. Ericsson, A. C. *et al.* Effects of vendor and genetic background on the composition of the fecal microbiota of inbred mice. *PLoS One* **10,** 1–19 (2015).

55. Cadwell, K. Expanding the role of the virome: commensalism in the gut. *J. Virol.* **89,** 1951–3 (2015).

56. Virgin, H. W. The virome in mammalian physiology and disease. *Cell* **157,** 142–150 (2014).

57. Mariman, R., Tielen, F., Koning, F. & Nagelkerken, L. The Probiotic Mixture VSL#3 Has Differential Effects on Intestinal Immune Parameters in Healthy Female BALB/c and C57BL/6 Mice. *J. Nutr.* **145,** 1354–61 (2015).

58. de Vooght, V. *et al.* Choice of mouse strain influences the outcome in a mouse model of chemical-induced asthma. *PLoS One* **5,** 1–9 (2010).

CHAPTER 5. DISCUSSION AND CONCLUSION

The use of bacteria in the food fermentation process has existed for millenia, and due to its long history of safe use in the food industry, many lactic acid bacteria have obtained the Generally Regarded As Safe (GRAS) status. Several of these bacteria are now considered a probiotic, meaning “for life” as derived from Latin and Greek, because of potential health benefits they confer. While the popularity of probiotics has grown with increased commercialization, the idea of consuming microbes to benefit health is by no means novel. The nobel laureate, Elie Metchnikoff, first proposed in the early 1900s that the consumption of the probiotic *Lactobacillus bulgaricus* could extend one’s lifespan [1]. He hypothesized that toxins produced by colonic bacteria were the cause for many age-related processes and lactic acid bacteria could counteract this. Interestingly, one of these ideas touched upon bone degeneration in old age being due to deleterious colonic bacteria dysregulating osteoclast differentiation. As a result, his revolutionary theories have contributed towards investigating the impact of probiotics on bone health.

Currently, the Food and Drug Administration does not regulate probiotics since it is categorized as a food supplement. Many have not undergone the rigors of clinical trials. As a result, specific claims about combating disease cannot be made. The current studies offer insight into how *L. reuteri* potentially suppresses bone loss in a mouse model of estrogen deficiency. This will guide future research that aims to further validate the therapeutic potential of *L. reuteri* in bone disease as well as improve upon decision-making regarding probiotic strain selection.

In the past 15 years, there have been a number of studies characterizing the positive impact of probiotics on bone health as described in Chapter 1. However, other than observing that bone health has improved following the administration of probiotics in *in vivo* animal models, many of the studies are still limited in terms of understanding the mechanisms involved in mediating this beneficial response. The work performed in this dissertation offers mechanistic insight into how

the probiotic *L. reuteri* is beneficial for bone health. In Chapter 2, we demonstrated that *L. reuteri* was efficacious in preventing the onset of osteoporosis in estrogen deficient mice. Through these studies, we observed that *L. reuteri* suppressed osteoclastogenesis, which is a crucial pathway involved in the development of osteoporosis. Upon further investigation, I was able to identify potential pathways that were impacted in RAW264.7 cells during osteoclastogenesis following *L. reuteri* treatment (Chapter 3). This led to studies demonstrating that p38 and NF-κB activation were decreased by *L. reuteri* during RANKL-induced RAW264.7 cell differentiation. Next, I discovered that Lactobacillic acid (LA), a long chain fatty acid produced by *L. reuteri*, was capable of suppressing osteoclastogenesis. By blocking GPR120, which is a receptor for long chain fatty acids, I demonstrated that the ability of *L. reuteri* to suppress osteoclastogenesis was diminished. Lastly, the impact of the microbiota on bone health was investigated in Chapter 4 using a germ free (GF) animal model. In contrast to a study performed by Sjögren et al., we demonstrated that colonization of GF mice did not lead to a decrease in bone mass [2]. This conflicting result was an indication of how little we understand about the regulation of bone metabolism by microbes.

5.1 *Future directions*

The number of studies demonstrating that probiotic treatment or modification of the microbial community is capable of impacting bone strongly suggests that this is an option worth exploring for the development of novel therapeutics. However, to continue gaining traction as a viable treatment option, a better understanding of the mechanisms responsible for therapeutic properties must be obtained. The studies carried out in this dissertation offer approaches to begin addressing this.

Despite making progress in characterizing the beneficial response to bone health by *L. reuteri* (Chapter 2) and identification of a molecule produced that holds promise as a bioactive compound (Chapter 3), many questions still remain. Our knowledge in terms of dosing is limited so future studies designed to answer that with a dose response in the Ovx animal model would address this gap in knowledge. *L. reuteri* appeared to be having an anti-catabolic effect in this model; however, it is possible that it also has an anabolic effect. In another animal model, it was demonstrated that *L. reuteri* promoted bone formation [3]. To test this, the addition of *L. reuteri* following a period of estrogen deficiency to allow for bone loss would help elucidate if *L. reuteri* promotes bone deposition. Currently, only one, FDA approved medication for osteoporosis is tailored for bone anabolism so this would provide a different strategy for treating this disease. Another area demanding attention is an understanding of how exclusive this activity is by testing various strains of probiotics would also be useful for several reasons. Further validation of strain-specific effects would offer power in probiotic strain selection. Additionally, this would also allow for identifying probiotic mechanisms of action through comparative genomic studies.

The identification of LA was an important first step towards potentially understanding the probiotic mechanism of action(s) by *L. reuteri* in the context of bone health. However, future studies still need to be performed to characterize this molecule. It is unclear whether this molecule targets the same signaling cascades that *L. reuteri* targets, so investigating its role in MAPK and NF-κB signaling activation could corroborate and validate our previous results. Its impact *in vivo* is also unclear, and this can be addressed by testing the efficacy of LA to prevent bone loss in our Ovx mouse model. Then, once LA is verified to have biological activity *in vivo*, questions regarding dosing and modes of delivery can also be addressed with the same model.

The ability to partially suppress osteoclastogenesis was still present in the *L. reuteri* mutant deficient in LA production indicating that other molecules are also involved. One strategy that

was used to identify these molecules was through the use of an *L. reuteri* mutant library generated by recombineering [4]. The screening of this library in the RAW264.7 cell differentiation assay allowed for the identification of three putative mutants that have a decreased ability to suppress osteoclastogenesis (Appendix A). Future studies focused on these mutants individually or in conjunction with other relevant mutations will provide further insight into the role of *L. reuteri* in regulating bone health.

While the gut microbiota has been the subject matter of many health-related studies, its impact on bone health has only been gaining interest recently. The goal of Chapter 4 was to investigate the impact of a defined microbial community on bone health in GF mice. By comparing different microbiotas used to colonize GF mice, I would be able to identify candidate organisms that putatively affected bone health. Although this study failed to yield the expected results, it is still an important contribution towards understanding how the gut microbiota impacts bone health. It is the first study with a detailed report of the bacteria present in the communities used to colonize the GF mice while monitoring bone health. This will serve as a reference database for future studies conducted in a similar manner to identify bacteria that impact bone health.

5.1.1 *Integration of other probiotic studies and potential mechanisms to consider*

Another topic of discussion pertains to whether the right pathways are being studied to understand how the microbiota impacts bone health. The importance of the microbiota on immune development has been extensively studied in many animal models [5–7]. Since the development of bone loss is highly impacted by cross talk between immune cells and monocytes that can differentiate into osteoclasts, early focus has been placed on the dysregulation of osteoclastogenesis [8–10]. However, one potential link that may be understudied is the connection between the gut microbiota, enteric nervous system, and bone in what can be referred to as a gut-brain-bone axis. The enteric nervous system is a communication system

between the brain and gastrointestinal tract [11,12]. Bidirectional signaling allows the brain to regulate a number of things including gastrointestinal motility, appetite, and central metabolism. Interestingly, the brain has also been linked to controlling bone metabolism [13].

In order to ensure survival, the brain has evolved to tightly regulate energy balance in the body. The hypothalamus is an extremely important portion of the brain involved with the secretion of endocrine hormones that are involved with growth, stress responses, sexual development, and blood pressure control to name a few [14–16]. It is surrounded by a capillary system that is semi-permeable to the blood-brain barrier to allow communication between the brain and the endocrine system. Through this interaction, the hypothalamus can respond to changes in hormone levels such as Neuropeptide Y (NPY) or leptin in the bloodstream to regulate energy homeostasis and bone mass [17–19]. Serotonin, an important neurotransmitter produced primarily in the small intestine, has also been shown to regulate bone mass [20–22]. Taken together, these studies strongly support a relationship between bone metabolism and the brain.

Several studies have been conducted to investigate the impact of the gut microbiota on NPY and leptin [23,24]. These studies were performed in the context of investigating obesity and metabolic disease. Additionally, a number probiotic studies have focused on mental health and involved the regulation of neurotransmitters and peptides [25,26]. For example, it has been demonstrated by another research group that the same strain of *L. reuteri* promoted wound healing and hair growth in different animal models. These observations were linked to an increase in oxytocin and testosterone, which are both hormones regulated by the hypothalamic-pituitary axis in the brain [27–29]. Another interesting observation was that *L. reuteri* was ineffective in vagotomized mice, which demonstrated the necessity of a neural connection between the brain and gut [27]. Despite the fact that bone health was not the primary focus of these studies,

the established links that have been made between microbes and gut hormones, and the brain and bone support the possibility of a novel gut-brain-bone regulatory axis.

5.2 *Conclusions*

The increase in life expectancy we are experiencing in the 21st century has also led to an increase in age-related diseases with one example being osteoporosis. According to the National Osteoporosis Foundation, 70 million Americans will have osteoporosis by the year 2025 and the healthcare cost for treating the disease or ailments that result from it is predicted to be $25 billion dollars. Due to the shortcomings of current treatment options, the development of novel therapeutics for osteoporosis is of utmost importance. To develop novel therapeutics, we must gain a better understanding of the disease. Due to the complexity of the human body, the understanding that bone metabolism can be regulated by the gut microbiota has not been recognized until recently. With the emergence of studies investigating the impact of the microbiota on human health, we are in a position to discover the potential of manipulating the microbiota or delivery of a probiotic to improve bone health.

BIBLIOGRAPHY

BIBLIOGRAPHY

1. Metchnikoff, É. Lactic acid as inhibiting intestinal putrefaction. *Prolong. Life Optimist. Stud.* 161–183 (1907). at <https://archive.org/details/prolongationofli00metciala>

2. Sjögren, K. *et al.* The gut microbiota regulates bone mass in mice. *J. Bone Miner. Res.* **27,** 1357–1367 (2012).

3. Mccabe, L. R., Irwin, R., Schaefer, L. & Britton, R. A. Probiotic use decreases intestinal inflammation and increases bone density in healthy male but not female mice. *J. Cell. Physiol.* **228,** 1793–1798 (2013).

4. Van Pijkeren, J. P. & Britton, R. a. High efficiency recombineering in lactic acid bacteria. *Nucleic Acids Res.* **40,** 1–13 (2012).

5. Cash, H. L., Whitham, C. V, Behrendt, C. L. & Hooper, L. V. Symbiotic bacteria direct expression of an intestinal bactericidal lectin. *Science* **313,** 1126–30 (2006).

6. Bouskra, D. *et al.* Lymphoid tissue genesis induced by commensals through NOD1 regulates intestinal homeostasis. *Nature* **456,** 507–10 (2008).

7. Hooper, L. V, Littman, D. R., Macpherson, A. J. & Program, M. P. Interactions between the microbiota and the immune system. *Science (80-.).* **336,** 1268–1273 (2015).

8. D'Amelio, P. & Sassi, F. Osteoimmunology: from mice to humans. *Bonekey Rep.* **5,** 802 (2016).

9. Weitzmann, M. N. & Pacifici, R. Estrogen regulation of immune cell bone interactions. *Ann. N. Y. Acad. Sci.* **1068,** 256–274 (2006).

10. Hirayama, T., Danks, L., Sabokbar, a & Athanasou, N. a. Osteoclast formation and activity in the pathogenesis of osteoporosis in rheumatoid arthritis. *Rheumatology (Oxford).* **41,** 1232–1239 (2002).

11. Forsythe, P. & Kunze, W. A. Voices from within: Gut microbes and the CNS. *Cell. Mol. Life Sci.* **70,** 55–69 (2013).

12. Hyland, N. P. & Cryan, J. F. Microbe-host interactions: Influence of the gut microbiota on the enteric nervous system. *Dev. Biol.* 1–6 (2016). doi:10.1016/j.ydbio.2016.06.027

13. Zofková, I. & Matucha, P. New insights into the physiology of bone regulation: the role of neurohormones. *Physiol. Res.* **63,** 421–7 (2014).

14. Han, C., Rice, M. W. & Cai, D. Neuroinflammatory and autonomic mechanisms in diabetes and hypertension. *Am. J. Physiol. - Endocrinol. Metab.* **311,** E32–E41 (2016).

15. Mooney-Leber, S. M. & Brummelte, S. Neonatal pain and reduced maternal care: Early-life stressors interacting to impact brain and behavioral development. *Neuroscience* (2016). doi:10.1016/j.neuroscience.2016.05.001

16. Cavadas, C., Aveleira, C. A., Souza, G. F. P. & Velloso, L. The pathophysiology of defective proteostasis in the hypothalamus — from obesity to ageing. *Nat. Rev. Endocrinol.* (2016). doi:10.1038/nrendo.2016.107

17. Baldock, P. A. *et al.* Neuropeptide Y knockout mice reveal a central role of NPY in the coordination of bone mass to body weight. *PLoS One* **4,** (2009).

18. Baldock, P. a *et al.* Hypothalamic regulation of cortical bone mass: opposing activity of Y2 receptor and leptin pathways. *J. Bone Miner. Res.* **21,** 1600–1607 (2006).

19. Steppan, C. M., Crawford, D. T., Chidsey-Frink, K. L., Ke, H. & Swick, A. G. Leptin is a potent stimulator of bone growth in ob/ob mice. *Regul. Pept.* **92,** 73–78 (2000).

20. Hage, M. P. & El-Hajj Fuleihan, G. Bone and mineral metabolism in patients undergoing Roux-en-Y gastric bypass. *Osteoporos. Int.* **25,** 423–439 (2014).

21. Quiros-Gonzalez, I. & Yadav, V. K. Central genes, pathways and modules that regulate bone mass. *Arch. Biochem. Biophys.* **561,** 130–139 (2014).

22. Sharan, K. & Yadav, V. K. Hypothalamic control of bone metabolism. *Best Pract. Res. Clin. Endocrinol. Metab.* **28,** 713–723 (2014).

23. Xiong, Y. *et al.* Short-chain fatty acids stimulate leptin production in adipocytes through the G protein-coupled receptor GPR41. *Proc. Natl. Acad. Sci. U. S. A.* **101,** 1045–50 (2004).

24. Schéle, E. *et al.* The gut microbiota reduces leptin sensitivity and the expression of the obesity-suppressing neuropeptides proglucagon (Gcg) and brain-derived neurotrophic factor (Bdnf) in the central nervous system. *Endocrinology* **154,** 3643–3651 (2013).

25. Mackos, A. R. *et al.* Social stress-enhanced severity of Citrobacter rodentium-induced colitis is CCL2-dependent and attenuated by probiotic Lactobacillus reuteri. *Mucosal Immunol.* **9,** 515–26 (2016).

26. Bravo, J. A. *et al.* Ingestion of Lactobacillus strain regulates emotional behavior and central GABA receptor expression in a mouse via the vagus nerve. *Proc. Natl. Acad. Sci. U. S. A.* **108,** 16050–5 (2011).

27. Poutahidis, T. *et al.* Microbial symbionts accelerate wound healing via the neuropeptide hormone oxytocin. *PLoS One* **8,** (2013).

28. Poutahidis, T. *et al.* Probiotic microbes sustain youthful serum testosterone levels and testicular size in aging mice. *PLoS One* **9,** (2014).

29. Ferrini, M. *et al.* Aging-related increased expression of inducible nitric oxide synthase and cytotoxicity markers in rat hypothalamic regions associated with male reproductive function. *Neuroendocrinology* **74,** 1–11 (2001).

APPENDIX

APPENDIX

Screening of the *Lactobacillus reuteri* 6475 secretome mutant library

Purpose

Lactobacillus reuteri ATCC 6475 has demonstrated the ability to inhibit osteoclastogenesis [1]. However, the mechanisms underlying this phenomenon have not been fully identified. Due to the importance of the osteoclastogenesis in osteoporosis, I believed that the identification of bioactive molecules or a better understanding of how *L. reuteri* impacts this pathway could lead to the development of novel therapeutics. The purpose of this study was to identify genes of *L. reuteri* 6475 that are involved with the suppression of osteoclastogenesis in an *in vitro* RAW264.7 cell differentiation assay. Since the activity was present in cell-free culture supernatant generated from *L. reuteri*, we hypothesized that a secreted product was responsible for the observed activity. Using a library of gene mutations in proteins predicted to be secreted, we conducted a screen to identify mutations that would attenuate the activity of *L. reuteri* on osteoclastogenesis.

Materials and methods

Bacterial strains and growth conditions

The method for culturing *L. reuteri* was identical to those described in Chapters 2 and 3. Briefly, *L. reuteri* was cultured anaerobically in deMan, Rogosa, Sharpe media (MRS, Difco) for 18 h at 37 °C.

Construction of mutant secretome library

The secretome mutant library was constructed based off of gene-encoding proteins that were predicted to be secreted using the SignalP 3.0 program [2,3]. Null mutations, through the introduction of a stop codon by recombineering, were made early in the coding sequence to halt transcription [4]. Several members of the Britton Laboratory contributed to the construction of the mutant library. J.P. van Pijkeren designed the oligonucleotides that introduced the desired mutations. Laura Ortiz, Javiera Ortega, Anthony Findlay, and Denise Sirias carried out the experiments that introduced, screened, and identified the mutants.

Preparation of cell-free supernatant from *L. reuteri*

The generation of CCS was identical to those described in Chapters 2 and 3. Briefly, an overnight culture of *L. reuteri* was grown in MRS for 18 h and then washed and resuspended in Minimum Essential Medium (MEM-α, Invitrogen) to an OD_{600} = 3.0 and incubated for 3 h at 37°C with gentle orbital shaking (60 rpm). Bacteria were pelleted and the supernatant was filter-sterilized and fractionated. The < 3 kDa fraction was used for the osteoclastogenesis assay.

Cell culture conditions and screening of mutant library

Cell culture protocols for the RAW264.7 cells were identical to those described in Chapters 2 and 3. *L. reuteri* CCS was generated from the secretome library mutants then lyophilized and stored at -80 °C. In 48-well culture grade plates (Costar), $2*10^4$ cells were seeded. Following one day of incubation, cells were stimulated for differentiation with the addition of receptor activator of NF-kappa B ligand (RANKL, 100 ng/ml, R&D systems). Lyophilized *L. reuteri* CCS from the mutant library was resuspended in culture medium and used to treat the cells. Fresh medium was replenished after every 2 days. On day 7, cells were fixed and stained for tartrate-resistant acid phosphatase (TRAP) using a commercially available staining kit (Cat. No. 387A,

Sigma). After identifying a candidate with suppressed inhibition, 2 additional biological replicates were performed. A total of 137 mutants were screened.

Statistical analysis

The results presented are as means +/- SD or SEM. An unpaired Student's *t* test was used to assess differences between groups. The cutoff for significance was $p \leq 0.05$. One-way ANOVA analysis was applied when more than 2 groups were being compared.

Results

Identification of *L. reuteri* genes that impacted osteoclastogenesis

Screening of the *L. reuteri* secretome library in the osteoclastogenesis assay identified 3 mutants with a decreased ability to suppress osteoclastogenesis in comparison to the wild type strain of *L. reuteri* (Figure A.1). Interestingly, the 3 genes identified were in close proximity to one another within the genome (Figure A.2).

Discussion and Future Directions

The identification of bioactive molecules that confer health benefits is of great importance in the field of probiotics research. Not only would this aid in elucidating possible mechanisms of action, but it would allow for the justification of strain selection. In Chapter 3, it was demonstrated that the *L. reuteri* mutant deficient in Lactobacillic Acid (LA) production retained the ability to partially suppress osteoclastogenesis. The additional mutants identified here may contribute to the remainder of the inhibition. Future studies investigating a multiple gene knockout containing mutations made in genes responsible for LA production in combination with the mutation(s) identified here will help elucidate this matter.

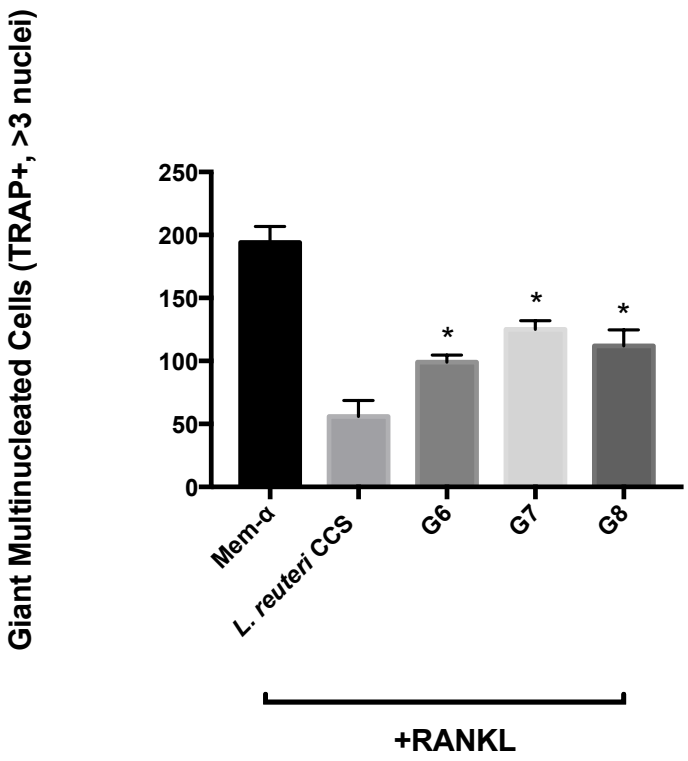

Figure A.1. Identification of mutants with decreased suppression of osteoclastogenesis.

RAW264.7 cells were stimulated for osteoclast differentiation with RANKL (100ng/ml) and treated with a vehicle (MEM-α) or *L. reuteri* CCS. This was performed three times in total and the reported result is a representative experiment with associated standard deviation, *$p < 0.05$ compared to MEM-α (vehicle control) and the *L. reuteri* WT CCS conditions as determined by one-way ANOVA.

Mutant	Locus Tag	Annotation	Pfam
G6	HMPREF0536_1674	Conserved hypothetical protein	ErfK family cell surface protein
G7	HMPREF0536_1675	Hypothetical surface protein	L,D transpeptidase catalytic domain
G8	HMPREF0536_1685	Probable Muramidase	LysM (lysin motif) Glucosaminidase

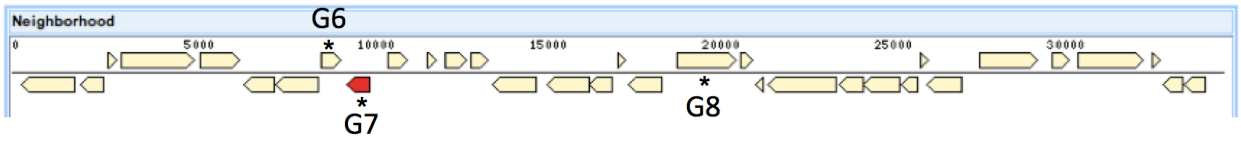

Figure A.2. Gene annotation of putative mutants and locus map.

The identified genes of interest are located in close proximity on the *L. reuteri* chromosome.

BIBLIOGRAPHY

BIBLIOGRAPHY

1. Britton, R. A. *et al.* Probiotic L. reuteri Treatment Prevents Bone Loss in a Menopausal Ovariectomized Mouse Model. *Journal of Cellular Physiology* **229,** 1822–1830 (2014).

2. Bendtsen, J. D., Nielsen, H., von Heijne, G. & Brunak, S. Improved prediction of signal peptides: SignalP 3.0. *J. Mol. Biol.* **340,** 783–795 (2004).

3. Boekhorst, J., Wels, M., Kleeberezem, M. & Siezen, R. J. The predicted secretome of Lactobacillus plantarum WCFS1 sheds light on interactions with its environment. *Microbiology* **152,** 3175–3183 (2006).

4. Van Pijkeren, J. P. & Britton, R. a. High efficiency recombineering in lactic acid bacteria. *Nucleic Acids Res.* **40,** 1–13 (2012).